MODULATING AUTOPHAGY AND GLUTAMINE METABOLISM IN CHO CELLS TO INCREASE FED-BATCH PROCESS PERFORMANCE

by

Mario A. Jardon

B.Sc. Université Laval, Québec, Canada, 1998

M.Sc. Université Laval, Québec, Canada, 2000

A THESIS SUBMITTED IN PARTIAL FULFILLMENT OF

THE REQUIREMENTS FOR THE DEGREE OF

DOCTOR OF PHILOSOPHY

in

The Faculty of Graduate Studies

(Chemical and Biological Engineering)

The University of British Columbia

(Vancouver)

June 2012

Abstract

Valuable recombinant therapeutic proteins are routinely produced from Chinese hamster ovary (CHO) cells in fed-batch cultivations. An improved understanding of the physiological factors that affect cell proliferation, survival, productivity and product quality in fed-batch could contribute to facilitate general access to these products. This work describes the investigation of autophagy and glutamine metabolism in CHO cells for the purpose of increasing fed-batch process performance. The close link between glutamine deprivation and autophagy was found to greatly affect process performance, with an increase of the cellular lysosomal compartment correlated with decreased cell-specific productivity. The increased autophagic activity upon glutamine withdrawal was confirmed by the formation of GFP-LC3 fluorescent puncta and by an LC3 autophagic flux assay. The use of 3-methyl adenine (3-MA) to inhibit autophagy increased the yield of recombinant tissue plasminogen activator (t-PA) by 2.8-fold, without compromising the glycosylation capacity of the cells given that the t-PA fucosylation, galactosylation and sialylation all increased. A more comprehensive study of glutamine metabolism and autophagy performed, including by investigating 2 additional CHO cell lines expressing different antibody proteins. The mitochondrial and lysosomal changes in response to glutamine deprivation varied substantially between cell lines, illustrating how the susceptibility to autophagy can be cell-line dependent. Integrating the combined effect of enhanced proliferation (achieved through modulation of glutamine metabolism) and inhibition of autophagy (by treatment with 3-MA), a maximum 4.6-fold increase of t-PA production was obtained in fed-batch culture. Finally, autophagy and glutamine metabolism were explored in cancer cell lines, and produced original findings on the potential for Raman spectroscopy to analyze live cell physiological responses to conditions that trigger autophagy. Overall, this study illustrates the potential for a fruitful interaction between basic scientific research and applied biotechnology. The investigation of response mechanisms to cellular stress provided opportunities to both improve industrial processing and open new perspectives for basic biological research.

Preface

Each chapter of this dissertation corresponds to a manuscript that either has been accepted or will be submitted for publication. For decisions regarding the general direction of this project, I was the major contributor along with my supervisor, James Piret. I contributed most of the experimental design and experimental work. I also participated in the training and supervision of an undergraduate student, Kelsey Marshal, and of a rotation graduate student, Sarah Natrasany, both of whom contributed manually to Chapter 4. Stanislav Konorov and I produced with equal contributions the experimental design and work reported in Chapter 5. James Piret was the main supervisor for all chapters, with significant input from Sharon Gorski (SFU and BCCA, Chapters 2 and 3), Hélène Côté (UBC, Chapters 2 and 3), Michael Butler (UoM, Chapter 2), Robin Turner (UBC, Chapter 5) and Michael Blades (UBC, Chapter 5). The detailed contributions were as follows:

Chapter 2. The manuscript "Inhibition of glutamine-dependent autophagy increases t-PA production in CHO cell fed-batch processes" has been accepted for publication in a peer-reviewed journal.

Mario Jardon: Contributed the experimental design, ~60% of experimental work, ~85% of the final data and text in the manuscript.

Katrin Braasch: ~20% of experimental work, 15% of the final data and text in the manuscript.

Beheroze Sattha: ~10% of experimental work.

Amy Leung: ~10% of experimental work.

Michael Butler: Supervision of Katrin, manuscript edition.

Hélène Côté: Supervision of Beheroze, manuscript edition.

Sharon Gorski: Supervision of Amy, manuscript edition.

James Piret: Supervision of Mario, manuscript edition.

Chapter 3. "Investigating glutamine metabolism and autophagy in various CHO cell lines" will be submitted to a peer-reviewed journal.

Mario Jardon: Contributed the experimental design, ~80% of experimental work, the final data and text in the manuscript.

Beheroze Sattha: ~10% of experimental work.

Amy Leung: ~10% of experimental work.

Hélène Côté: Supervision of Beheroze, manuscript edition.

Sharon Gorski: Supervision of Amy, manuscript edition.

James Piret: Supervision of Mario, manuscript edition.

Chapter 4. "Integrating autophagy and glutamine metabolism in process strategies to increase fed-batch performance" will be submitted to a peer-reviewed journal.

Mario Jardon: Contributed the experimental design, ~60% of experimental work, the final data and text in the manuscript. Supervision of Kelsey and Sarah.

Kelsey Marshal: ~20% of experimental work.

Sarah Natrasany: ~20% of experimental work.

James Piret: Supervision of Mario, manuscript edition.

Chapter 5. "Exploring autophagy and glutamine metabolism in cancer systems" is being submitted to a peer-reviewed journal.

Mario Jardon: Contributed ~80% of the experimental design, ~50% of experimental work, ~50% of the final data and ~50% of the text in the manuscript.

Stanislav Konorov (equal contribution): Contributed ~20% of the experimental design, ~50% of experimental work, ~50% of the final data and ~50% of the text in the manuscript.

Robin Turner: Supervision of Stanislav, manuscript edition.

Michael Blades: Supervision of Stanislav, manuscript edition.

James Piret: Supervision of Mario, manuscript edition.

Ethical approval

Work with biohazards (level 2) in all chapters was approved by the UBC BioSafety Committee (protocol # B09-0105).

Table of Contents

List of Tables

List of Figures

Nomenclature

3-MA	3-methyladenine
CHO	Chinese hamster ovary
ETC	Electron transfer chain
GS	Glutamine synthetase
GU	Glucose units
IgG	Immunoglobulin G
MAb	Monoclonal antibody
Mc/mL	10^6 cells per milliliter
MOMP	Mitochondrial outer membrane permeabilization
mtDNA	Mitochondrial DNA
OUR	Oxygen uptake rate
PAT	Process analytical technology
PE	Phosphatidyl ethanolamine
PGR	Partial glutamine replacement
PS	Phosphatidyl serine
PTP	Permeability transition pore
RH	Relative humidity
ROS	Reactive oxygen species
shRNA	Short hairpin RNA
siRNA	Small interfering RNA, short interfering RNA or silencing RNA
TCA	Tricarboxylic acid
TEM	Transmission electron microscopy
t-PA	Tissue plasminogen activator
$\Delta\Psi m$	Mitochondrial transmembrane potential

Dedication

To all my family: Mom and Dad, Nacho, Sabel, Eliud, Bruno, Paola, Rodri and Yola, thank you. I hope you may be one day as proud of me as I am of you. Even though physically far away, I know you are very close. Aunts, uncles and cousins: thanks.

Thank you to all in Glenwood and to all who make Glenwood possible.

To the graduate students – Derek, Corinne, Davis, Nicole, John, Sandra, Siva, Jana, Alex and James – with whom I interacted in the CHBE Graduate Club and the CHBE Sustainability Club: the lessons I learned at your side are among the most valuable from my experience at UBC. Thanks. To all those involved with the CHBE Grad Club, the CHBE Sustainability Club, the CHBE Arts Club or the MSL Grad Student and Postdoc Association: thank you for making a difference with your generosity.

1 Introduction

1.1 Mammalian cell culture for the production of biopharmaceuticals

Numerous studies (Pavlou and Reichert, 2004; Werner, 2004; Wurm, 2004) have reported an increasing demand over decades for recombinant proteins with clinical applications. These proteins are used for the treatment or diagnosis of cancer, diabetes, blood diseases, central nervous system disorders and infectious diseases including HIV, and they account for multi-billion dollar yearly sales (Pavlou and Reichert, 2004). More than half of such products are manufactured from mammalian cell cultures (Pavlou and Reichert, 2004), which are currently the only system capable of performing complex posttranslational processing – particularly the glycosylation pattern – required for the proper biologic activity of these proteins (Butler, 2005).

In order to become commercially available, biopharmaceuticals must undergo a long and often unsuccessful path. The time range from product development to market availability is typically 10 years (Wurm, 2004). Limited availability of valuable novel products affects first of all the patients, depriving them of effective treatments. However, it can also burden health care systems, increasing therapy costs. Finally, delayed access to market of these products may become a financial challenge for industries trying to obtain regulatory approval. Accelerating the development of processes for the manufacture of advanced biopharmaceuticals can therefore benefit public health, health care systems and industry. Engineering disciplines integrating science and technology to improve process can be a key contributor in this pursuit.

1.2 Current industrial practice

Industrial production of recombinant proteins from mammalian cells is mostly performed in instrumented stirred-tank reactors, using fed-batch cultivations with serum-free media (Butler, 2005; Chu and Robinson, 2001; Hu and Aunins, 1997). Stirred-tank reactors are a well-established, scalable and robust technology. Serum-free media are used for safety purposes, to avoid concerns with animal-derived products, and to facilitate product

purification. The cell lines most commonly used are derived from Chinese Hamster Ovary (CHO) cells and the murine myeloma cell lines NS0 and SP2/0 (Chu and Robinson, 2001).

Fed-batch processes are the most widely used since they provide high product yields with relatively simple operations. A fed-batch process can be defined as a cultivation in which nutrients are added (fed) over time. This feeding can be continuous or discontinuous, although the most common feeding protocols of industrial relevance are discontinuous.

Such media additions result in non-negligible changes over time of the culture volume and in variations of numerous process parameters such as cell, nutrient and product concentrations, osmolality, volume, etc.
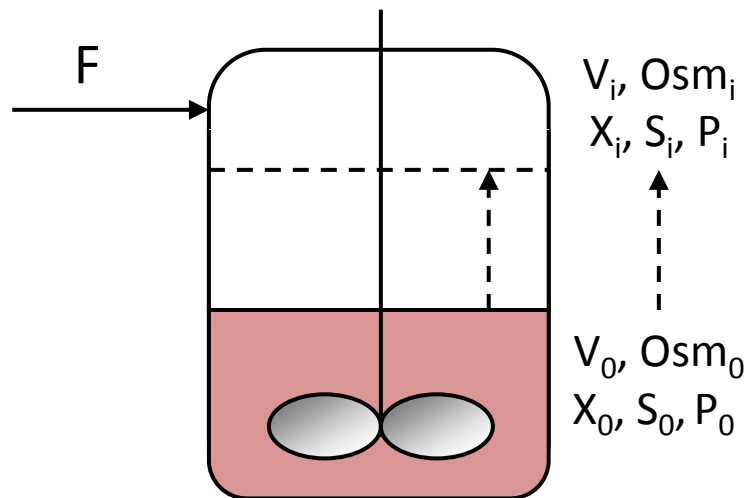
Figure 1.1.   Schematic of a fed-batch process.
During fed-batch cultivations numerous process parameters change: volume (V), osmolality (Osm), cell concentration (X), nutrient concentrations (S), product concentrations (P). Parameter subscripts in the diagram refer to the time (0 for initial and i for any other). The feed is designated by F; its units are generally volume per time.

Literature on fed-batch processes for the cultivation of mammalian cells is very abundant. However, it is often not revealing, in part because it is generated by industrial research groups with restrictions on intellectual property. Studying mammalian cell fed-batch process research and development in a mechanistic and systematic way from an academic

2

perspective can therefore contribute to both scientific literature and industrial practice, while addressing a public health need.

1.3   Fed-batch processes

1.3.1   Overview

The primary purpose of a feeding operation is to overcome the depletion of nutrients that cells consume over time. However, it is not possible to provide such nutrients from the beginning of the culture, due to solubility limits or to potential undesirable effects of high nutrient concentrations (toxicity, substrate inhibition, etc.). Thus, compared to a batch cultivation (with no feeding), the nutrient additions in a fed-batch cultivation are intended to achieve higher cell concentrations and sustain cell productivity, while extending cell viability. In order to have industrial potential, the feeding operation should not alter the product quality attributes or impair the ability of cells to perform the posttranslational modifications that determine product quality.

1.3.2   Results in published literature

Most reports on fed-batch processes deal with the production of monoclonal antibodies (MAb), often from hybridoma cell lines in the 1990s and increasingly from more industrially relevant NS0 and CHO cells. Cell lines, experimental conditions and actual results for cell density, product concentration and maximum cultivation time vary considerably. Monoclonal antibody concentrations in the order of grams per liter and cell concentrations around 10 million cells per milliliter are current expectations for industrial mammalian cell processes (Wurm, 2004). Comparatively, fewer published results are available for other recombinant proteins. Table 1.1 presents a summary of some of these published results, in decreasing order of product concentration.

Numerous feeding strategies aim at maintaining low levels of glucose with the purpose of limiting lactate production. However, the highest product titers do not always correspond to the lowest glucose levels reported. A closer correlation can be found between maximum product titer and maximum viable cell concentration, but the differences may also be influenced by the productivity of the cell lines used.

Table 1.1.   Published results on feeding protocols.

Reference	Cell line	Product	Glucose conc. during fed-batch	Max. Product Conc. (mg/L)	Max. Viable Cell Conc. (Mc/mL)	Max. Duration (days)
Li et al., 2012a	CHO DUK-XB11	MAb	17-33 mM	8000	20	18
Yu et al., 2011	CHO DUK-XB11	Humanized IgG1 MAb	Not reported	7500	8	20
Luo et al., 2012	CHO DUK-XB11	Humanized MAb	11-45 mM	4800	18	12
Li et al., 2012b	NS0.CF	MAb	>10 mM	4608	12.8	15
Combs et al., 2011	CHO K1SV	IgG1 MAb	3-30 mM	4000	14.2	14
Zhang et al., 2006	CHO K1SV	IgG4 MAb	2-40 mM	3000	13	14
Tabuchi et al., 2010	CHO-DXB11	MAb	~25 mM	2890	Not reported	42
Zhou et al., 1997a	Amplified GS-NS0 myeloma	Humanized anti-CD18 MAb	ca 5 mM	2700	6.6	28
Burky et al., 2007	NS0	MAb, IgG1, IgG4	>16 mM	2640	10	13
Xie et al., 1996	CRL-1606 hybridoma	Anti-fibronectin IgG	ca 0.5 mM	2400	17	23
Ref. in Bibila et al., 1995	Amplified GS-NS0 myeloma	MAb	Not reported	1800	Not reported	Not reported
Jo et al., 1993	2c3.1 Hybridoma	Anti HBs IgG1 MAb	5.6-14 mM	1560	10	104
Han et al., 2011	CHO	Humanized MAb	0-38 mM	1123	9	14
Li et al., 2009	GS-NS0	Anti-CD25 MAb	10-18 mM	1005	8.9	9
Bibila et al., 1994	Amplified GS-NS0 myeloma	MAb	15-50 mM	1000	2.0	20
Sellick et al., 2011	CHO	IgG4 MAb	Not reported	820	13	12
Sauer et al., 2000	Sp2/0 myeloma	Humanized IgG4 MAb	5.0-30.5 mM (SP: 22.5-30.5)	750	9.6	10
Majors et al., 2009	CHO DG44	Humanized IgG MAb	Not reported	700	6	14
Dorai et al., 2009	CHO EAX197	MAb	60 mM	687	Not reported	15
Xie et al., 1994	CRL-1606 hybridoma	Anti fibronectin IgG MAb	0-20 mM	551	6.0	17
Jardon et al., 2012	CHO CRL-9096	t-PA	>20 mM	536	5.9	12
Dempsey et al., 2003	GS-NS0	MAb	11-22 mM	508	2.7	17
Moran et al., 2000	GS-NS0	Humanized IgG1 MAb	Not reported	500	4.7	7
Zhang et al., 2004	WuT3 hybridoma	IgG2a	1-3 mM	350	6.1	15
Frahm et al., 2003	NS0 6A1 Bcl-2	Chimeric IgG MAb	16 mM	340	1.1	9
Zhou et al., 1997b	MAK	IgG MAb	0.55 mM (SP)	250	10	6
Takagi et al., 2001	CHO 1-15500	t-PA	Not reported	250	2.3	30
Stansfield et al., 2007	GS-NS0	IgG4 MAb	Not reported	240	2.4	14
Sanfeliu et al., 1996	KB-26.5 murine hybridoma	Anti red-cell A1 IgG3 MAb	Not reported	200	2.5	15
Jang et al., 2000	AFP-27 murine hybridoma	Anti α-fetoprotein IgG1 MAb	Near 0 (starvation)	180	0.8	Not reported
Kurokawa et al., 1994	16-3F mouse-mouse hybridoma	Anti α-amylase MAb	1.1 mM	172	4.1	6
Ryu et al., 1999	S3H5/g2bA2 murine hybridoma	IgG2b MAb	Not reported	122	3.9	13
Zhou et al., 1995	MAK	IgG MAb	0.83 mM (SP:0.55)	58	13.6	9
Wang et al., 1995	BHK	t-PA	5.6 mM	15	1.2	8

1.3.3 Classification of feeding protocols

Feeding protocols can be classified according to: (1) the mode of addition, (2) the nutrient target concentrations (glucose is the nutrient most commonly reported), or (3) the method of determining the feeding profile.

Table 1.2.   Types of feeding protocols.

According to the mode of addition

    Discontinuous (or pulsed)
        Constant volume additions
        Variable volume additions (pre-specified or adaptive)
    Continuous
        Constant flow (pre-specified)
        Variable flow (pre-specified or adaptive)

Based on nutrient levels during cultivation

    High (e.g., glucose >10 mM)
    Low (e.g., glucose 1 – 10 mM)
    Limitation (e.g., glucose 0.5 – 1.0 mM)
    Starvation (glucose-limited to the extent that cell growth rate decreases)

According to the method of determining the feeding profile

    Pre-specified feeding
        Based on pre-specified volume to add
    Adaptive feeding
        Based on pre-specified target concentrations
        Based on off-line estimation of nutrient consumption
        Based on indirect on-line estimation of nutrient consumption
        Based on on-line monitoring of nutrient consumption

Table 1.3.   Comparison of feeding protocols.

Type of Feeding Protocol	Examples	Mode of Addition of Feeding Medium	Type of Control	Minimal Automation Requirements	Required Previous Knowledge of Cell Metabolism	Operation Requirements
Based on on-line monitoring of nutrient consumption	On-line HPLC (Kurokawa 1994)	Continuous, adaptive	On-line feedback	Automated sampling device Automated on-line analyzer Communication protocol between analyzer and system control Standard requirements for feedback control	No particular knowledge	General equipment supervision (system fully automated)
Based on indirect on-line estimation of nutrient consumption	OUR-based (Zhou 1995)	Continuous, adaptive	On-line feedback	Standard requirements for feedback control	Yield coefficient between OUR and nutrient consumption rate(s)	General equipment supervision. Feed flow adjustment according to OUR (if not automated)
Based on off-line estimation of nutrient consumption	Off-line GUR-based (Frahm 2003, Zhou 1997, Xie 1996)	Continuous or pulsed	Off-line feedback, predictive	None	Determination of a strategy for prediction of GUR over the next sampling period	General equipment supervision Manual sampling – nutrient levels Calculation of GUR prediction Addition of volume or feed flow adjustment
Based on pre-specified target concentrations	Addition of feed medium upon sampling for nutrient levels (Sauer 2000)	Pulsed	Off-line feedback, non-predictive	None	Definition of specifications for target concentrations and feeding frequency	General equipment supervision Manual sampling – nutrient levels Calculation of volume to add Addition of calculated volume
Based on pre-specified volume to add	Addition of specified volume of feed medium (Bibila 1994)	Continuous or pulsed	No control	None	Definition of specifications for volume to add and feeding frequency	General equipment supervision Addition of specified volume

The potential advantages and inconveniences of various degrees of complexity in feeding protocols are compared in Figure 1.2. Dark shading indicates situations generally considered undesirable, whereas the light shading indicates desirable attributes of these protocols.

Feeding Protocol	Cost of Implementation	Control Algorithm	Variability of Key Parameters	Manual Interventions
Based on on-line monitoring of nutrient consumption	High	Complex	Low	Minimal
Based on indirect on-line estimation of nutrient consumption				
Based on off-line estimation of nutrient consumption				
Based on pre-specified target concentrations				
Based on pre-specified volume to add	Low	Simple	High	Maximal

Figure 1.2.   Advantages and limitations of various feeding protocols.

This analysis indicates that a feeding protocol somehow involves a compromise between desirable and undesirable conditions. Most reports from industrial sources indicate a clear preference for simple processes, even though they may result in greater variability of key parameters and require more manual interventions.

1.3.4   Analysis of some examples of published feeding protocols

In the feeding protocol presented by Zhou et al., 1995, nutrient consumption is estimated on-line through oxygen uptake rate (OUR), which serves as a basis for the definition of the feeding pattern, converting OUR to glucose required.

Another approach is the predictive estimation of nutrient consumption over the period between sampling. Such protocols are represented by Zhou et al., 1997, and Xie and Wang, 1996. The predictive estimation of nutrient consumption in order to meet the metabolic requirements can be simplified or calculated through more complicated means such as metabolic models.

7

A simpler approach, proposed by Sauer et al., 2000, determines the feeding profile by a target concentration. Glucose is measured at specific intervals and the volume required to reach the target is calculated.

The simplest approach, described by Bibila et al., 1994, uses pre-defined volumes of nutrient concentrates (feed medium) for culture supplementation at pre-specified times.

Table 1.4.   Description of examples of feeding protocols

Type	Feeding Protocol	Reference
Indirect online estimation of nutrient consumption	$$F_{t_i} = \frac{\int_{t_i}^{t_{i+1}} OUR \cdot V \ dt}{\alpha_i \ C_f \ (t_{i+1} - t_i)}$$ $$\alpha_i = \frac{\int_{t_{i-1}}^{t_i} OUR \cdot V \ dt}{GC_{t_i} \cdot V_{t_i} - GC_{t_{i-1}} \cdot V_{t_{i-1}}}$$ $$GC_{t_i} \cdot V_{t_i} = GC_{t_{i-1}} \cdot V_{t_{i-1}} + C_f \int_{t_i}^{t_{i+1}} F \ dt + C_{t_i} \cdot V_{t_i} - C_{t_{i-1}} \cdot V_{t_{i-1}}$$	Zhou et al., 1995
Off-line predictive estimation of nutrient consumption	$$V_i = \frac{q_i \left[(X_v)_{n+1} + (X_v)_n \right](t_{n+1} - t_n) V_c}{2C_i}$$	Zhou et al., 1997
Off-line predictive estimation of nutrient consumption	$$V_R = \frac{\beta \ \Delta N_t}{C_t}$$ $$\Delta N_t = N_t - V_0 \ X_{t,0}$$ $$N_t = N_t^n + \frac{\mu \ N_{v,n}}{\mu - \alpha} \left[e^{(\mu - \alpha)(t - t_n)} - 1 \right]$$	Xie and Wang, 1996
Pre-specified target concentrations	$$V_{feed} = \left(\frac{glc_{tar} - glc}{glc_{feed} - glc_{tar}} \right) \cdot V$$	Sauer et al., 2000
Pre-specified volumes to add	*10X medium concentrates* *1L vol eq = 100 mL 10X medium + 60 mL suplements* *Optimum = 3 vol eq* *Starting at 1x10⁶ c/mL, following at 48 h intervals*	Bibila et al., 1994

1.4 Physiological indicators to guide process development

Process performance can be described as a double objective function encompassing high product yield and acceptable quality. In the case of cell culture processes, the yield component of performance can be further divided in a double objective of cell proliferation and productivity. However, processes face perturbations or stresses that may decrease their performance or even cause it to fail. Resilience to disturbances with no loss of performance is process robustness (Stelling et al., 2004). Robust process performance (Figure 1.3) is the goal of process optimization. Robust processes are able to meet both economic and regulatory requirements.

Understanding cellular stress can provide a guiding rationale to developing robust bioprocesses. Lack of nutrients can be a stress encountered during fed-batch cultivations, particularly at high cell concentrations under periodic discontinuous feeding. Two major physiologic responses can arise in such conditions, namely apoptosis and autophagy. Apoptosis is a well-studied mechanism that leads to cell demise (Betenbaugh and Arden, 2004). Autophagy is another known response to metabolic stress (Ferraro and Cecconi, 2007); however it has been given so far little attention in literature related to bioprocess development.
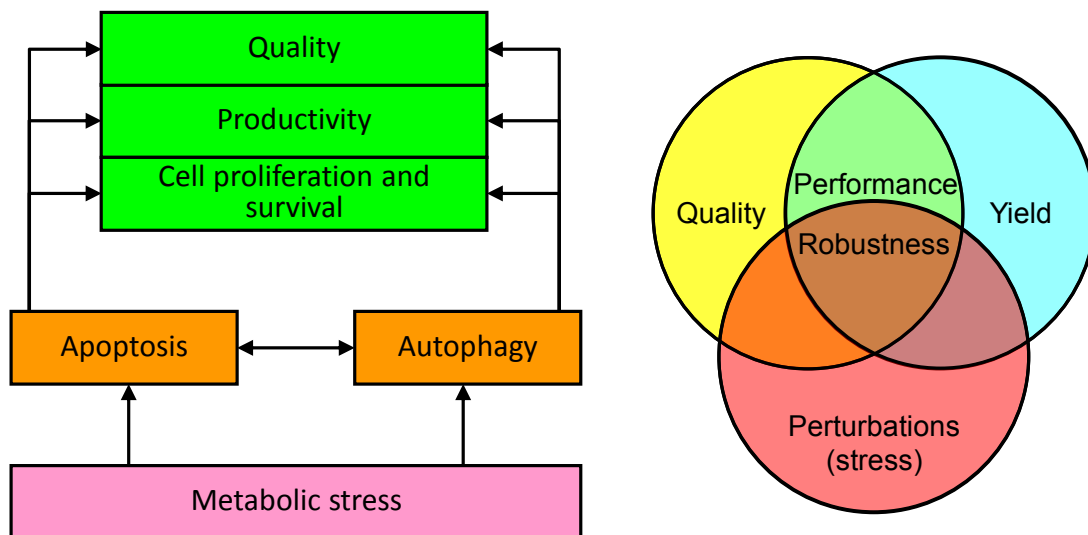
Figure 1.3.   Process performance and biologic stress

In spite of their high product value, fed-batch processes are often developed empirically, using trial-and-error methodologies. Considering the cell physiology and sources of cellular stress can contribute to the rational design of robust bioprocesses. Such an approach for process development is fully compatible with new regulatory initiatives, such as Process Analytical Technology (PAT). PAT is defined as a ''system for designing, analyzing, and controlling manufacturing through timely measurements (i.e., during processing) of critical quality and performance attributes of raw and in-process materials and processes with the goal of ensuring final product quality'' (FDA Guidance for Industry, 2004). Timely identification of the cellular responses involved in product performance (yield and quality) can provide effective means of monitoring the process to maximize its robustness.

1.4.1 Apoptosis

Apoptosis is a physiological process that actively effects cell death, with distinct morphological and biochemical features. Morphologically, it is characterized by condensation of cytoplasm, cell shrinkage, separation from neighbouring cells, condensation of chromatin (pyknosis), nuclear fragmentation (karyorrhexis), blebbing and formation of apoptotic bodies, along with preservation of cellular membranes and organelles (Bouchier-Hayes et al., 2008). These morphological features reflect biochemical events caused primarily by the activation of a family of intracellular proteases known as caspases (cysteine-dependent aspartate-specific proteases). Caspase cleavage inactivates a wide assortment of proteins involved in cell adhesion (catenins, cadherins), cytoskeletal structure (actin, fodrin, tubulin, vimentin), nuclear structure (lamin, nucleoporins), cell cycle (cyclin, MDM2), DNA synthesis and repair (PARP-1), survival signals (ICAD, NF-κB, NRF2, HSF, AKT, Bcl-2, Bcl-x$_L$), RNA synthesis and splicing, protein translation and other vital cellular functions (Fischer et al., 2003). Catalytic cleavage by caspases, on the other hand, activates a number of death-promoting (acinus, gelsolin) and inflammation-related proteins (interleukin precursors). Execution of apoptosis also involves the activation of endonucleases by caspase-dependent (CAD) or independent mechanisms, such as AIF or EndoG (Fischer et al., 2003). Another biochemical feature of apoptosis is given by changes that occur on the plasma membrane, namely permeability changes to specific stains and translocation of phosphatidyl-

serine (PS) from the inner to the outer cell membrane leaflet. This redistribution of PS serves as a recognition signal of apoptotic cells by phagocytes. An additional trait of apoptosis is the dissipation of the mitochondrial transmembrane potential ($\Delta\Psi$m), the electrochemical potential across the internal mitochondrial membrane caused by the proton export from the mitochondrial matrix during the electron transport chain (ETC). $\Delta\Psi$m is the driving force for ATP production by mitochondria and its loss is due to the opening of a high-conductance channel called permeability transition pore (PTP). It is still controversial whether loss of $\Delta\Psi$m causes apoptosis, contributes to it or is simply an end result.

Apoptosis can be caused by multiple stimuli involved in developmental cues, stress or infection: growth factor withdrawal, glucocorticoids, drugs, UV radiation, DNA damage, nutrient depletion, anoxia, reactive oxygen species (ROS) production. Apoptosis can be divided into two major signaling pathways: intrinsic or extrinsic.

The intrinsic (or mitochondrial) pathway is mediated by the action of proteins Bax (Bcl-2-associated X protein) or Bak (Bcl-2 antagonist/killer). These pro-apoptotic proteins oligomerize and form a pore on the mitochondrial outer membrane that enables the release of proteins resident in the mitochondrial intermembrane space (Cytochrome c, AIF, EndoG, Smac). This event is termed mitochondrial outer membrane permeabilization (MOMP). Activity of Bax/Bak is counteracted by two anti-apoptotic proteins Bcl-2 and Bcl-xL. Once Cytochrome c is released, it interacts with Apaf-1 (Apoptotic protease activating factor 1) and forms an oligomer called apoptosome which recruits and activates procaspase-9, whose function is to activate executioner caspases 3 and 7, responsible for the apoptotic hallmarks (Green and Reed, 1998).

The extrinsic pathway is induced when death ligands bind to death receptors. Examples of ligands and their respective receptors are: tumour necrosis factor (TNF) and TNFR1, Fas ligand (FasL) and Fas (also named APO1 and CD95). The extrinsic pathway can directly mediate mitochondria- and caspase-independent apoptosis by induction of the JNK (c-Jun N-terminal Kinases) pathway or activate Caspase 8, which cleaves the protein Bid. Truncated Bid (tBid) induces MOMP and recruits the downstream effects of mitochondrial permeabilization. Active caspase 8 can also directly activate executioner caspases 3 and 7 (Chipuk and Green, 2006).

The most common methods to measure apoptosis at the single-cell level include the visualization of Cytochrome c release (by immunostaining or by stable expression of the fusion protein Cytochrome c-GFP), loss of $\Delta\Psi$m (by fluorescent cationic lipophilic dyes), translocation of Bcl-2 family proteins, caspase activation, PS translocation (by staining with PS-reactive Annexin V) and cell membrane selective permeability to apoptosis-specific stains. Such methods have enabled the detailed characterization of the kinetics of apoptosis events. Other population-based methods are also commonly used, such as western blots of processed or translocated proteins, such as PARP1 cleavage, cytosolic fraction of Cytochrome c, active caspases, etc (Bouchier-Hayes et al., 2008).

1.4.2 Autophagy

Autophagy is a degradative process present in all eukaryotes by which intracellular components are delivered to lysosomes for breakdown and reuse. Unlike apoptosis, which merely leads to cell death, autophagy can participate in both cell survival and cell death in response to various stresses.

Three types of autophagy have been described: macroautophagy, microautophagy and chaperone-mediated autophagy (Cuervo, 2004; Klionsky et al., 2007; Mizushima, 2007). **Macroautophagy** is the most prevalent form of autophagy (Figure 1.4). Once induced, it begins with the formation of a double- or multi-membrane vesicle (called phagophore) which sequesters cytoplasm, organelles, protein aggregates and/or invading pathogens. The phagophore expands and eventually closes to form the autophagosome, which then fuses with the lysosome thus forming the autolysosome, where its contents are degraded by hydrolases and recycled back into the cytoplasm through permeases. The fusion of the autophagosome with the lysosome may be preceded by its fusion with a late endosome, in which case, the resulting hybrid acidic organelle is called an amphisome. Macroautophagy is generally considered a non-specific degradative process (Klionsky, 2007; Cao and Klionsky, 2007; Ferraro and Cecconi, 2007), but a growing body of literature indicates that it can also be observed for specific targets. **Microautophagy** is characterised by the formation of invaginations in the lysosomal membrane which are then pinched off and degraded intralysosomally along with their contents of cytoplasm (Klionsky et al., 2007). **Chaperone-mediated autophagy** involves the transport of unfolded proteins directly across the

lysosomal membrane (Mizushima and Klionsky, 2007). Conventionally, the term autophagy is used to refer to macroautophagy (Ferraro and Cecconi, 2007; Mizushima, 2007). Following this convention, the term autophagy will be used in this document to refer to macroautophagy, unless otherwise noted.
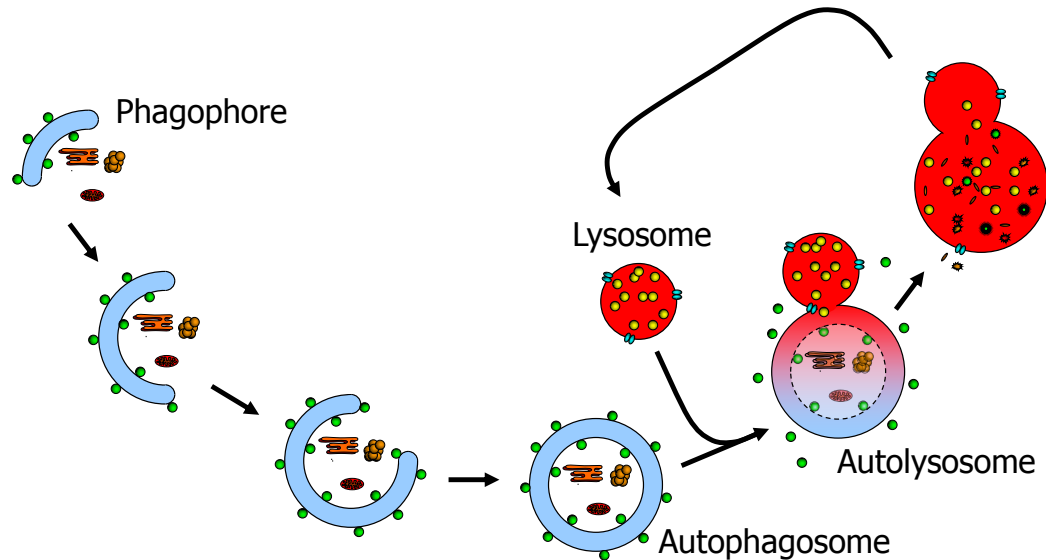
Figure 1.4.   **Representation of the autophagic process.**

About 40 genes that participate in autophagy have been identified. By convention most of these genes are referred to according to the unified ATG gene nomenclature (Klionsky et al., 2003).

Basal autophagic activity is observed in cells at low, constitutive levels, with homeostatic functions for the turnover of macromolecules and organelles. It is the main mechanism for the turnover of long-lived proteins (Meijer and Codogno, 2004). However, it can be upregulated by various stress signals, such as nutrient starvation (mainly carbon sources in yeast and amino acids in higher eukaryotes), growth factor depletion, metabolic hormone stimulation (e.g., glucagon), pathogen invasion (Cao and Klionsky, 2007), unfolded protein accumulation or oxidative stress (Meijer and Codogno, 2004). It has been shown that mitochondria with decreased transmembrane potential and producing reactive oxygen species are particularly sensitive to autophagic sequestration (Meijer and Codogno, 2004). Autophagy is also observed in the clearance of superfluous organelles upon differentiation, e.g. during erythroid maturation (Meijer and Codogno, 2004).

13

Therefore, the physiological role of autophagy can be summarized in three categories: (1) cell remodeling during development and differentiation; (2) production of amino acids upon nutrient shortage; and (3) elimination of unnecessary or damaged molecules and organelles (Meijer and Codogno, 2004).

Naturally, autophagy also plays a role in pathophysiology if its normal function is somehow disrupted. Numerous examples are found in literature, including tumor progression, neurodegenerative diseases and myopathies (Cuervo, 2004; Meijer and Codogno, 2004; Kundu and Thompson, 2008; Rubinsztein, 2006).

The autophagic process can be divided in the following phases or steps, each related to characteristic molecular events:

Induction: In most cellular settings, induction of autophagy takes place when the serine/threonine kinase mTOR (mammalian target of rapamycin) is inhibited which in its turn stimulates the catalytic activity of the ULK1/2 kinases (the yeast orthologue is known as Atg1). Some cases of mTOR-independent induction of autophagy have been reported, in the presence of reactive oxygen species, ceramide, tumor necrosis factor, ER stress, AMPK activation, NFκB (Maiuri et al., 2007; Kroemer et al., 2010).

Nucleation: After induction, the initial steps of vesicle nucleation include the activation of mammalian Vps34, a class III phosphatidylinositol 3‑kinase (PI3K), also known as PIK3C3. PIK3C3 activation depends on the formation of a multiprotein complex composed by Beclin-1 (Becn1, mammalian orthologue of Atg6), Atg14L, p150 (a myristylated kinase, also named Vps15 in yeast) and Ambra1 (Maiuri et al., 2007; Yang and Klionsky, 2010).

Vesicle elongation: Two conjugation systems involving ubiquitin-like proteins are part of the process of sequestering vesicle elongation. Both systems involve Atg7, a homologue of the ubiquitin activating enzyme (E1-like enzyme) and another conjugating protein, either Atg10 or Atg3 (E2-like enzymes). In the first system, Atg12 is conjugated to Atg5, with the help of Atg7 and Atg10. The complex Atg12-Atg5 then binds to Atg16, which multimerizes into a large complex. The second conjugation system involves the modification of MAP1-LC3 (microtubule associated protein 1 light chain 3, referred to normally as LC3, the mammalian homologue of Atg8 in yeast) by Atg4, followed by its conjugation with phosphatidyl ethanolamine (PE) by Atg7 and Atg3. Once LC3 becomes lipidated, it remains

anchored to the membrane of the autophagic vesicle and is named LC3-II, as opposed to its soluble form LC3-I (Maiuri et al., 2007).

Fusion, breakdown and efflux: Fusion of amphisomes and autophagosomes with lysosomes to form autolysosomes is mediated by various proteins, among which LAMP2 (Lysosomal-associated membrane protein 2) seems to be essential for fusion. These proteins participate in tethering the two organelles and their fusion (Luzio et al., 2007). In the autolysosomes, the inner autophagosomal membrane as well as the luminal content of the autophagic vacuoles is degraded by lysosomal enzymes (Maiuri et al., 2007).

There is consensus (Klionsky et al., 2008; Mizushima et al., 2010) about the importance of two phenomena to be considered while monitoring autophagy: autophagic induction (generation of autophagic compartments) and autophagic flux (degradation of such compartments), which have opposite effects on autophagosome levels and can be independently modulated according to the treatment. The proper interpretation of the various assays available for the monitoring of this process therefore requires the consideration of both phenomena. A great variety of analytical techniques have been applied to the study of autophagy. Since all of them have some limitation and provide a partial representation, it is generally recommended to use various techniques in combination for the study of autophagy. The most commonly used techniques are presented below, along with some cautionary notes on their use.

Electron microscopy: Sequestered areas of cytoplasm in various degrees of degradation within a double membrane structure are used to identify and quantify autophagic compartments. This technique can be prone to misinterpretation, due mainly to the potential for sampling artifacts (Klionsky et al., 2008).

Atg8/LC3 western blotting: As discussed earlier, LC3-II is a protein marker reliably associated with autophagic compartments. LC3 conversion (from LC3-I to LC3-II) can be detected by immunoblot and is correlated with the amount of autophagosomes. However the adequate use of this assay to study autophagy requires taking in account various considerations. First, LC3-II is degraded upon fusion with the lysosome. Second, the levels of LC3-II are indicative of autophagosomes, but not of autophagic flux. Third, LC3-II is more sensitive to detection than LC3-I and therefore a comparison of the two forms of the

protein, or a summation for ratio determinations may not be appropriate (Klionsky et al., 2008; Mizushima and Yoshimori, 2007).

GFP-LC3 and fluorescence microscopy: GFP–LC3 fusion protein has been widely used to monitor autophagy since its lipidation and association to autophagic organelles produces a shift in its fluorescence from diffuse to punctate. Detection of this fusion protein has been used in numerous *in vivo* studies and to monitor co-localization with targets (such as organelle degradation or pathogen sequestration). Besides the difficulty of quantifying the number of GFP-LC3 puncta, the main limitation of this technique resides in the fact that this fusion protein can associate with aggregates, particularly if expressed at high levels and therefore, GFP-LC3 puncta may represent a mix of protein aggregates in the cytoplasm, protein aggregates within autophagosomes and autophagic membrane-bound lipidated protein (Klionsky et al., 2007; Klionsky et al., 2008).

Acidotropic dyes and fluorescence microscopy: A very common method to monitor autophagy involves staining with acidotropic dyes, such as mondansylcadaverine (MDC), acridine orange (AO), and LysoSensor or LysoTracker stains. While MDC is able to stain autophagosomes, it also stains late endosomes, amphisomes and lysosomes. In the case of AO and the LysoTracker probes, they detect primarily lysosomes, but since they accumulate in acidic organelles, they also stain late endosomes and amphisomes. Despite their lack of specificity, these stains are commonly used to produce correlative data, but they must be used in combination with other techniques in order to provide convincing evidence of autophagic activity (Klionsky et al., 2008).

1.4.3   Interplay between apoptosis and autophagy

Since apoptosis and autophagy are both stress responses, various aspects of cellular physiology can influence both of them. A great variety of situations has been reported where autophagy has a survival role and apoptosis the opposite, both responses being mutually exclusive. However, other scenarios have also been observed where autophagy contributes concomitantly to cell demise. The interplay between these two responses may be dependent on the cell line and/or the treatment used. A key regulatory role in both apoptosis and autophagy is played by the anti-apoptotic proteins Bcl-2 and Bcl-X_L, which can also interact with Beclin-1, thereby inhibiting autophagy (Cao and Klionsky, 2007; Levine et al., 2008).

Three major interrelated aspects of cell physiology can affect both apoptosis and autophagy, namely mitochondrial physiology, metabolism and redox homeostasis, as described below.

1.4.3.1 Mitochondrial physiology

Mitochondria play a central role in the intrinsic pathway of apoptosis through the release of Cytochrome c and other pro-apoptotic proteins from the mitochondrial intermembrane space. Mitochondria that undergo PTP opening and loss of $\Delta\Psi m$ can be selectively removed by autophagy, a process called mitophagy (Kundu and Thompson, 2005; Rodriguez-Enriquez et al., 2004; Kim et al., 2007). The autophagy proteins Ulk1 (Kundu et al., 2008) and Atg4 (Scherz-Shouval et al., 2007) play a critical role in mitophagy. Successful removal of the damaged organelles followed by repair and adaptation allow for survival, while failure to restore homeostasis can result in apoptosis.

Calcium transfer from the endoplasmic reticulum to mitochondria is required to support oxidative phosphorylation and ATP production. The absence of this transfer can induce energy stress and activation of pro-survival autophagy (Cardenas et al., 2010).

1.4.3.2 Metabolism

Lack of specific nutrients is known to induce both apoptosis and autophagy. However, a wide variety of interactions has been reported, that ranges from both processes inducing cell death to cases where they have opposite functions. In the context of cell survival, autophagy is the default pathway induced upon nutrient deprivation, which enables cells to restore ATP levels to an extent that apoptosis can be prevented (Maiuri et al., 2007).

Of particular interest is the mitochondrial glutamine metabolism, since it plays a major role in the proliferation of mammalian cells. Glutamine is used in proliferating cells as a means to supply TCA cycle intermediates, particularly citrate and malate, which are exported from the mitochondrial matrix and consumed for the *de novo* production of lipids and to provide reducing power for lipid and DNA synthesis (DeBerardinis et al., 2008). So far, glucose metabolism has received more attention regarding its effect on the TCA cycle and lactate production. Consideration of glutamine mitochondrial metabolism can provide useful insights on the interplay between apoptosis and autophagy (Yuneva et al., 2007).

Another interesting interaction between metabolism and apoptosis is the function of p53, a transcription factor able to induce apoptosis when activated. The protein TIGAR (p53-induced glycolysis and apoptosis regulator), a target of p53, modulates glucose metabolism at a key node, inhibiting phosphofructokinase-1 (PFK-1) activity, which diverts glucose metabolism from glycolysis into the phosphate pentose pathway, enabling cells to survive by maintaining a reduced pool of NADPH and glutathione (Bensaad et al., 2006). Cytoplasmic p53 exerts an inhibitory function toward autophagy, in contrast to nuclear p53, which has the opposite function (Tasdemir et al., 2008).

1.4.3.3 Redox homeostasis

Reactive oxygen species (ROS) are generated in several physiological processes by the reduction of molecular oxygen. The most common ROS are hydrogen peroxide (H_2O_2), the superoxide anion ($O_2^{\bullet -}$), the hydroxyl ($^{\bullet}OH$) and peroxyl ($ROO^{\bullet}$) radicals (Jaiswal McEligot et al., 2005; Trachootham et al., 2008; Valko et al., 2007). Most of the ROS are generated in mitochondria and peroxisomes. ROS are extremely reactive and when present at high concentrations cause oxidative damage to DNA, lipids and proteins. Generation of high levels of ROS is also called oxidative stress.

Cells possess various mechanisms against oxidative stress, including enzymatic and non-enzymatic antioxidants. Some important enzymatic antioxidants include superoxide dismutase (SOD), glutathione peroxidase (GPx), catalase (CAT) and the thioredoxin (TRX)/thioredoxin reductase (TR) couple. The major non-enzymatic redox couple is the tripeptide glutathione (GSH), which dimerizes when oxidized (GSSG). The GSH/GSSG couple is one of the major reductants in eukaryotic cells and is maintained at high cell concentrations (1-10 mM). Other non-enzymatic redox species include ascorbic acid (Vitamin C), α-tocopherol (Vitamin E), carotenoids and flavonoids (Jaiswal McEligot et al., 2005; Valko et al., 2007). The two most abundant redox couples (GSH/GSSG and TR/TRX) require transfer of electrons from NADPH for their regeneration.

The redox state of a cell needs to be kept within a narrow range and is the result of the balance between the rates of ROS production and removal by antioxidants. Two major means for cells to generate reducing power in the form of NADPH are (1) the pentose-phosphate pathway (particularly through glucose-6-phosphate-dehydrogenase, G6PDH) and (2) the

malic enzyme (ME), a NADP-dependent dehydrogenase that can produce high levels of NADPH in actively proliferating cells (DeBerardinis et al., 2008).

Generally, a reducing intracellular environment promotes proliferation. Mild shift toward oxidizing conditions induces a series of signaling events and has been observed to cause cell differentiation. An even more oxidizing environment (caused, for example by the depletion of the reduced glutathione pool) can induce MOMP-dependent apoptosis. However, after Cytochrome c is released in the cytoplasm, only its oxidized form is able to initiate apoptosis. On the other hand, if the intracellular environment is too oxidizing, caspases become inactivated and cells may die instead by necrosis (Vaughn and Deshmukh, 2008).

With regard to autophagy, generation of ROS from mitochondria inhibits the proteolytic activity of Atg4, thereby favoring the formation of autophagosomes around mitochondria (Scherz-Shouval et al., 2007). ROS generation seems to be a signaling for mitochondrial removal by autophagy.

1.5   Research goals

CHO cells are commonly used for the production of valuable biopharmaceuticals. The cost of producing these recombinant proteins is becoming increasingly important due to many factors, including the more widespread generic manufacturing. An improved understanding of the physiological influences on cell proliferation, survival, productivity and product quality – process performance – can thus have a great impact on the global access of healthcare systems to modern biotechnology therapeutics.

The overall goal of this project was **to explore the physiology of CHO cells with the purpose of generating a methodology applicable to the development of high-performance fed-batch processes**. The underlying hypothesis was that a deeper understanding of the physiological factors affecting the ability of mammalian cells to produce glycosylated recombinant proteins would lead to methods to improve the design of high-performance fed-batch processes. Autophagy became the main physiological factor that was investigated, partly out of an interest to explore a novel cellular process that has been little studied in bioprocess-related research. Yet, the main reason for focusing on autophagy was driven by the remarkable discovery that its modulation was able to influence process performance in substantial ways. It also became clear that the metabolic stress imposed by fed-batch processing was a potent physiological trigger of this cellular process. The main goal of this research was divided into specific objectives, each covered in an individual chapter of the present dissertation.

The first specific objective, covered in Chapter 2, was to establish the significance of autophagy in fed-batch process performance and **to demonstrate that inhibition of glutamine-dependent autophagy increases t-PA production in CHO cell fed-batch processes**. In order to accomplish this objective, first, the changes in the lysosomal compartment of cultures were evaluated and compared to changes in productivity, as a preliminary assessment of the presence of autophagy in fed-batch processes. Secondly, more definitive evidence of autophagy in this system was obtained. Then, the effects of chemical inhibition of autophagy on cell proliferation, viability, protein production and glycosylation were evaluated.

The second specific objective of this research, developed in Chapter 3, was **to compare glutamine metabolism and autophagy in three CHO cell lines**. The work in this chapter expanded the analysis of Chapter 2, including two other CHO cell lines producing different recombinant antibody proteins. This objective was achieved by evaluating first the effect of glutamine deprivation on factors that directly affect process performance (cell proliferation, viability and protein production). Secondly, the effect of glutamine deprivation on other physiological factors (energy metabolism, mitochondrial and lysosomal abundance) was also determined. Lastly, the sensitivity of the three cell lines to induction of autophagy by glutamine deprivation was compared.

The third specific objective of this project, presented in Chapter 4, was **to combine autophagy inhibition and glutamine metabolism-based process strategies to increase fed-batch performance**. This objective involved first the evaluation of potential substitutes for glutamine to increase cell proliferation and protein production by using a scale-down system in short-term cultivations. The next step was to test the combined effect of enhanced proliferation (achieved through modulation of glutamine metabolism) and inhibition of autophagy (by treatment with 3-MA) in fed-batch cultivations. The third part of this objective was to evaluate potential alternatives to the use of 3-MA for the inhibition of autophagy.

Finally, Chapter 5 provides the fourth specific objective of this work, which was **to explore autophagy and glutamine metabolism in cancer cell lines**. Raman spectroscopy (RS) was used to probe the response of cancer cells to glutamine deprivation. First, the effect of glutamine deprivation on autophagy reporters was quantified in two different cancer cell lines. Then, RS was used to measure the changes produced by glutamine deprivation on cells. Thirdly, this technology was used to analyze in live cells the recovery process from glutamine deprivation. Finally, the potential of RS to probe cell populations for heterogeneity in the response to starvation stimuli was evaluated.

This research project ventured in unexplored areas of research at the crossroads between engineering and biology, generating original results and opening new perspectives. The work described in this dissertation produced the first report showing that inhibition of autophagy could result in as much as a 2.8-fold increase of a secreted recombinant protein, without compromising the protein glycosylation. This could be considered the most significant contribution of this investigation. Further analysis revealed the importance of glutamine

metabolism and its interplay with autophagy in process performance. The process strategy resulting from the integration of autophagy and glutamine metabolism resulted in an additional yield enhancement, to a maximum 4.6-fold increase compared to the initial conditions. Finally, interactions between autophagy and glutamine metabolism were explored in cancer cell lines, and produced original findings on the potential of Raman spectroscopy to probe the cellular response to cell starvation.

Overall, this study illustrates the potential of fruitful interplay between basic scientific research and applied biotechnology. The investigation of response mechanisms to cellular stress provided opportunities to both improve industrial processing and open new perspectives for basic biological research aiming to elucidate the mechanism by which autophagy inhibition results in increased recombinant protein secretion.

2 Inhibition of glutamine-dependent autophagy increases t-PA production in CHO cell fed-batch processes [1]

Understanding the cellular responses caused by metabolic stress is crucial for the design of robust fed-batch bioprocesses that maximize the expression of recombinant proteins. Chinese hamster ovary (CHO) cells were investigated in chemically defined, serum-free cultures yielding 10^7 cells/mL and up to 500 mg/L recombinant tissue plasminogen activator (t-PA). Upon glutamine depletion increased autophagosome formation and autophagic flux were observed, along with decreased proliferation and high viability. Higher lysosomal levels correlated with decreased productivity. Chemical inhibition of autophagy with 3-methyl adenine (3-MA) increased the t-PA yield by 2.8-fold. Autophagy-related MAP1LC3 and LAMP2 mRNA levels increased continuously in all cultures. Analysis of protein quality revealed that 3-MA treatment did not alter glycan antennarity while increasing fucosylation, galactosylation and sialylation. Taken together, these findings indicate that inhibition of autophagy can considerably increase the yield of biotechnology fed-batch processes, without compromising the glycosylation capacity of cells. Monitoring or genetic engineering of autophagy provides novel avenues to improve the performance of cell culture-based recombinant protein production.

2.1 Introduction

To manufacture the ever-increasing number of valuable recombinant therapeutic proteins, high performance mammalian cell fed-batch processes have been developed (Wurm, 2004; Aggarwal, 2010). However, operating a process at or close to its performance limits increases the risks of failure, especially given the inevitable variability of biological processes. The ideal high-performance upstream process should successfully optimize cell proliferation, productivity and product quality within a well-characterized design space.

Process development should be consistent with the FDA Process Analytical Technology and Quality by Design initiatives, and meet their emphasis on process monitoring and understanding.

Discerning the sources and effects of cellular stresses can therefore provide valuable guidance for robust bioprocess design. Metabolic stress caused by nutrient limitation is a common perturbation in fed-batch cultivations given the widespread use of periodic feeding, particularly during the later stages when cell concentrations are high. Two major physiologic responses that can arise in such conditions are apoptosis and autophagy. Whereas apoptosis is a well-studied cell death response to nutrient limitations in bioprocesses and has been manipulated to increase product yields (Dorai et al., 2009, Durocher and Butler, 2009), much less investigation has focused on autophagy. Besides a few reports in batch cultures (Meneses-Acosta et al., 2001; Hwang and Lee, 2008; Kim et al. 2009) the activation of autophagy has recently been reported in fed-batch (Han et al., 2011). In that study inhibition of autophagy by Bafilomycin A1 did not significantly increase production. In order to understand how best to modulate this pathway to improve process performance further investigation is required.

Autophagy is a highly dynamic process by which intracellular material is sequestered in double-membrane vesicles called autophagosomes. Once these vesicles are closed, they fuse with lysosomes and their contents are degraded. Unlike other proteins involved in this process, microtubule-associated protein 1 light chain 3 (MAP1LC3 or simply LC3) is associated with both nascent and mature autophagosomes, making LC3 a useful marker of these organelles. Once synthesized, pro-LC3 is cleaved at its C-terminus, becoming LC3-I. Upon autophagosome formation, soluble cytoplasmic LC3-I is lipidated to become LC3-II and associates with both the inner and outer membranes of autophagosomes (Mizushima et al., 2010). In this work LC3 processing was monitored by immunoblotting and by fluorescence microscopy using expression of LC3 tagged at its N terminus with the fluorescent GFP. GFP-LC3 was then visualized as a diffuse cytoplasmic pool (corresponding to LC3-I) or in autophagosome-bound punctate structures (corresponding to LC3-II) (Mizushima et al., 2010, Klionsky et al., 2008).

In contrast to the apoptosis cell death pathways, autophagy has a wide range of physiological roles, mainly related to cell survival (Mizushima et al., 2008, Kundu and

Thompson, 2008). For example, basal autophagic activity is observed at constitutive levels in cells, with homeostatic functions for macromolecule and organelle turnover (Meijer and Codogno, 2004; Mathew et al., 2007; Kundu and Thompson, 2008). Under stresses such as nutrient starvation, autophagy enables cells to survive by delivering macromolecules to lysosomal hydrolases for reuse of their components (Mizushima and Klionsky, 2007). Another survival function is to remove damaged organelles, such as permeabilized or depolarized mitochondria, which could otherwise cause apoptosis (Kim et al., 2007). Although autophagy has been associated with type II programmed cell death, loss of viability may result when the survival functions of autophagy are unsuccessful (Boya et al., 2005), or when autophagy is excessively or ectopically activated (Kourtis and Tavernarakis, 2009; Kroemer and Levine, 2008).

In the present study, based on cell physiological changes in fed-batch cultures producing t-PA, we investigated the cellular autophagic response, with particular attention to glutamine metabolism. In order to meet this objective, the effects of glutamine deprivation on viability, proliferation, lysosomal content and cell productivity were analyzed. The induction of autophagic flux by glutamine limitation was further confirmed. The effect of 3-methyl adenine-mediated autophagy inhibition on t-PA production was also investigated. The impact of this inhibition on cell proliferation, viability, autophagy-related gene expression and t-PA glycosylation were also evaluated.

2.2   Materials and methods

2.2.1   Cell culture

Chinese hamster ovary (CHO) cells (Drouin et al., 2007) expressing human tissue-type plasminogen activator (t-PA) were cultured in shake flasks in a humidified incubator (Infors, Basel, Switzerland) at 37 ˚C, 5% CO_2 and 140 rpm. The cells were grown in chemically defined CD CHO medium, supplemented with 25 ng/mL IGF, 4X anti-clumping agent and 4 mM glutamine (Invitrogen, Grand Island, NY). Fed-batch cultures were supplemented daily with CHO CD Efficient Feed A (hereafter referred to as Feed A, Invitrogen) and additional mixtures of concentrated amino acids. Amino acid mixture 1 contained 10 mM L-cystine disodium salt hydrate (MP Biomedicals, Illkirch, France), 15 mM L-tyrosine disodium salt

(Sigma, St. Louis, MO) and 10 mM aspartic acid (Invitrogen) dissolved in 0.1 N HCl; mixture 2 contained 10 mM L-glutamic acid (Sigma) and 75 mM L-asparagine (Sigma) in 0.1 N NaOH; mixture 3 contained 10 mM L-Cystine (Sigma), 20 mM L-glutamic acid (Sigma), and 50 mM L-asparagine (Sigma) in 0.1 N HCl. The feeding protocols consisted of daily additions of pre-specified volumes of these solutions, expressed as a percentage of initial culture volume per day (*e.g.* 3.3% corresponds to the daily addition of 1 mL to a culture of initially 30 mL). After feeding, the pH was measured with a RapidLab 348 blood gas analyzer (Bayer, Leverkusen, Germany) and adjusted to 7.0 with a solution of 7.5% w/v NaHCO$_3$ (Invitrogen). Chemical inhibition of autophagy was done using 3-methyl adenine (3-MA, Sigma), from a 500 mM stock prepared in 0.5 N HCl; the final concentration in cultures treated with 3-MA was 10 mM.

2.2.2   Generation of autophagy reporter cell line

The phrGFP II-N expression vector (Stratagene, La Jolla, CA) was used to produce a hrGFP-tagged microtubule-associated protein 1-light chain 3B (MAP1-LC3B). EcoRI and BamHI restriction sites were added to the human MAP1-LC3β cDNA (NCBI accession: BC067797) for in-frame fusion to the C-terminus of hrGFP. The final construct was verified by sequencing. The t-PA producing cell line described above was transfected with the construct containing the GFP-LC3 sequence, using Lipofectamine 2000 in OptiMEM transfection medium (Invitrogen), according to the manufacturer's protocol. The transfected cells were sorted after 7 days of expansion and maintained under G418-free conditions for more than 3 months to demonstrate stable transfection.

2.2.3   Flow cytometry

Cell-permeable stains (Molecular Probes, Eugene, OR) were used to analyze selected physiological parameters by flow cytometry: LysoTracker Green DND-26 (LTG), to stain lysosomes and propidium iodide (PI), to identify dead cells. Samples were mixed with a solution of PBS, glucose and trypsin and incubated with 75 nM LTG for 15 min at 37˚C. Stained cells were pelleted, resuspended in PBS with 10 mM glucose and 0.5 μg/mL PI and placed on ice until analysis. Flow cytometry was performed in a FACScalibur (BD

Biosciences, Franklin Lakes, NJ) with 488 and 633 nm lasers. FlowJo (Tree Star, Ashland, OR) was used for data analysis.

2.2.4 Fluorescence microscopy

GFP-LC3-expressing cells were imaged in confocal mode directly after sampling to obtain resolution of autophagosomes. Fluorescence microscopy was performed on an IX81 motorized inverted microscope (Olympus Life Science, Hamburg, Germany) with filters for DAPI and GFP, using Z-increments of 0.5 μm. Image acquisition, deconvolution and projection was performed using Slidebook (Leeds Precision Instruments, Minneapolis, MN).

2.2.5 Western blotting of LC3 and autophagic flux assay

To monitor autophagy, Western blotting was performed to assess LC3 conversion from its cleaved cytosolic (LC3-I) form to its lipidated autophagosomal membrane-bound (LC3-II) form, indicative of autophagosome formation. After sampling, cells were washed in cold PBS and lysed with cold RIPA Lysis Solution (Santa Cruz Biotechnology, Santa Cruz, CA). Fifty μg of protein were loaded per lane in a NuPAGE Novex 12% Bis-Tris Gel (Invitrogen) and resolved at 200 V. Anti-LC3 antibody was rabbit polyclonal (PN ab48394, Abcam, Cambridge, MA), diluted 1:1000; anti-β-actin loading control antibody was mouse monoclonal (PN ab6276, Abcam), diluted 1:20000. The autophagic flux assay was performed by comparing the levels of LC3-II in control and glutamine-deprived cells in the presence and absence of chloroquine (Sigma; 2 hour treatment with 20 μM chloroquine). Blots were scanned with an Odyssey infrared imaging system (LI-COR Biosciences, Lincoln, NE).

2.2.6 Transmission Electron Microscopy (TEM)

Samples were high pressure frozen with a Leica HPM100 (Leica Microsystems, Wetzlar, Germany) using Type A aluminum planchettes and freeze-substituted firstly in tannic acid followed by osmium tetroxide and uranyl acetate. Samples were embedded in Spurr's resin. Ultra-thin sections were stained in uranyl acetate (12 min) and Sato's lead (6 min). TEM imaging used a Hitachi H7600 (Hitachi, Tokyo, Japan) operated at 80 kV.

2.2.7 Quantification of mRNA levels

Total DNA and RNA were extracted from cells using the AllPrep DNA/RNA Mini kit (Qiagen, Germantown, MD). Reverse transcription was done on total RNA samples using QuantiTect RT kit (Qiagen) and real-time quantitative RT-PCR using LightCycler 480 SYBR Green I Master kit (Roche, Basel, Switzerland). PCR reactions were performed on a Lightcycler 480 (Roche) at 95°C for 10 min (1 cycle), followed by 95°C for 5 s, 60°C for 10 s, and 72°C for 5 s (45 cycles). The mRNA levels were expressed as the average levels of microtubule-associated protein 1 light chain 3 beta (MAP1LC3B), lysosomal-associated membrane protein 2 (LAMP2), or Beclin-1 (BECN1), normalized to the level of beta-actin (ACTB). Primers designed based on sequence homology are listed in Table 1.5.

Table 2.1.   **Primer sequences for autophagy genes mRNA levels quantification.**

CHO gene	qRT-PCR Primers (5'-3')
Microtubule Associated Protein – Light Chain 3β (LC3B)	Forward: 5'- CTT YGA ACA AAG AGT RGA AGA TGT CCG -3'
	Reverse: 5'- ACC ATG CTG TGY CCR TTC ACC A -3'
Lysosomal Associated Membrane Protein 2 (LAMP2)	Forward: 5'- CAA GCT TTT GTC CAR AAT GGY ACA GTG AG -3'
	Reverse: 5'- TTC AGC TGC AGC CCC ATG GTA G -3'
Beclin-1 (BECN1)	Forward: 5'- TTC TGG GAC AAC AAG TTT GAY CAT GC -3'
	Reverse: 5'- GTC CAC TGY TCC TCM GAG TTA AAC TG -3'
β-Actin (ACTB)	Forward: 5' - CCA CTG GCA TTG TGA TGG A - 3'
	Reverse: 5' - GCA ACA TAG CAC AGC TTC TCT - 3'

2.2.8 Glycan analysis

An in-gel method was used for t-PA purification (Royle et al., 2006), in tubes treated with Sigmacote, omitting treatment with formic acid, which can disturb glycan sialylation. The glycans were cleaved from the core protein and fluorescently labelled with 2-aminobenzamide (Sigma), passed through a GlycoClean S cartridge (Prozyme, Hayward, CA) and analyzed by Normal Phase -HPLC (Guile et al., 1996). The profiles obtained for all peptide N-glycosidase F and exoglycosidase digests (including dextran ladder standard) were

analyzed to determine the glucose unit (GU) values that were translated into structures using Glycobase (Dublin-Oxford Glycobiology site, NIBRT) as a guide.

2.2.9   Other analytical techniques

Viable cell concentration was measured by trypan blue exclusion using a Cedex automated cell counting system (Innovatis, Bielefeld, Germany). Samples were diluted 1:2 in a 0.25% trypsin-EDTA solution, incubated 15 min at 37 °C. Glucose, lactate and glutamine concentrations were measured by electrogenic enzymatic reactions with a 7100 MBS analyzer (YSI Life Sciences, Yellow Springs, OH). Quantification of t-PA was performed using a colorimetric activity assay (Fann et al., 2000; protocol in Appendix F) and the conversion factor of 630,000 U/mg (specific activity of the standard) to obtain t-PA concentrations.

2.3   Results and discussion

2.3.1   Cell physiology changes during fed-batch cultivations

Figure 2.1 presents the results of three feeding regimes: (1) fed-batch, (2) enriched fed-batch and (3) unfed (batch) control. The fed-batch culture was supplemented with daily 3.3% (of initial culture volume) Feed A and 1.7% amino acid mix 3, while the enriched fed-batch culture was supplemented with daily 10% Feed A. These feeding strategies resulted in contrasting cell proliferation and productivity performance. The fed-batch yielded the highest viable cell concentration (Figure 2.1A) at 1.14×10^7 cells/mL, more than 1.6 times higher than the enriched fed-batch protocol (6.93×10^6 cells/mL) and 1.8 times higher than the unfed control (6.33×10^6 cells/mL). Despite this, the maximal t-PA concentration (Figure 2.1B) achieved in both the fed-batch and the unfed control was 31 mg/L, whereas the enriched fed-batch reached a maximum of 122 mg/L, four times higher than the other cultures. The higher t-PA production observed in the enriched fed-batch compared to the other fed-batch culture illustrates how bioprocess optimization involves complexities beyond simply maximizing cell proliferation and viability.

All three cultures had similar glutamine concentration profiles, becoming undetectable by day 4 (<0.05 mM, data not shown). This time point corresponded to the maximum t-PA

concentration reached in both the fed-batch and the unfed cultures whereas t-PA continued to accumulate in the enriched fed-batch. From day 3 onwards, the lysosomal compartment increased in all cultures, although at different rates (Figure 2.1C). The initial rate of lysosomal accumulation was greatest in the unfed culture, as could be expected due to the earlier and sustained nutrient limitations in the absence of nutrient feeding. The sudden decrease of lysosomal signal observed on day 6 in the unfed culture coincided with glucose depletion (data not shown). Ultimately, the expansion of the lysosomal compartment was greatest in the fed-batch culture: by day 11, the cellular lysosomal content in this culture was more than 4.5-fold greater than that in the enriched fed-batch culture.
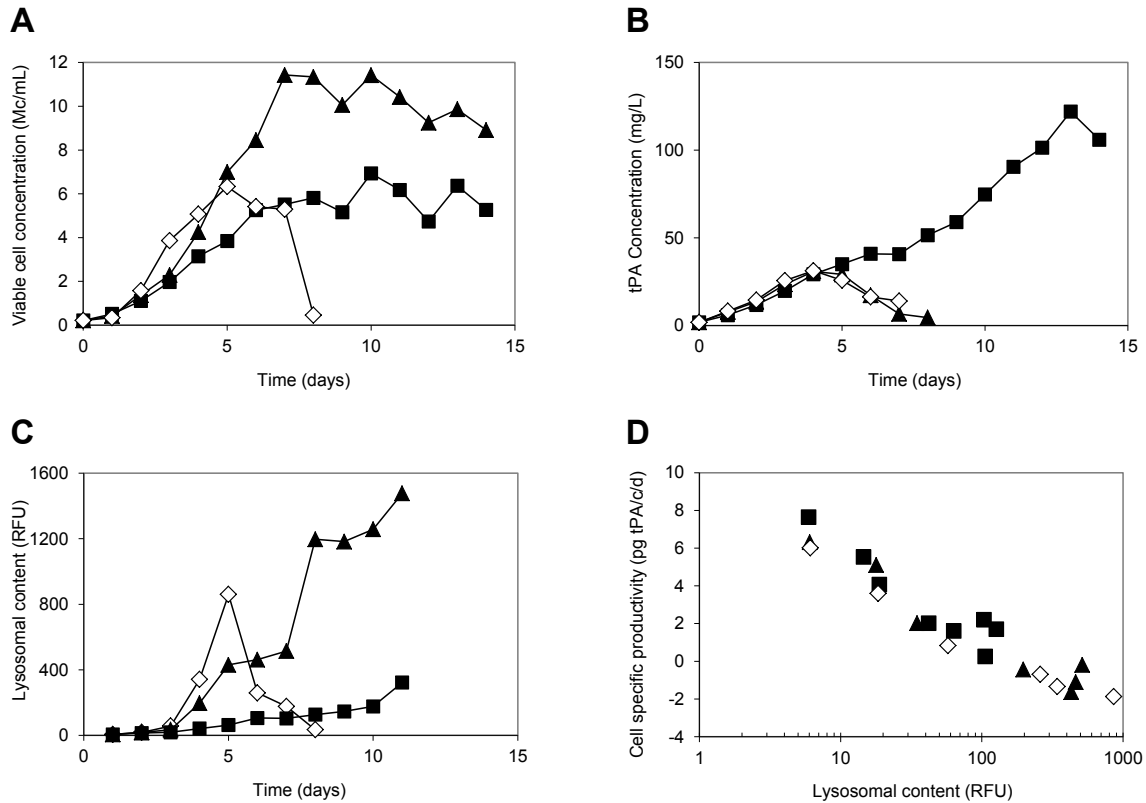
Figure 2.1.   Lysosomal content and protein production.
Comparison of cultures with three different feeding regimes: no feed control (◇), fed-batch (▲), enriched fed-batch (■). Viable cell concentration (A), t-PA concentration (B) and lysosomal content (C) as a function of time. Cell-specific productivity as a function of lysosomal content for the first 7 days of culture (D).

Lysosomal content was negatively correlated with productivity (Figure 2.1D) for the first 7 days of culture, even while the cells retained a high viability which was above 90% in

30

both fed batch cultures until day 8 and up to day 7 in the unfed culture (data not shown). Thus, high lysosomal content appeared to be compatible with high cell viability but not with high cell-specific productivity. This suggested that preventing the accumulation of lysosomes could provide a means to retain high productivity in cultures. Since the increased presence of lysosomes can be associated with autophagic activity (Klionsky et al., 2008), these results also suggested that decreased t-PA production could be related to increased autophagic activity.

2.3.2   Glutamine deprivation upregulates autophagic activity

It has been reported that the absence of glutamine can induce autophagy via TOR inhibition in human and *Drosophila* cells (Nicklin et al., 2009). We developed a GFP-LC3 autophagy-reporter CHO cell line to explore this phenomenon in this widely used cell type for industrial protein production. Exponential phase growing GFP-LC3 CHO cells were resuspended in fresh medium with or without glutamine. They were incubated for 1 day and then analyzed by fluorescence microscopy for the presence of green fluorescent puncta in the cytoplasm, indicative of autophagosomes. As can be seen in Figure 2.2A, higher numbers of autophagosomes were consistently observed in cells deprived of glutamine. Electron micrographs (Figure 2.2B) confirmed the appearance of double-membrane autophagic vesicles upon glutamine deprivation.

To monitor autophagic flux a Western blot of endogenous LC3 was used to assess its conversion and turnover, both in the presence and absence of chloroquine, a lysosomal inhibitor (Mizushima et al., 2010). Non-GFP transfected t-PA producing cells were incubated without glutamine for 0, 1, 2 or 3 days. CHO cells stopped proliferating in the absence of glutamine but retained a high viability (>95%) throughout the experiment (data not shown). Figure 2.2C shows the Western Blot of the autophagic flux assay, in which cells were treated with (20 μM) or without chloroquine for 2 h prior to harvesting. Inhibition of lysosomal function by chloroquine resulted in increased autophagosome-bound LC3-II as observed in all chloroquine-treated samples. This increase was further enhanced in the glutamine-deprived cultures treated with chloroquine, reflecting an increased delivery to the lysosomal

compartment (autophagic flux). These results show that the absence of glutamine alone is sufficient to cause autophagosome formation, and increased autophagic flux.
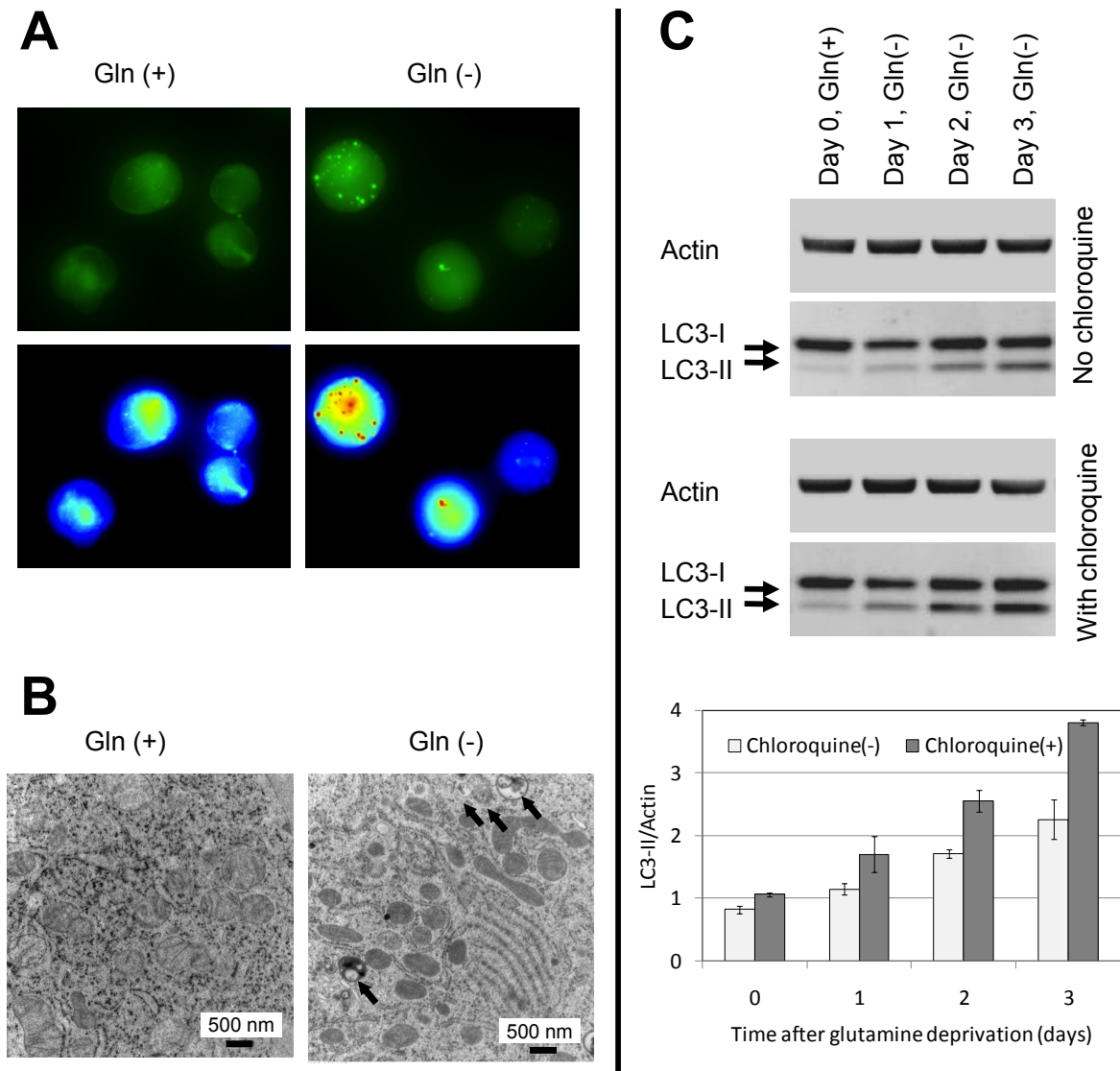
Figure 2.2.   Glutamine-dependent autophagy regulation.
(A) Fluorescence micrographs and heat-map representations of fluorescence intensity of GFP-LC3 expressing CHO cells incubated for 1 day in the presence or absence of glutamine (Gln). (B) Electron micrographs of CHO cells incubated under the same conditions. (C) Western blot of CHO cells incubated in the presence (Day 0, Gln+) or absence of glutamine (Gln-) for 1, 2 and 3 days. Error bars indicate the SEM from two biological replicates.

It appears that induction of autophagy is an early step in the CHO cell response to glutamine limitation. To sustain the proliferation and productivity of these cells in culture,

additional glutamine could be provided, but this would yield increased ammonia generation. Ammonia is an undesirable metabolic byproduct of glutaminolysis since it can both be toxic to cells and impair the glycosylation quality of recombinant proteins (Gawlitzek et al., 2000). Furthermore, ammonia has recently been reported to increase basal autophagy (Eng et al., 2010). These observations thus suggest that increasing process performance may involve autophagy induction, either through the absence of glutamine or because of ammonia generation. Although the multiple roles of glutamine metabolism in cell proliferation, survival, redox balance and mitochondrial function are the object of intensive research (DeBerardinis and Cheng, 2010), the role of autophagy in response to glutamine limitation has seldom been explored.

2.3.3   Inhibition of autophagy with 3-methyl adenine enhances t-PA production

In order to extend to the fed-batch context this analysis of the interplay between glutamine metabolism, autophagy and protein production, three fed-batch protocols were evaluated: (1) a control fed-batch, (2) on day 7 the control culture was divided in 2 and the second fed-batch treated with a single addition of 10 mM 3-MA, a chemical inhibitor of autophagy, and (3) a fed-batch supplemented with glutamine (~4 mM) on a daily basis matching the consumption of this amino acid. All 3 fed-batch cultures were supplemented with daily 3.3% (of initial culture volume) of Feed A and 1.7% of amino acid mixes 1 and 2 from days 1 to 3. The daily feeding volumes were increased 3-fold starting on day 4, i.e. 10% Feed A and 5% of amino acid mixes 1 and 2. The initial glutamine concentration was 4 mM and additional glutamine was only added to the third culture as described above.   The aminopurine derivative 3-MA is widely used to inhibit autophagy (Klionsky et al., 2008); it inhibits the lipid kinase activity of phosphoinositide-3-kinases (PI3Ks). PI3Ks phosphorylate the 3' hydroxyl group on the inositol ring of phosphoinositides. The activity of class III PI3K (PIK3C3, also known as Vps34), producing phosphatidylinositol 3-phosphate PtdIns(3)P, is required for autophagy (Petiot et al., 2000; Wu et al., 2010). Even though 3-MA also inhibits class I and II PI3Ks, accounting for some of its non-specific effects, it does inhibit preferentially the class III member of the family (Miller et al., 2010).

Figure 2.3 shows various cellular responses observed in these cultures. In the control culture, the cells grew exponentially until day 3, when glutamine became depleted (data not

shown) and there was a shift to a lower rate of proliferation. The maximum cell concentration of 8 x 10^6 cells/mL was observed between days 9 and 11 (Figure 2.3A), with viability higher than 80% (Figure 2.3B). Due to batch-to-batch variability in production, the t-PA concentration was normalized to the final concentration of the fed-batch control, increasing gradually up to day 12 (Figure 2.3C). The feeding with excess glutamine resulted in continued proliferation to a maximum cell concentration of 12 x 10^6 cells/mL and a greater t-PA production (1.3-fold increase compared to the control). However, the viability decreased more rapidly than in the control fed-batch.
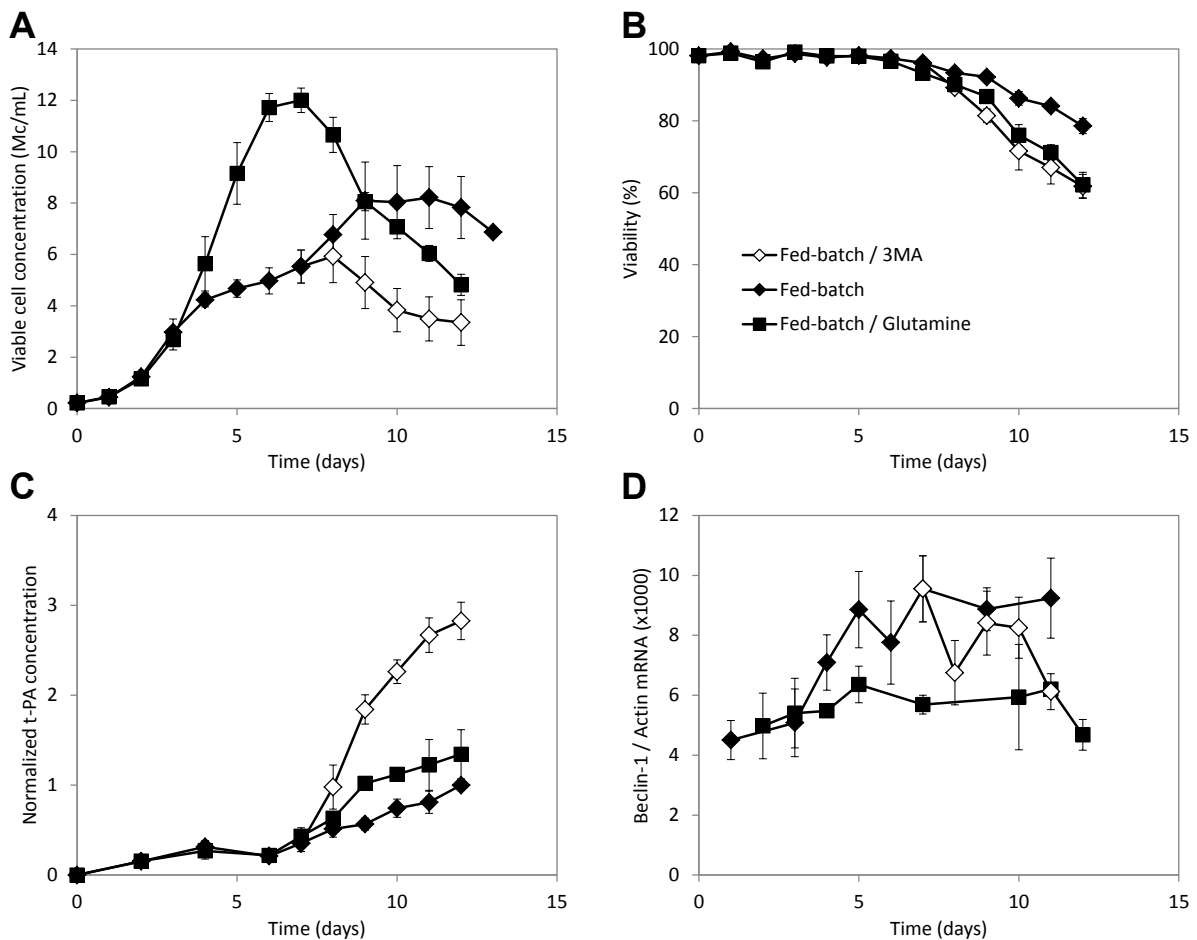
Figure 2.3.   **Use of 3-MA in fed-batch cultures to increase protein production.**
Effect of 3-MA treatment on (A) viable cell concentration, (B) viability, and (C) t-PA production (normalized to the maximum control fed-batch production). (D) Quantification of mRNA levels of Beclin-1, normalized to cellular β-actin. Legend: Control fed-batch (◆), fed-batch treated with 10 mM 3-MA at day 7 (◇) and fed-batch supplemented with excess glutamine (■). Error bars represent the SEM of biological triplicates.

34

Addition of 3-MA resulted in a decreased cell concentration compared to the other cultures, although the viability was similar to the glutamine-fed culture. However, in the 3-MA treated culture, a striking 2.8-fold increase in t-PA production relative to the untreated culture was observed (Figure 2.3C), corresponding to a maximum active t-PA concentration of 536 mg/L. Analysis of samples by ELISA using a detection antibody complementary to both active and inactive t-PA showed the same trend in fold increase (data shown in Appendix A), indicating that the t-PA yield increase upon 3-MA treatment was not due to a change in its specific activity. These results suggest that while autophagy enables cell survival under the nutrient limitations of fed-batch, it also decreases recombinant protein production.

To determine whether differences in the 3 fed-batch protocols were reflected further at the mRNA level, we investigated expression of selected autophagy related genes. Three genes involved in different stages of autophagy progression were chosen for this purpose: Beclin-1, LC3 and LAMP2. Beclin-1 is a component of three regulatory protein complexes involved in autophagosome nucleation and maturation (Yang and Klionsky, 2010), and was thus selected as a potential indicator of early-stage autophagy. Since LC3 is associated with phagophores and mature autophagosomes (Klionsky et al., 2008), this protein is commonly used as a reporter of autophagy. LAMP2 (lysosomal-associated membrane protein 2) is a protein resident in lysosomes and required for their fusion with autophagosomes (Malicdan et al., 2008); it was selected as a possible indicator of late-stage autophagy. The mRNA levels of LAMP2 (Supplementary Figure A.3A) increased 4-fold with little difference between the three cultures. LC3 mRNA levels (Supplementary Figure A.3B) increased almost 3-fold and showed the greatest rise in the control fed-batch culture after day 3, correlating with the time of glutamine limitation. After treatment with 3-MA, higher mRNA levels of LC3 and LAMP2 could be observed, whereas mRNA levels of Beclin-1 decreased (Figure 2.3D), although not in a sustained way. These minor transcriptional level effects of 3-MA treatment may be the result of 3-MA being a PI3K inhibitor that operates at the post-translational level and not transcriptionally. On the other hand, Beclin-1 mRNA levels began to rise following day 3 in the control fed-batch culture, while remaining relatively constant throughout the glutamine-supplemented culture. These findings suggest that glutamine limitation may result in increased Beclin-1 transcription.

Table 2.2.   HPLC analysis of glycans released from t-PA

Peak No.	GU	Structure Name	Structure Image	Area (%)		
				Fed-batch + Glutamine	Fed-batch	Fed-batch + 3-MA
1	4.95	F(6)M3		4.96	2.61	
2	5.48	A2		12.90	7.26	
3	5.96	A3		9.51	6.10	3.65
4	6.17	M5		5.28		
5	6.29	A2[6]G(4)1		15.71	16.28	17.40
6	6.84	F(6)A2[3]G1		6.86	5.91	3.75
7	7.14	A2G2		11.12	9.13	12.83
8	7.46	F(6)A1G1S(3)1		4.01		3.55
9	7.91	A2G2S(3)1		18.29	27.57	11.89
10	8.13	F(6)A2G2S1				13.57
11	9.04	F(6)A3G3S(3)1		11.36	17.10	13.03
12	9.31	F(6)A2G2S(6)2				9.62
13	10.15	A3G(4)3S3			6.32	8.49
14	11.09	N/Av	N/Av		1.72	2.22
			Sialylated glycans (%)	**33.7**	**51.0**	**60.2**
			Fucosylated glycans (%)	**27.2**	**25.6**	**43.5**
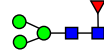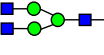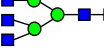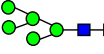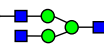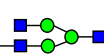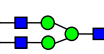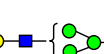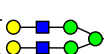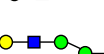
Where

A= N-acetylglucosamine (■); F = Fucose (▼); G = Galactose (○); M = Mannose (●);

S = Sialic acid (◆); N/Av = structure identification not available; GU = glucose unit

2.3.4 Treatment with 3-methyl adenine does not compromise t-PA glycosylation

Figure 2.4 and Table 2.2 show the HPLC glycan profiles of t-PA purified from samples obtained at the end of the Figure 2.3 cultures. The high glutamine fed-batch t-PA had the lowest peaks of complex glycans with high glucose unit (GU) values, whereas the 3-MA treated culture produced the highest levels of complex, high GU value glycans. Conversely, the opposite trend was observed for low GU value glycans (notably the first three peaks, corresponding to shorter glycan chains with terminal mannose and terminal GlcNAc). Higher abundance of short glycans is indicative of a lower degree of carbohydrate processing in the Golgi, particularly if such glycans lack peripheral GlcNAc, galactose and sialic acid, incorporated in later steps of the glycan extension (Butler, 2006; Hossler et al., 2009). The extent of fucosylation (peaks 1, 6, 8 and 10 to 12), galactosylation (peaks 5 to 13) and sialylation (peaks 8 to 13) was also highest in the 3-MA treated fed-batch. Abundance of triantennary complex glycans was similar in t-PA from the 3-MA treated culture and the untreated control (21.5% and 23.4%, respectively). Taken together, these results indicate that the glycosylation efficiency was highest in the 3-MA treated culture. Overall, autophagy inhibition with 3-MA enhanced fed-batch t-PA production by almost 3 fold without impairing t-PA glycosylation and even enhancing this critical feature of product quality.
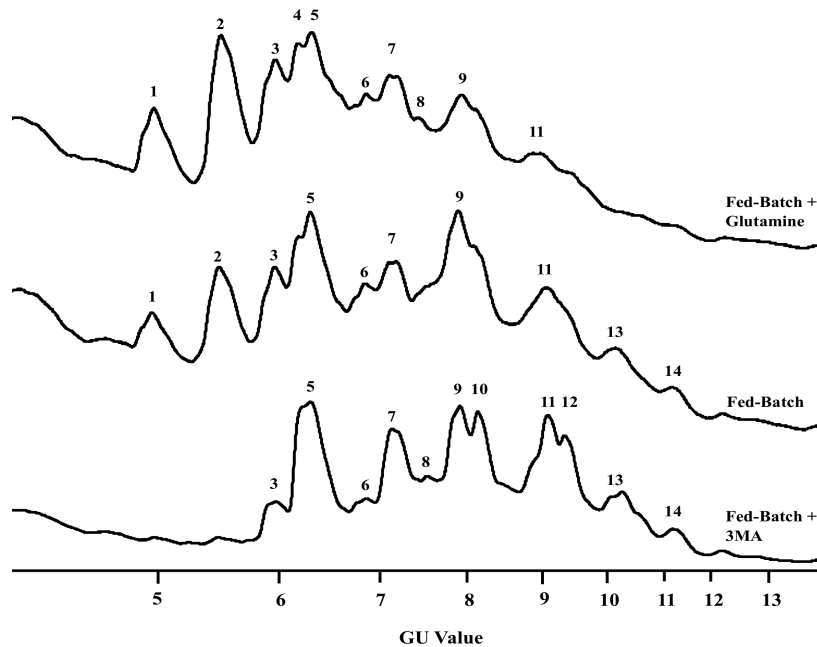
Figure 2.4.   Identification of t-PA glycans in fed-batch cultures.
NP HPLC profiles of t-PA glycans purified from fed-batch cultures.

2.4 Conclusions

Process optimization of protein production using recombinant mammalian cells requires a careful balance of multiple cellular functions such as proliferation, survival, productivity and glycosylation capacity. In this study, autophagy was shown to play a key role in cell physiology, especially by decreasing protein productivity in the presence of metabolic stress. The mechanism by which autophagy decreases protein secretion may involve the degradation of the production machinery (ribosomes, endoplasmic reticulum) as well as of protein-containing vesicles in the secretory pathway. Chemical modulation of autophagy provides an approach to investigate this phenomenon and to enhance process performance. Blocking lysosomal degradation using chloroquine did not yield clear increases in protein production (data not shown) perhaps at least in part because it does not prevent autophagic sequestration of protein production machinery. Consistent with the need to block autophagy at an earlier stage to prevent autophagic sequestration, the PI3K inhibitor 3-MA yielded the most promising results in this strategy. Nonetheless, investigating the influence of other PI3K inhibitors such as wortmannin or more specific inhibitors of other autophagy gene products would also be of interest. Since 3-MA also inhibits class I PI3Ks, this treatment also impairs cell proliferation. It has been reported that 3-MA can even induce autophagy under nutrient-rich conditions (Wu et al., 2010). Thus, to maximize protein yields, dosing and timing need to balance the cytotoxic effects with the benefit of increased productivity.

The lower glycosylation efficiency of the glutamine-supplemented culture is likely due to the higher levels of ammonia generated by higher glutamine consumption, which are known to impair galactosylation and sialylation (Gawlitzek et al., 2000). Another possible explanation for decreased glycosylation efficiency could be that the substantially higher cell proliferation in that culture led to decreased oxygen availability, which could have affected galactosylation (Butler, 2006) and subsequent sialylation. Mannose and galactose receptors in the liver can clear t-PA (Smedsrod and Eiarsson, 1990). The mannose receptor also recognizes terminal GlcNAc and binds to it initiating clearance (Jones et al., 2007). Furthermore, asialoglycoprotein receptors found in the liver remove non-sialylated glycoproteins from the circulatory system (Weiss and Ashwell, 1989). These findings indicate that a high level of sialylation in glycoproteins is important to maintain the half-life of a therapeutic. Thus, it was particularly important to demonstrate that treatment with 3-MA

not only increased production of t-PA, but also 3-MA treatment did not compromise these aspects of the t-PA glycan profile.

The use of 3-MA as an additive in industrial fed-batch cell cultures may not be acceptable given the requirement to ensure safety for the production of biopharmaceuticals. Nonetheless, these results have demonstrated the influence that autophagy can have on productivity and should lead to exploring novel strategies for the production of biopharmaceuticals. For example, autophagy could be more safely modulated by genetically engineering producer cells. Overall, the CHO fed-batch process strategy presented in this study proposes initial glutamine supplementation for enhanced proliferation, followed by inhibition of glutamine-depletion-induced autophagy near the maximum cell proliferation point, in the context of a fed-batch process that provides the nutrients required to sustain production.

This work describes the importance of autophagy in the cellular response to fed-batch culture conditions that are currently widely used for the industrial production of recombinant proteins. Autophagy was activated in particular upon glutamine limitation and correlated with a decrease in cell-specific productivity. The activation of cell survival mechanisms under stress conditions will prevent loss of cell viability, but the autophagy of cellular components can also decrease recombinant protein production. Understanding the importance of this mechanism suggested strategies to enhance process performance, including the inhibition of autophagy, which yielded a 2.8-fold increase in t-PA production. This remarkable increase in t-PA production was not accompanied by compromised complex glycosylation quality as is required for the therapeutic applications of numerous recombinant proteins. These results suggest that monitoring and modulating the cellular process of autophagy, using inhibitors or through genetic engineering of production cell lines, could lead to significant improvements in the performance of biotechnology protein production processes.

3   Comparison of glutamine metabolism and autophagy in three CHO cell lines

Cell proliferation, cell productivity and product quality need to be reproducibly obtained within a well-characterized process to be considered high-performance and robust. Statistical design of experiments methods provide an empirical approach to reach this goal and generate a robust design space for production process operations. Understanding and modulating the cell physiological factors that affect recombinant protein production cell cultures should complement those approaches and enable improved bioprocess design.

It was described in the previous chapter how autophagy inhibition can significantly increase cell-specific t-PA productivity without adverse effects on protein glycosylation. The present chapter presents the investigation of glutamine metabolism and autophagy for this cell line and two other CHO cell lines producing different recombinant antibodies. For all of these cell lines, glutamine deprivation decreased cell proliferation, glucose uptake and lactate production, without adverse effects on cell viability. However, mitochondrial and lysosomal changes varied substantially between cell lines, illustrating how the susceptibility to autophagy was cell-line dependent. A western blot LC3 turnover assay confirmed that the three cell lines have varied susceptibility to glutamine deprivation and this should guide the design of strategies based on autophagy and glutamine metabolism modulation to increase process performance.

3.1   Introduction

Glutamine is a central metabolite in mammalian cell culture, often consumed at rates only second to glucose and oxygen. Glutamine has long been known as an alternative energy source, especially due to mitochondrial oxidation (Neermann and Wagner, 1996; Zielke et al., 1980). Recent literature shows that the role of glutamine extends far beyond this function (Dang et al., 2011; DeBerardinis and Cheng, 2010), with especially important contributions to cellular biosynthesis and cell survival. Through its role in anaplerosis (replenishment of the pool of TCA cycle intermediates) and NADPH regeneration, glutamine can sustain lipid and nucleic acid biosynthesis (DeBerardinis et al., 2007). Glutamine can also influence glutathione levels (Shanware et al., 2011), the most abundant non-enzymatic cellular antioxidant (Schafer and Buettner, 2001), necessary for repair functions and redox

homeostasis (Franco and Cidlowski, 2009), therefore playing an important role in cell survival and resilience to stress. Further roles of glutamine in survival mechanisms include the transcriptional regulation of stress responses: its presence prevents the activation of NFκB (Brasse-Lagnel et al., 2009) and enhances expression of HSP70 (Hamiel et al., 2009), which has a cytoprotective role.

The influence of glutamine on protein product quality is likewise a key aspect of the production of therapeutic recombinant proteins. A toxic by-product of glutamine metabolism, excess ammonia accumulation due to overfeeding glutamine can compromise protein glycosylation above 10 mM (Gawlitzek et al., 2000). However, glutamine levels below threshold concentrations can result in down-regulation of genes required for glycosylation, producing glycans with decreased antennarity and lower sialic acid content (Wong et al., 2010).

Reports on the effect of glutamine on productivity vary considerably. Both positive (Jeong and Wang, 1995) and negative (Mancuso et al., 1998) correlations between glutamine and cell-specific productivity have been reported. Perhaps this dependence is cell-line dependent and, in any case, the cellular mechanisms for glutamine metabolism influences on protein productivity are not well understood. Recently, it was shown that autophagy induced by glutamine depletion can significantly decrease cell-specific productivity and chemical inhibition of autophagy using 3-methyladenine (3MA) yielded an almost 3-fold increase in production of t-PA (Chapter 2; Jardon et al., 2012). In order to evaluate the applicability of these findings to other cell lines and products, the interplay between autophagy and glutamine metabolism was investigated in three different CHO cell lines producing recombinant t-PA or antibodies. The applicability of autophagy inhibition to increase antibody production is of particular importance since this is the largest class of therapeutic proteins currently in development.

3.2 Materials and methods

3.2.1 Cell culture

Three different CHO cell lines (Table 3.1) were used for this study. The first one, referred to as CHO-t in this work, produces tissue plasminogen activator (Jardon et al.,

2012). The second cell line (Kennard et al., 2009) produces a human anti-interleukin 1 beta monoclonal IgG1 antibody and will be referred to as CHO-m. The third cell line used produces EG2-hFC, a human-llama chimeric single domain antibody against epidermal growth factor receptor (Bell et al., 2010) and hereafter will be referred to as CHO-l.

Table 3.1.   Cell lines used in this study

Cell line	Name	Product	Parental cell line
CHO-t	CHO 540/24	t-PA	CRL-9096 (CHO duk-)
CHO-l	CHO EG2 1A7	EG2-hFC	CHO-DXB11
CHO-m	ChK2 437.89.56	Anti-IL1β IgG1	CHOK1SV

Culture conditions were the same as previously described (Jardon et al., 2012) for maintenance cultures of CHO-t and CHO-l cells that were in chemically defined CD CHO medium, supplemented with 25 ng/mL IGF, 4X anti-clumping agent and 4 mM glutamine (Gibco-Invitrogen, Grand Island, NY). CHO-m maintenance cultures were in CD CHO, supplemented with 6 mM glutamine (Gibco), 0.1 mg/mL hygromycin B (Gibco) and 0.45 μg/mL bleocin (Calbiochem, La Jolla, CA).

Fed-batch cultures were supplemented daily with CHO CD Efficient Feed A (Gibco). The feeding protocol consisted of daily addition of 6.7% (expressed as percentage of initial culture volume per day) Feed A and, for specified cultures, a daily addition of 2 mM glutamine (Gibco).

3.2.2   Flow cytometry

The following stains (Molecular Probes, Eugene, OR) were used to analyze selected physiological parameters by flow cytometry: LysoTracker Green DND-26 (LTG) to stain lysosomes, propidium iodide (PI) to identify dead cells, $DiIC_1(5)$ to stain predominantly in mitochondria with high transmembrane potential ($\Delta\Psi m$), and 10-n-nonyl acridine orange (NAO) which binds cardiolipin, staining mitochondria independently from their $\Delta\Psi m$. For this analysis, 1×10^5 cells were resuspended in a solution of PBS, 10 mM glucose and 0.09% trypsin and incubated with 75 nM LTG and 50 nM $DiIC_1(5)$ for 15 min at 37ºC or with 2 μM NAO and 50 nM $DiIC_1(5)$ for 10 min at 37ºC. Stained cells were pelleted, resuspended in

PBS with 10 mM glucose and 0.5 µg/mL PI and placed on ice until analysis. Flow cytometry was performed in a FACScalibur (BD Biosciences, Franklin Lakes, NJ) with 488 and 633 nm lasers. FlowJo (Tree Star, Ashland, OR) was used for data analysis.

3.2.3 LC3 autophagic flux assay

Western blotting was performed to monitor autophagy, as previously described (Jardon et al., 2012). Samples were incubated in a tube rotator (Sarstedt, Nümbrecht, Germany) at 37ºC in a humidified CO_2 incubator for 2 h in the presence or absence of 20 µM chloroquine. Preliminary work confirmed that this concentration of chloroquine saturated all three cell lines to block lysosomal degradation without negative effects on cell viability within the specified incubation time (Rubinsztein et al., 2009).

3.2.4 Quantification of mRNA levels and mitochondrial over nuclear DNA ratios

Total DNA and RNA extraction, reverse transcription and real-time quantitative RT-PCR were performed as previously reported (Jardon et al., 2012). The mRNA levels were expressed as the average levels of lysosomal-associated membrane protein 2 (LAMP2), microtubule-associated protein 1 light chain 3-β (MAP1-LC3B, or simply LC3), or Beclin-1 (BECN1), normalized to the mRNA level of β-actin (ACTB). The mitochondrial DNA (mtDNA) content, was calculated from the average ratio of mtDNA-encoded Cytochrome Oxidase Subunit 1 (COX-1) over chromosomal β-actin (BACT) COX-1/BACT and referred to as the mitochondrial over nuclear DNA ratio (mtDNA/nDNA). Probes used for mtDNA content are listed in Table 3.2. Primers for mRNA quantification were the same as previously reported (Jardon et al., 2012).

Table 3.2.   Probe sequences for mtDNA content determination

CHO Gene	Probes (mtDNA/nDNA)
Cytochrome Oxidase Subunit 1 (COX-1)	Fluorescein: 5' - CCT CCA TTA GCA GGA AAT CTA GCC CA - 3'
	LC Red 640/P: 5' - GCA GGA GCT TCG GTA GAC CTA ACC - 3'
β-Actin (BACT)	Fluorescein: 5' - CGT GGC TAC AGC TTT ACC ACC AC - 3'
	LC Red 640/P: 5' - GCT GAG AGG GAA ATT GTG CGT GAC - 3'

3.2.5   Other techniques

Viable cell concentration was measured by trypan blue dye exclusion using a Cedex automated cell counting system (Innovatis, Bielefeld, Germany), as previously described. Glucose, lactate and glutamine concentrations were measured by electrogenic enzymatic reactions with a 7100 MBS analyzer (YSI Life Sciences, Yellow Springs, OH). Quantification of t-PA produced by CHO-t cells was performed using a colorimetric activity assay previously described (Jardon et al., 2012) using a conversion factor of 630,000 U/mg (specific activity of the standard) to report t-PA concentration. Chimeric EG2hFC produced by CHO-l cells was quantified by ELISA, using an immunoperoxidase assay, Fc-specific human IgG1 kit (Immunology Consultants Laboratory, Portland, OR). Monoclonal IgG1 antibody produced by CHO-m cells was quantified by ELISA (adapted from Kennard et al., 2009), using goat anti-human IgG Fcγ fragment as coating antibody and goat alkaline phosphatase-conjugated anti human IgG (H+L) as conjugate antibody (Jackson ImmunoResearch Laboratories, West Grove, PA). Statistical significance was determined using a two-tailed t-test.

3.3   Results and discussion

3.3.1   Glutamine deprivation does not compromise cell viability but significantly decreases cell proliferation

In order to evaluate in detail the effect of glutamine on process performance, the three cell lines were cultured in short-term (3-day) fed-batch regimes, using the protocol described in the Materials and methods section. The fed-batch regime was chosen because the alternative of running these cultures for 3 days in batch mode would risk exposing cells to other nutrient limitations, unless very low cell concentrations were used. Extremely low cell concentrations could in turn decrease the sensitivity of some of the readouts planned. The fed-batch mode of cultivation was thus particularly suitable for the purpose of this experiment, enabling to limit the confounding effects of medium changes and illustrating how glutamine differences influence process performance. Cultures were inoculated at 2.5 x 10^5 cells/mL in shake flasks. The effect of glutamine on cell viability and proliferation after 3 days of culture is presented in Figure 3.1. Viability (Figure 3.1A) in all glutamine-deprived

cultures was higher than 90%. In fact, after 3 days of culture CHO-l cells had a slightly lower viability (82%) in the presence of glutamine, probably due to higher lactate and ammonia accumulation. Within 3 days (Figure 3.1B) CHO-t, CHO-l and CHO-m cells reached average concentrations of 3.7, 2.3 and 1.8 x 10^6 cells/mL respectively, in the presence of glutamine, and 0.3, 0.6 and 0.6 x 10^6 cells/mL respectively, in the absence of glutamine. These differences correspond to 12.3, 3.8 and 3-fold higher cell proliferation in the presence of glutamine. CHO-t cells proliferated at much higher rates than the other cell lines in the presence of glutamine and, conversely, these cells expanded the least upon glutamine deprivation, suggesting a particularly strong dependence of this cell line on glutamine. The lower susceptibility of CHO-m cells to glutamine depletion is likely due to these cells having been derived from the CHOK1SV cell line (Kennard et al., 2009) and expressing glutamine synthetase (GS). Even these GS-expressing cells proliferated more slowly in the absence of exogenous glutamine and their proliferation increased significantly with glutamine supplementation. These results suggest that glutamine supplementation can be an important variable to consider in process development strategies even for GS-exprressing cell lines that are less dependent on this amino acid.
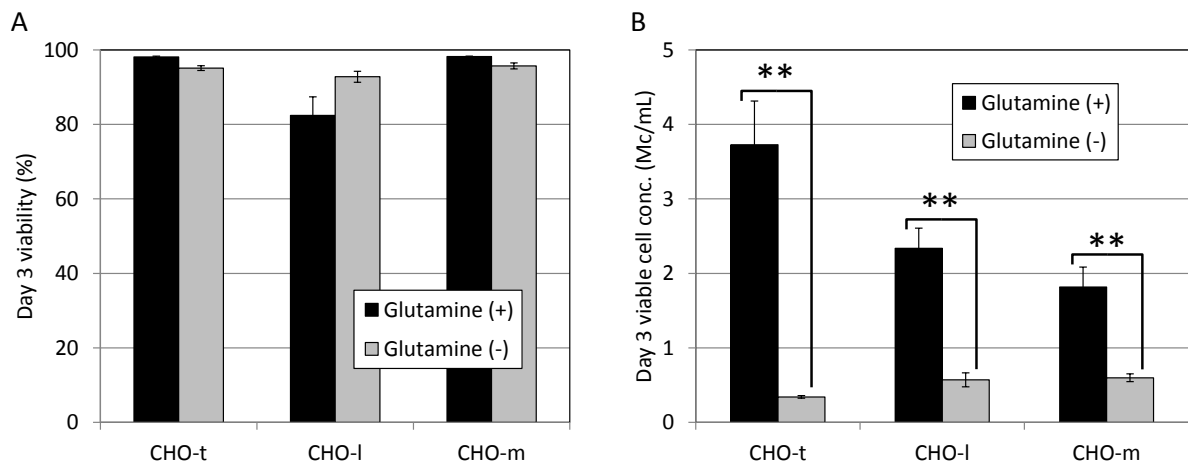
Figure 3.1.   Effect of glutamine deprivation on viability and proliferation.
(A) viability and (B) viable cell concentration after 3 days of fed-batch culture. Error bars represent the SEM of biological triplicates. ** p value < 0.05

3.3.2 Glutamine deprivation can lead to decreased recombinant protein concentrations but not necessarily due to lower cell-specific productivity

The quantification results of the secreted recombinant proteins produced by each cell line are shown in Figure 3.2. After the 3 day fed-batch culture of CHO-t, CHO-l and CHO-m cells (Figure 3.2A), their respective recombinant product reached average concentrations of 28, 7.5 and 12 μg/mL in the presence of glutamine, whereas in the absence of glutamine the final concentrations were 2.9, 3.0 and 8.0 μg/mL respectively. In other words, the final recombinant protein concentration was 9.6, 2.5 and 1.5 times higher in the presence of glutamine, respectively for each cell line.
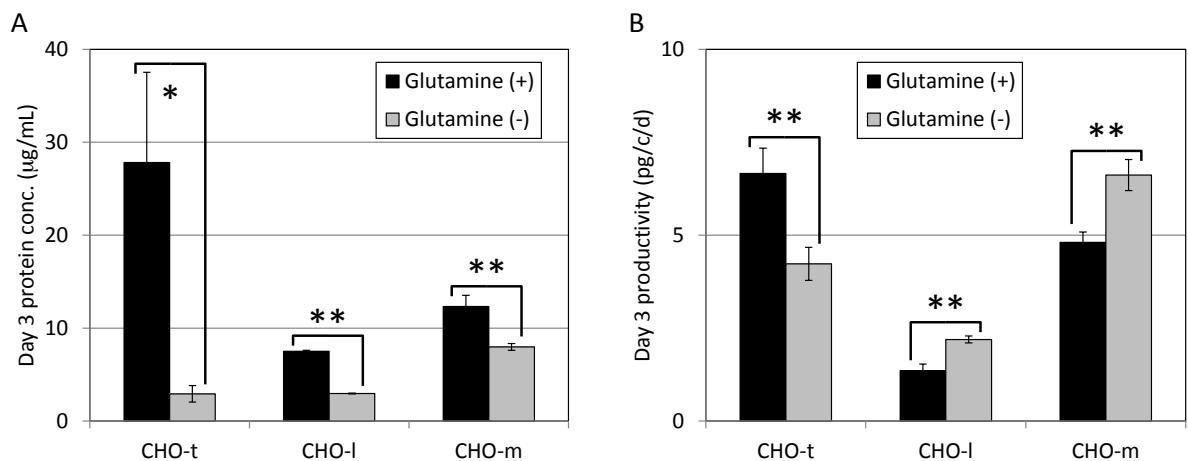
Figure 3.2.   Effect of glutamine deprivation on yield and productivity.
(A) protein concentration and (B) cell-specific productivity at the end of the experiment. Error bars represent the SEM; for CHO-t and CHO-m, n=3; for CHO-l n=2. * p value < 0.1; ** p value < 0.05

The cell-specific productivity between day 2 and day 3 is shown in Figure 3.2B. CHO-t cells, the most significantly affected by the absence of glutamine in terms of proliferation, also showed a decreased cell-specific productivity (63% of the productivity in the presence of glutamine). The cell-specific productivity in CHO-l and CHO-m cells had a different trend: 1.5-fold and 1.4-fold higher than in the absence of glutamine. However, despite the higher cell-specific productivity in the absence of glutamine in these two cell lines, the final protein concentration reached a higher level in all of the cultures supplemented with glutamine, due to the higher cell proliferation. Once again, the GS-expressing cells were least

sensitive to the absence of glutamine and yet the addition of glutamine increased the final protein concentration. These results illustrate how increasing only cell-specific productivity may not be enough to increase the final product yield if the proliferation is somehow compromised.

3.3.3 Glucose consumption and lactate production decrease in the absence of glutamine

Figure 3.3 shows the results obtained on day 2, at which the largest differences between glutamine-supplemented and glutamine-limited cultures were observed. Particularly in the case of cultures with high lactate levels, pH differences would have introduced biases by day 3. The cell-specific glucose consumption (qGlc, Figure 3.3A) and lactate production (qLac, Figure 3.3B) rates were significantly lower in the absence of glutamine in all three cell lines. Under glutamine deprivation, glucose consumption rates were 6%, 58% and 75% of the corresponding rates in glutamine-supplemented cultures for CHO-t, CHO-l and CHO-m cells, respectively. Similarly, lactate production rates in glutamine-deprived CHO-t, CHO-l and CHO-m cells were 22%, 41% and 65%, of their respective rates in cultures with glutamine. As expected, CHO-m cells were the least sensitive to glutamine deprivation, yet interestingly their metabolism was also affected by the absence of this amino acid.
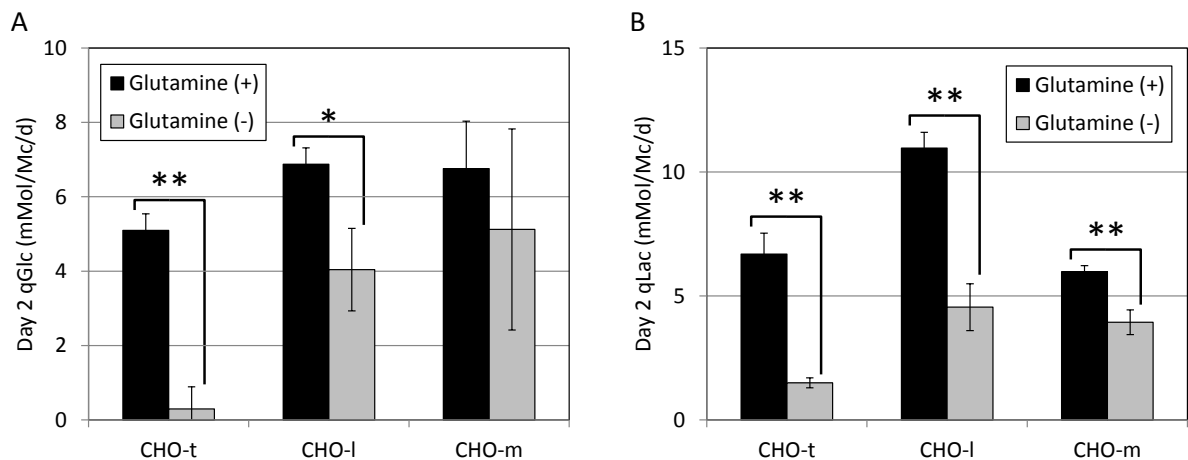
Figure 3.3.   Effect of glutamine deprivation on energy metabolism.
Cell-specific (A) glucose consumption and (B) lactate production rates on day 2 of the experiment. Error bars represent the SEM of biological triplicates. * p value < 0.1; ** p value < 0.05

Proliferating cells need to successfully combine ATP production with increasing cellular mass, which requires protein, nucleic acid and lipid biosynthesis. In order to meet these needs, they require energy, biosynthetic precursors and reducing power, notably in the form of NADPH, to assemble the required macromolecules (Figure 3.4). Mitochondrial metabolism plays a major role in sustaining all these requirements (DeBerardinis et al., 2008). Building blocks for carbon backbones are provided by the TCA cycle in the form of citrate, which is converted by the ATP-citrate lyase (ACL) into cytoplasmic acetyl-CoA (Vander Heiden et al., 2009). Malate, another TCA cycle intermediate, is also exported from the mitochondrial matrix in proliferating cells as a substrate of the malic enzyme (ME) to regenerate the NADPH pool, required for the assembly of lipids and nucleic acids (DeBerardinis et al., 2007). The extensive use of TCA cycle intermediates by proliferating cells requires the replenishment of this pool, a process named anaplerosis. Glutamine has been shown to be a major anaplerotic substrate in proliferating cancer cells (DeBerardinis, 2007) and thereby contributes to their core metabolic requirements by taking part in bioenergetics, supporting regeneration of reducing power and complementing glucose metabolism for macromolecule production (DeBerardinis, 2010).
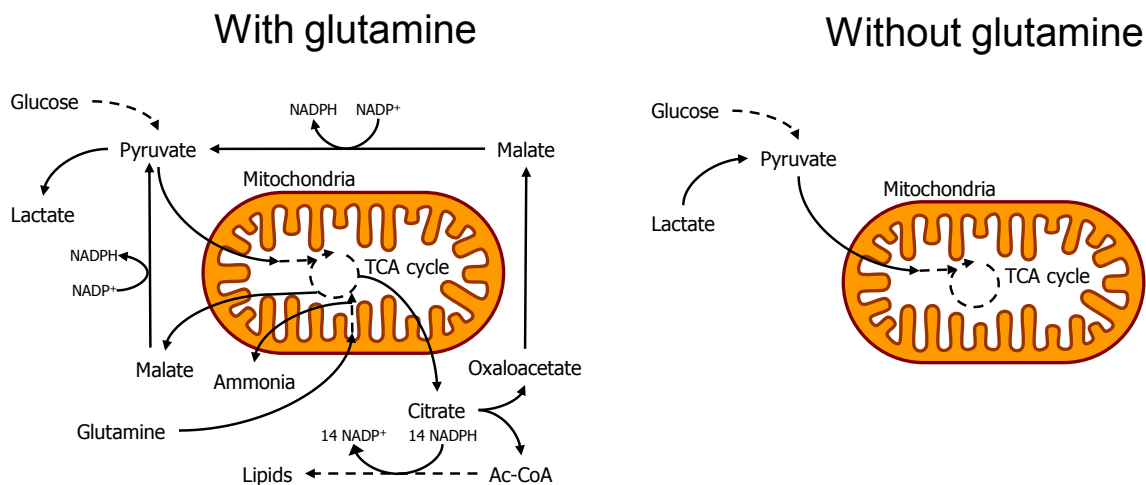
Figure 3.4.   Model of mitochondrial metabolism in the presence or absence of glutamine.
Proliferating cells require energy, macromolecules and reducing power for their biosynthesis. Glutamine enables them to meet such requirements by providing TCA cycle intermediates citrate, which is consumed particularly for lipid biosynthesis, and malate, which is mainly used to regenerate NADPH.

These features of proliferating mammalian cells are compatible with anaerobic metabolism - high glucose consumption and lactate production - even when oxygen is available (Vander Heiden et al., 2009). This metabolic state is termed aerobic glycolysis, also known as the Warburg effect. The results presented in this work are consistent with the perspective that glutamine supports, at least in part, aerobic glycolysis and that this may not be an exclusive feature of cancer cells but of proliferating mammalian cells in general.

3.3.4 Absence of glutamine leads to mitochondrial and lysosomal changes in a cell-line dependent manner, consistent with the differences in autophagic activity

To further understand the extent of the physiological changes produced by glutamine deprivation, lysosomal content (Figure 3.5A) and mitochondrial mass (Figure 3.5B) were estimated by staining with LysoTracker Green DND-26 (LTG) and 10-n-nonyl acridine orange (NAO), respectively, and quantified by flow cytometry. The initial levels of the lysosomal and mitochondrial compartments were remarkably different between cell lines but remained at comparable levels for the duration of all the glutamine-supplemented cultures. Three days of glutamine deprivation resulted in a 4.9-fold increase of the lysosomal compartment in CHO-t cells and a 34% decrease of mitochondrial mass. These observations suggest the presence of mitophagy, i.e. targeted mitochondrial clearance by the autophagic-lysosomal machinery (Kundu and Thompson, 2008). On the other hand, CHO-l cells showed a lesser expansion of the lysosomal compartment in the absence of glutamine whereas the mitochondrial mass estimated by NAO did not change significantly. The 3-fold increase of the lysosomal compartment in CHO-l cells was similar to the increase for the CHO-t cells but the initial CHO-l levels were so low that the lysosomal signal of CHO-l cells remained 10 times lower than in the CHO-t cells. These results suggest that the lysosomal compartment expansion in the CHO-l cells in the glutamine-deprived cultures was not sufficient to produce any observable difference in the mitochondrial compartment. In CHO-m cells, the lysosomal compartment estimated by LTG did not change significantly, nor did the mitochondrial content estimated by NAO (less than 10%).

Since LAMP-2 is a structural protein of the lysosomal membrane, it was hypothesised that its mRNA levels could be used to estimate lysosomal abundance by qRT-PCR. Comparison of LAMP-2 mRNA levels with flow cytometry data supports this hypothesis: a

significant change (38% increase) in LAMP-2 mRNA levels (Figure 3.5C) due to glutamine deprivation was detected only in the CHO-t cells. These results suggest that the increased lysosomal biogenesis likely taking place in CHO-t cells due to glutamine deprivation entails the sustained production of mRNA for gene products destined to the lysosomes, such as LAMP-2. The results for mitochondrial DNA content estimated by the mtDNA/nDNA ratio (Figure 3.5D) also agree with the flow cytometry data: a significant change (45% decrease) of mtDNA content upon glutamine depletion was observed only for the CHO-t cells. Also, the magnitude of this decrease is comparable to the change estimated by NAO fluorescence.
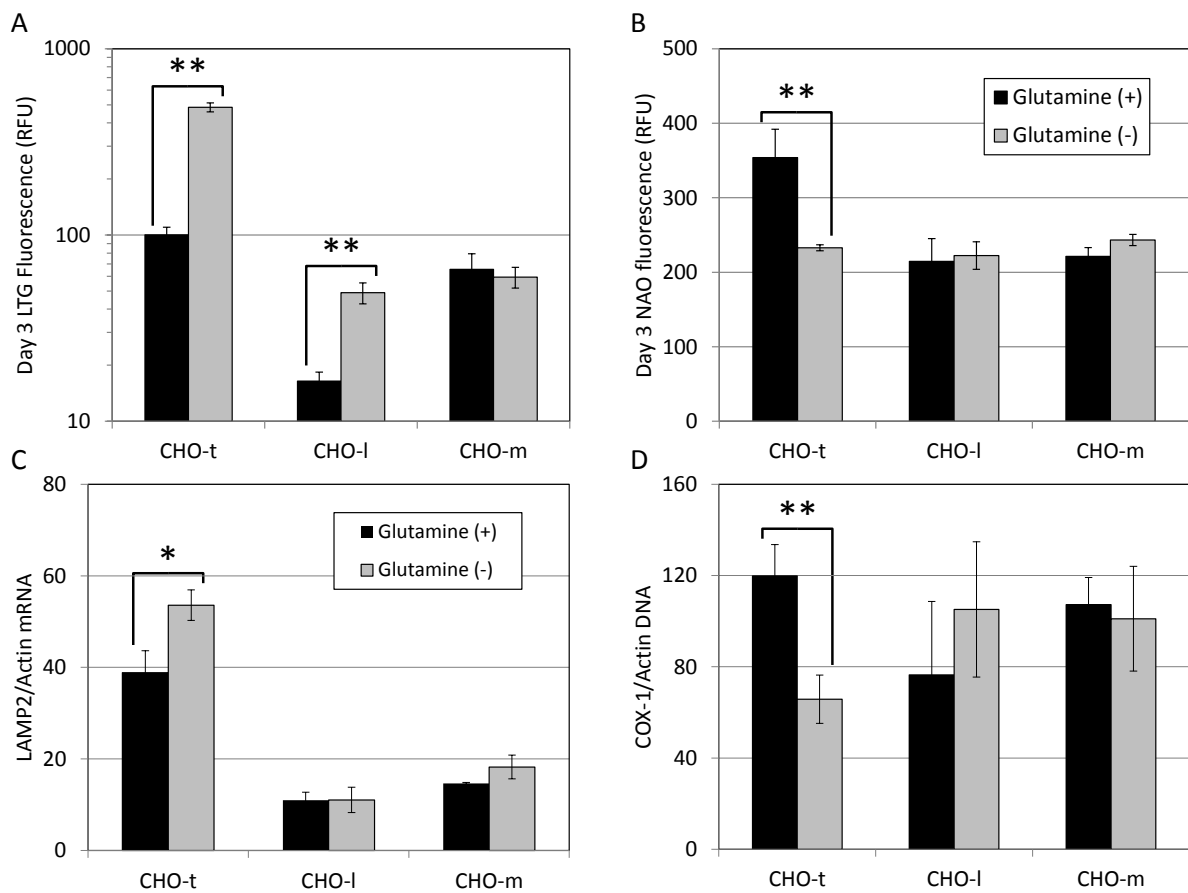
Figure 3.5.   Effect of glutamine deprivation on lysosomal and mitochondrial content. (A) lysosomal content and (B) mitochondrial mass, determined by flow cytometry. Quantification of (C) LAMP-2 mRNA levels and (D) mitochondrial over nuclear DNA levels. All results are from day 3 of the experiment. All error bars represent the SEM of biological triplicates. * p value < 0.1; ** p value < 0.05

A flux assay (LC3 turnover) was performed in order to determine if the results on mitochondria and lysosomal content correlated with changes in autophagic flux (Figure 3.6). In this assay (Mizushima et al., 2010; Klionsly et al., 2008), the amount of autophagy cargo delivered to the lysosomes is inferred by the differences in LC3-II levels between samples treated or not with lysosomal inhibitors (20 μM chloroquine in this study). Inhibition of the lysosomal function prevents the degradation of LC3-II and of other autophagy cargo, resulting in increased levels of this autophagy marker. Whereas increased LC3-II levels in the absence of lysosomal inhibitors indicates a higher abundance of autophagosomes, a further increase in LC3-II levels in the presence of lysosomal inhibitors shows that more cargo is being delivered to the lysosomal compartment for degradation, i.e. an increase in autophagic flux.
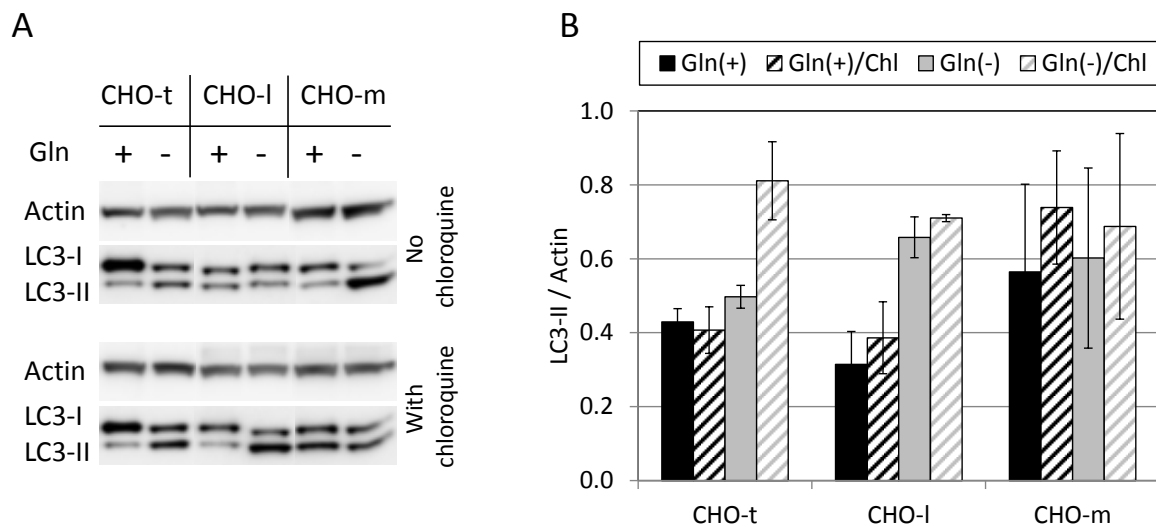
Figure 3.6. **Effect of glutamine (Gln) deprivation on autophagy flux.**
(A) Western blot of samples incubated with and without chloroquine (Chl, 20 mM) for 2 hours. (B) Protein quantification from western blots. Error bars represent the SEM of biological duplicates. All results are from day 3 of the experiment.

The LC3-II turnover assay revealed that CHO-t and CHO-l cells undergo an increase in autophagic flux upon glutamine deprivation. On the other hand, the autophagic activity of CHO-m cells does not significantly increase in absence of exogenous glutamine.

Interestingly, the basal levels of LC3-II (with glutamine) in CHO-m cells are higher than in the other cell lines, suggesting that their basal autophagic activity is also higher.

Based on the LC3-II turnover assay, the more drastic lysosomal and mitochondrial changes observed in CHO-t cells under glutamine deprivation coincides with a greater autophagic activity. For the least glutamine sensitive CHO-m cells there was not an increase of autophagic activity nor organellar remodelling under lack of exogenous glutamine. CHO-l cells, in the middle of this spectrum, also display increased autophagic flux upon glutamine deprivation, but without the extensive physiologic reconfiguration observed in CHO-t cells. It is possible that longer exposure to this metabolic stress would be required to observe similar changes as in the CHO-t cells.

Finally, the mRNA levels of two core autophagy genes, LC3 (Figure 3.7A) and Beclin-1 (Figure 3.7B), were quantified by qRT-PCR. The results for LC3 were consistent with other data presented in this work. On the one hand, the LC3 mRNA levels were highest in the CHO-t cells and lowest in the CHO-l cells, similar to what was observed in terms of lysosomal content (LTG staining) and LAMP-2 mRNA levels. Also, LC3 levels increased in the CHO-t cells after 3 days of glutamine deprivation. It appears that the CHO-t cells have higher abundance of both LC3-I and LC3-II, as was also observed for the mRNA quantification for this protein. It is difficult to interpret the biological significance of the higher LC3 mRNA levels in CHO-m cells without glutamine, since they do not seem to correlate with other markers of autophagic activity. Perhaps the kinetics of autophagy were not fully captured by this experiment. It is also difficult to interpret the biological significance of beclin-1 mRNA levels, since the trends are opposed to the other markers used in this study.
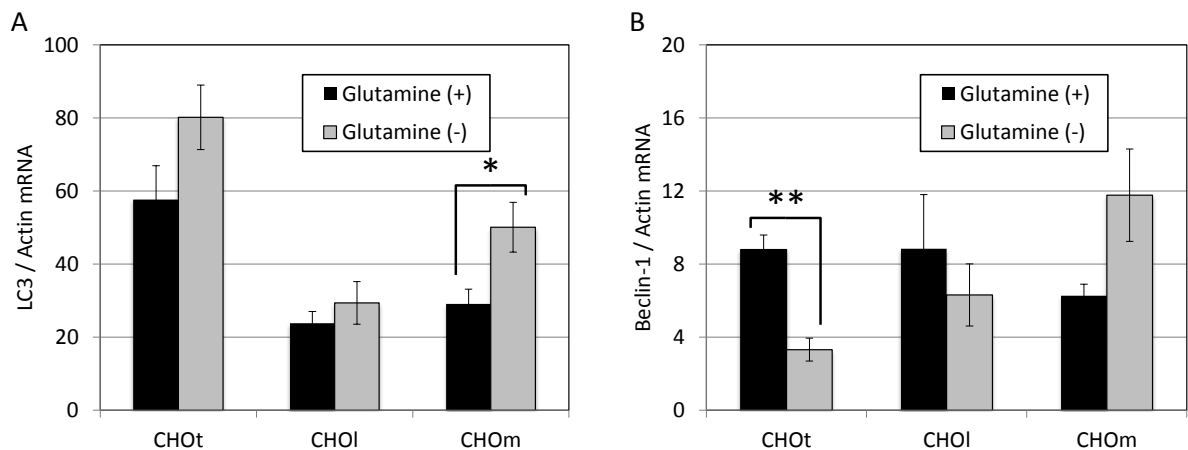
Figure 3.7.   Effect of glutamine deprivation on mRNA levels of core autophagy genes.
(A) LC3 and (B) Beclin-1. All results are from day 3 of the experiment. Error bars represent the SEM of biological triplicates. * p value < 0.1; ** p value < 0.05

3.4   Conclusions

The results presented in this work have provided a deeper insight into the interplay between autophagy and glutamine metabolism by analyzing 3 different cell lines. This insight can be useful when defining strategies to increase fed-batch process performance and understanding that the same responses will not be obtained with all CHO cell lines.

The CHO-t, CHO-l and CHO-m cells overall responded in a decreasing order of susceptibility to exogenous glutamine deprivation. The CHO-t cells were the most sensitive of the three to glutamine deprivation, developing under this stress robust lysosomal expansion and loss of mitochondrial mass, paired with increased induction of autophagy. This appears to explain their loss of cell-specific productivity in the absence of glutamine and the successful manipulation with chemical autophagy inhibitors to increase process performance. The CHO-m cells were on the other extreme of the glutamine sensitivity spectrum, with no significant induction of glutamine-dependent autophagy. It remains to be seen whether these cells have indeed higher basal autophagy, and to what extent its inhibition may increase recombinant protein production. Lastly, the CHO-l cells were intermediate in their glutamine susceptibility and glutamine-dependent autophagy. However, the benefit of autophagy modulation in this cell line may prove to be more difficult to demonstrate, because the cell specific productivity was not considerably affected by autophagy and because their

autophagy response does not appear to be strong enough in the short term to produce the extensive physiological reconfiguration observed in the glutamine-sensitive cells.

The exogenous glutamine deprivation did not reduce the viability but produced a dramatic decrease of the proliferation capacity and energy metabolism of all three CHO cell lines tested. However, each of them had different responses in terms of autophagic activity, organellar reconfiguration, and cell-specific productivity. These observations can be useful in the design strategies, particularly aiming at maximizing proliferation, which can have a significant impact on overall process performance.

This study thus highlights the unique role of glutamine in fed-batch bioprocesses. A revealing follow-up to this work could be to compare in terms of gene expression profiles matching conditions of glutamine supplementation and deprivation. Such follow-up, coupled with functional assays, could reveal strategies to engineer cells to become more resistant to autophagy induction (as would be the case of the glutamine-sensitive CHO-t cells) or to have them proliferate more while retaining their productivity (as would be the case of the CHO-m cells). Another follow-up of this work would be an analysis of the impact of glutamine deprivation on protein glycosylation, an important dimension of process performance.

4 Combining autophagy inhibition and glutamine metabolism-based process strategies to increase fed-batch performance

The previous chapter explored the interplay between glutamine metabolism and autophagy and its effect on the key process performance parameters, i.e. cell proliferation, cell productivity and product yield. This included an analysis of the varying response of 3 different cell lines. The present chapter presents work to influence CHO cell metabolism by adding TCA intermediates to further increase fed-batch process performance.

Simply replacing glutamine with TCA intermediates was not effective and this was likely due to glutamine having several roles in cellular physiology besides its anaplerotic function in mitochondria. Therefore a strategy of partial glutamine replacement was devised to combine the supplementation of low glutamine levels and TCA cycle intermediate additions. In particular, α-ketoglutarate feeding had a proliferative capacity comparable to cultures with excess glutamine and yet the ammonia accumulation was even lower than that of fed-batch controls. Once these cultures with maximal proliferation were treated with 3-MA, the overall t-PA yield was increased to a maximum 4.5-fold over the control fed-batch, whereas (as discussed in Chapter 2), treatment with 3-MA alone had enabled a 2.8-fold increase. Finally, another potential autophagy inhibitor, STO-609, was tested as an alternative method to increase recombinant protein production.

4.1 Introduction

The benefit of glutamine for mammalian cell proliferation is well known (Jeong and Wang, 1995). Numerous efforts have aimed at finding suitable replacements for this amino acid such as by supplementing mammalian cell cultures with glutamate and/or asparagine (Christie and Butler, 1999) or pyruvate (Genzel et al., 2005). While reducing ammonia accumulation, glutamine replacement often results in decreased proliferation rates. In biological research literature cell-permeable molecules such as methyl-pyruvate (Buzzai et al., 2005) or dimethyl α–ketoglutarate (Eng et al., 2010) have been reported to partially rescue cells from depletion of energy sources or from extrinsic death-inducing signals. The critical role of glutamine in cell proliferation is at least in part explained by the efficiency with which this amino acid functions in the replenishment of the TCA cycle intermediate

pool, anaplerosis, notably citrate and malate levels (DeBerardinis et al., 2008). These metabolites are heavily consumed by proliferating cells to produce biosynthetic precursors and reducing power to fuel cell expansion.

New perspectives on the importance of glutamine in bioprocess performance come from recent work demonstrating that glutamine depletion can induce autophagy (Nicklin et al., 2009) and thereby decrease protein productivity in CHO cells (Chapter 2, Jardon et al., 2012). Given that unlimited glutamine supplementation results in the production of unacceptable ammonia levels (Schneider et al., 1996), detrimental to protein quality (Gawlitzek et. al, 2000), a viable bioprocess design strategy should incorporate a mechanistic understanding of the key role glutamine plays in cell physiology.

The successful use of the chemical inhibitor of autophagy 3-methyl adenine (3-MA) to increase production of recombinant t-PA with uncompromised glycosylation (Jardon et al., 2012), suggests that another approach would be to add other chemicals to modulate this pathway to increase product yield. Autophagy decreases cell-specific productivity likely through clearance of ribosomes or recombinant protein from the secretory pathway (Jardon et al., 2012). Therefore, it was of interest to interfere in this pathway at its earliest stages or in upstream pathways, to prevent its activation. The adenosine monophosphate–activated protein kinase (AMPK) pathway, is an intracellular energy sensor. When AMPK is activated, it interacts with ULK1/2 to initiate autophagy (Egan et al., 2011) and so this was targeted using the inhibitor STO-609 (Høyer-Hansen et al., 2007).

4.2   Materials and methods

4.2.1   Cell culture

CHO540/24 cells, producing tissue plasminogen activator were used in this study. Recent work (Chapter 2, Jardon et al., 2012) has shown their sensitivity to glutamine-dependent autophagy, greater than for two other cell lines studied (Chapter 3). Maintenance and fed-batch cultures were performed as previously described (Jardon et al., 2012). Supplementation with α-ketoglutarate (Sigma, St. Louis MO) used a 400 mM solution in 0.8 N NaOH. As reported previously, chemical inhibition of autophagy used 3-methyl adenine (3-MA, Sigma), from a 500 mM stock prepared in 0.5 N HCl; the final concentration in

cultures treated with 3-MA was 10 mM. Volume differences between the 3-MA treated and each respective untreated control culture were less than 5%. STO-609 (Sigma) was diluted in DMSO and used at a working concentration of 25 μM.

A scale-down system was devised to operate multiple simultaneous cultures with various supplementation conditions, while reducing culture volumes compared to shake flask cultures. This system allows up to 22 independent cultures in suspension with volumes as low as 1 mL. Cultures were inoculated in 5 mL round bottom culture tubes (Falcon-BD Biosciences, Franklin Lakes, New Jersey) at a cell concentration of 3 x 10^6 cells/mL and placed in a fixed speed rotator (Sarstedt, Nümbrecht, Germany) inside a 37 ºC, 95% RH and 5% CO2 incubator for the duration of the experiment. Initial volume was 1.5 mL, sampling volume was 0.5 mL and daily fed-batch additions were 0.5 mL.

4.2.2   Analytical techniques

Viable cell concentration was measured by trypan blue dye exclusion using a Cedex automated cell counting system (Innovatis, Bielefeld, Germany), as previously described. Quantification of t-PA produced by CHO-t cells was performed using a colorimetric activity assay previously described (Jardon et al., 2012) using a conversion factor of 630,000 U/mg (specific activity of the standard) to report t-PA concentration. Ammonia was quantified using a gas-sensing electrode (Cole Parmer, Vernon Hills, IL).

4.3   Results and discussion

4.3.1   Glutamine plays a unique role in cell proliferation and cannot be entirely replaced

Figure 4.1 shows the results of the screening experiment for TCA cycle intermediates as potential glutamine replacements. The selection of these metabolites was based on stability, water solubility and cost. The cultures supplemented with 4 mM glutamine or with no addition of glutamine served as positive and negative controls, with the cell concentration reached 4.2 and 1.8 x 10^6 c/mL, respectively, after a 3-day fed-batch culture. The t-PA concentrations in these positive and negative controls were 42 and 15 μg/mL, respectively. Cultures supplemented with only α–ketoglutarate, citrate, malate or succinate reached a

57

maximum of 2.0 x10^6 c/mL, comparable to the negative control. Similarly to the cell proliferation results, t-PA concentration in these cultures was also comparable with the negative control. On the other hand, cultures supplemented with TCA cycle intermediates as well as a low level of glutamine, reached approximately 3 x 10^6 c/mL, i.e. ~75% of the positive control. Despite the slightly lower proliferation in these cultures, production of t-PA was comparable to that of the positive control, indicating a higher cell-specific productivity than the 4 mM glutamine control. The culture supplemented with only low levels of glutamine (1mM) yielded similar results as the parallel cultures with additional TCA cycle intermediates. This observation suggests that the main effect observed in this experiment was due to the presence or absence of the daily 1 mM glutamine additions. However, on day 2 there was an encouraging result, with the t-PA accumulation 15% higher in cultures treated with any of the TCA cycle intermediates and 1 mM glutamine, in comparison with the 1 mM glutamine alone (data not shown). Overall, in this experiment supplementation with TCA cycle intermediates did not restore growth or t-PA production, unless at least low levels of glutamine were provided.

	A												B										
Glutamine	-	4	-	-	-	-	1	1	1	1	1		-	4	-	-	-	-	1	1	1	1	1
α-Ketoglutarate	-	-	4	-	-	-	4	-	-	-	-		-	-	4	-	-	-	4	-	-	-	-
Citrate	-	-	-	4	-	-	-	4	-	-	-		-	-	-	4	-	-	-	4	-	-	-
Malate	-	-	-	-	4	-	-	-	4	-	-		-	-	-	-	4	-	-	-	4	-	-
Succinate	-	-	-	-	-	4	-	-	-	4	-		-	-	-	-	-	4	-	-	-	4	-
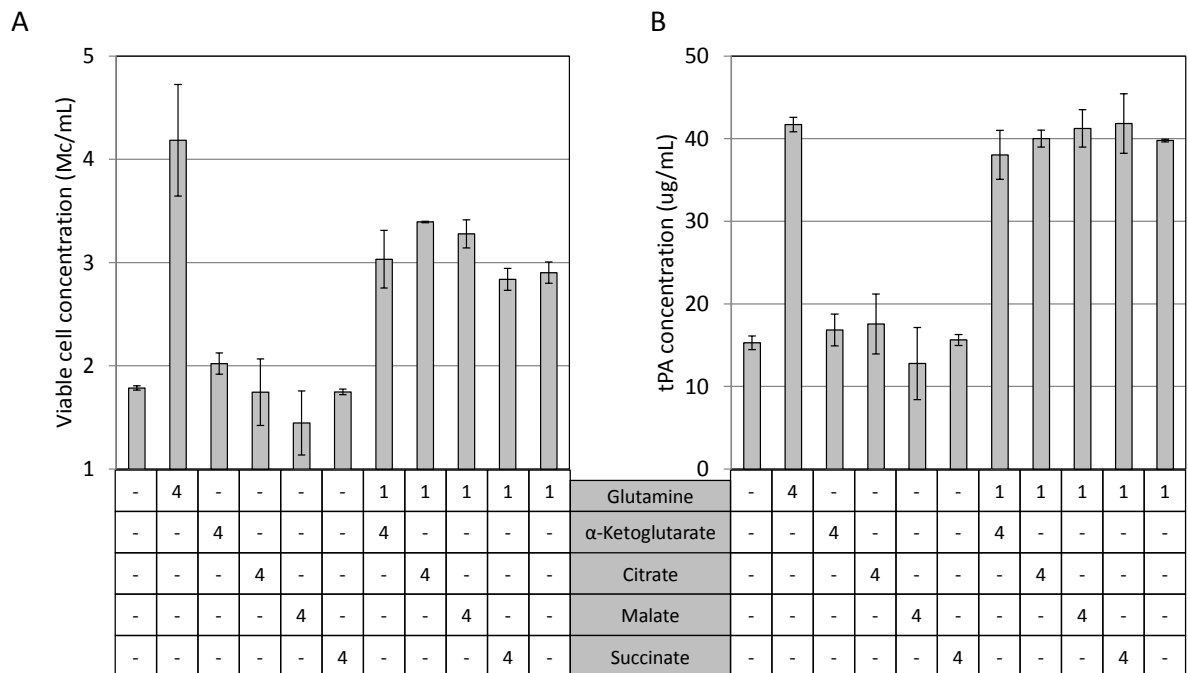
Figure 4.1.   Screening of TCA cycle intermediates for use as glutamine replacements. Viable cell (A) and t-PA (B) concentrations on day 3. Values in the design matrix indicate concentration in mM. Error bars represent the standard deviations of biological duplicates.

A cell-permeable TCA intermediate derivative, di-methyl succinate was used to test the hypothesis of whether facilitated transport to the mitochondria could rescue the proliferation capacity of cells in the absence of glutamine (Figure 4.2). However, only in the presence of at least 0.5 mM glutamine, did the di-methyl succinate addition increase cell proliferation and t-PA production. In cultures with 1 mM glutamine cell proliferation and t-PA production levels were comparable to the 4 mM glutamine control. Thus, facilitated transport into the mitochondria of di-methyl succinate alone was not sufficient to restore proliferation in glutamine-deprived CHO cells.

As in the previous experiment, supplementation of TCA cycle intermediates or cell-permeable derivatives required daily 1 mM glutamine addition to restore growth and t-PA production. A dose response down to 0.5 and 0.1 mM daily additions revealed diminishing cell and protein production responses.

4	1	0.5	0.1	-	1	0.5	0.1	-	0.5	-	Glutamine	4	1	0.5	0.1	-	1	0.5	0.1	-	0.5	-
-	-	-	-	-	4	4	4	4	-	-	α-Ketoglutarate	-	-	-	-	-	4	4	4	4	-	-
-	-	-	-	-	-	-	-	-	4	4	Di-methyl Succinate	-	-	-	-	-	-	-	-	-	4	4
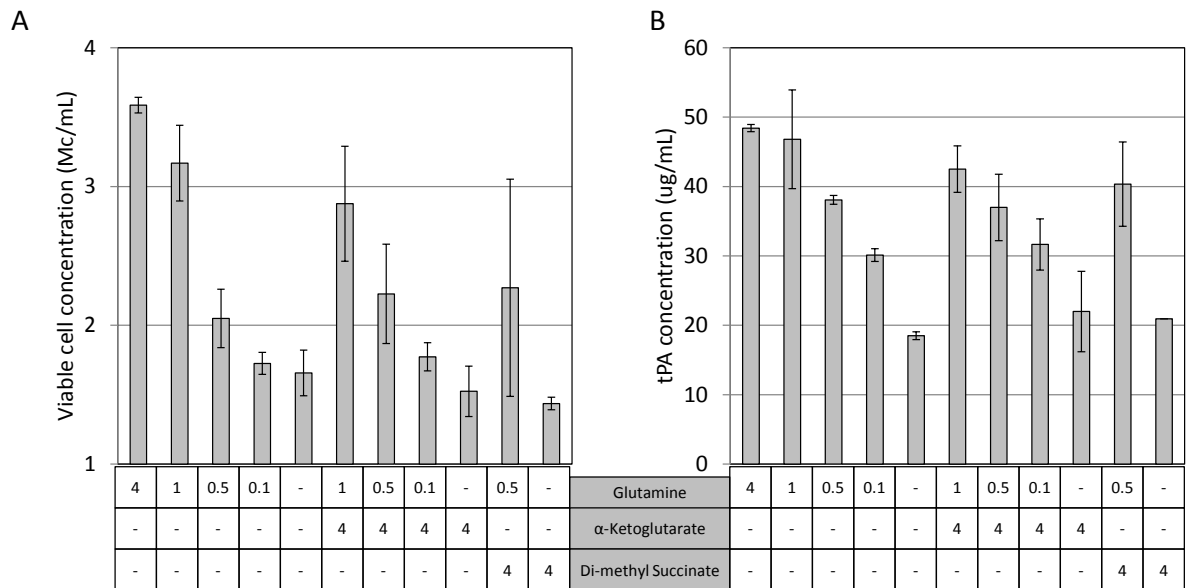
Figure 4.2.   Testing of cell-permeable derivatives of TCA cycle intermediates for use as glutamine replacements.
Viable cell and t-PA concentrations on day 3. Error bars represent the standard deviations of biological duplicates.

These results agree with previous work (Nicklin et al. 2009) showing that intracellular glutamine is indirectly necessary for the effective activation of the mammalian target of rapamycin (mTOR) kinase, which regulates protein translation, cell growth and autophagy. A

key aspect is that transport across the plasma membrane of leucine and other essential amino acids that regulate mTOR activity requires simultaneous glutamine efflux, carried out by the bidirectional transporter SLC7A5/SLC3A2. This transport system is highly specific to glutamine, which cannot be replaced by glutamate or α–ketoglutarate (Nicklin et al., 2009). Thus, in the absence of intracellular glutamine, essential amino acids cannot be imported into the cell even if they are present in the extracellular environment. The source of the intracellular glutamine can be endogenous if cells express glutamine synthetase or exogenous, through the Na^+-dependent amino acid transporter SLC1A5. Figure 4.3 illustrates this mechanism in a simplified diagram.
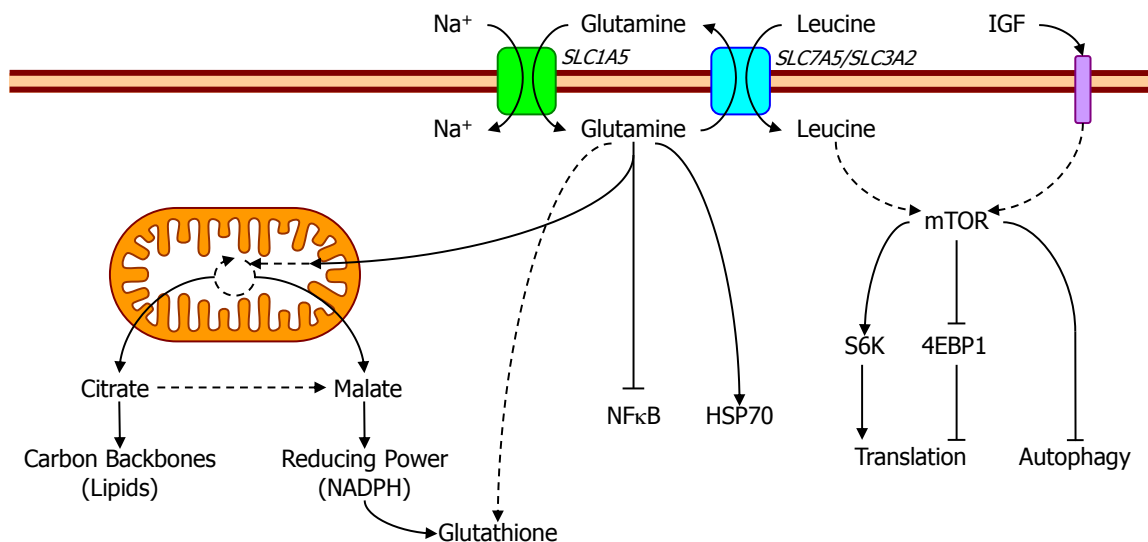
Figure 4.3.   Physiological roles of glutamine
Glutamine sustains multiple physiological functions required for cell proliferation, survival and resistance to stress

It was based on this insight that a process strategy of partial glutamine replacement was devised to combine supplementation of low glutamine levels (1 mM per day), to maintain active the transmembrane amino acid transport system, and a TCA cycle intermediate (α-ketoglutarate), to provide the anaplerotic substrate (4 mM per day). This process strategy is designated hereafter as PGR (for partial glutamine replacement).

4.3.2 Partial glutamine replacement reduces ammonia accumulation and improves cell viability

Figure 4.4 presents the outcome of the PGR strategy in terms of cell viability (Figure 4.4A) and ammonia accumulation (Figure 4.4B), compared to a fed-batch supplemented with glutamine, roughly matching the cellular consumption (FB-Gln) and a control fed-batch (FB) with only 4 mM initial glutamine and no further glutamine supplementation. Cell viability was maintained above 90% until day 10 in the PGR and control FB cultures, whereas it started declining by day 8 in the FB-Gln. Treatment with 3-MA produced a clear decrease in cell viability in the FB and FB-Gln. Interestingly, the viability of the PGR fed-batch treated with 3-MA remained higher and was comparable to the non-treated cultures. With and without 3-MA addition, the maximum ammonia accumulation was considerably reduced in the control FB, compared to the FB-Gln, reaching 19 and 28 mM, respectively. The ammonia concentration in the PGR fed-batch was even lower, at 11 mM. It may be that the higher susceptibility to 3-MA treatment in terms of viability decrease in the control FB and FB-Gln cultures is related to their higher ammonia levels. Future experiments will need to distinguish the effects of glutamine and α-ketoglutarate in the improved PGR fed-batch performance.
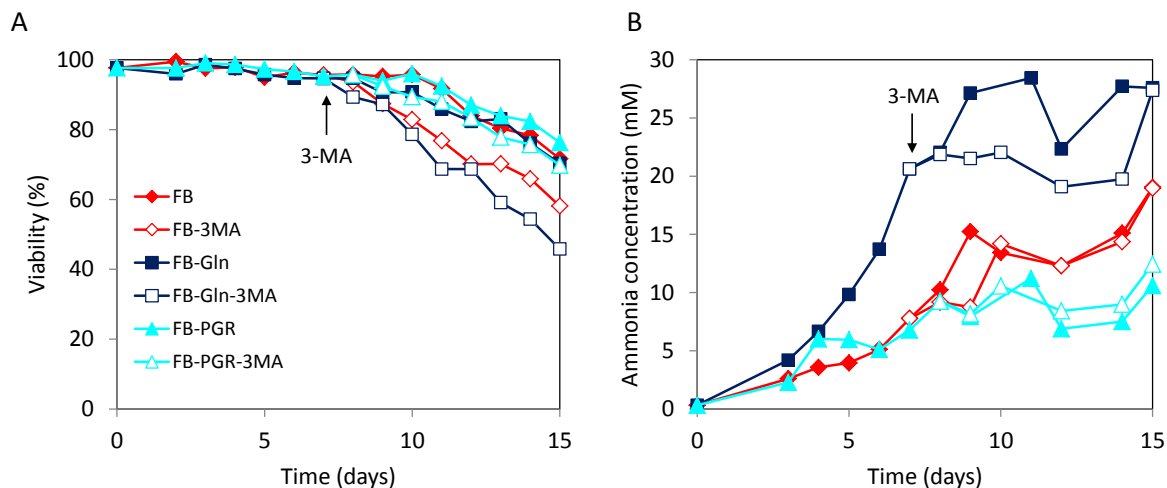
Figure 4.4. Cell viability and ammonia accumulation with partial glutamine replacement.
Legend: FB (red): control fed-batch with 4 mM initial glutamine and no further glutamine supplementation; FB-Gln (dark blue): fed-batch with glutamine supplementation, matching the cellular consumption; FB-PGR (light blue): fed-batch with partial glutamine replacement. Open symbols refer to cultures treated with 3-MA and closed symbols to the equivalent non-treated controls. The arrow indicates time of 3-MA treatment.

4.3.3 Combination of partial glutamine replacement with 3-MA treatment further increases t-PA yield

The viable cell concentrations (Figure 4.5A), were practically identical for all cultures until day 3, after which the FB-Gln and the PGR fed-batch continued proliferating at a faster rate than the control FB. The FB-Gln, control FB and PGR fed-batches reached maximal cell concentrations of 8.8, 9.1 and 11 x 10^6 cells/mL, respectively, with the FB-Gln and the PGR fed-batches reaching this peak 3 to 4 days earlier than the control FB. Thus, the PGR method restored the rapid cell growth as in the FB-Gln, but with reduced ammonium generation. As observed in previous similar experiments, upon treatment with 3-MA, the viable cell concentration decreased continuously in all the treated cultures.

The production of t-PA (Figure 4.5B) was normalized with respect to the final total mass of active t-PA in control FB. The total t-PA mass was calculated by multiplying the assayed t-PA concentration by the culture volume. This total mass is shown instead of the t-PA concentration so as to account for the greater dilution in the FB-Gln and the PGR cultures. The t-PA production in the 3-MA treated control FB was 2.7 times higher than the control, comparable to the 2.8 times reported in Chapter 2. With 3-MA addition the FB-Gln and the PGR fed-batch production increased 2.1 and 1.7 times, respectively. The 3-MA treated FB-Gln and PGR fed-batches produced 4.6 times more t-PA than the control FB without 3-MA addition.

Overall, by combining the maximized cell proliferation obtained by PGR with inhibition of autophagy by 3-MA both higher cell and t-PA concentrations were obtained. This yielded an overall 4.6 fold increase of t-PA produced compared to the FB. These results have been duplicated (see Appendix A), producing the same trends as in Figures 4.4 and 4.5, but with differences in sampling times and total culture duration that do not allow estimation of variance. In the replicate experiment, the overall t-PA yield on day 13 in the PGR was 3.6-fold that in the control FB. At that time point, the replicate experiment was stopped prematurely, although the increasing trend appears to continue.
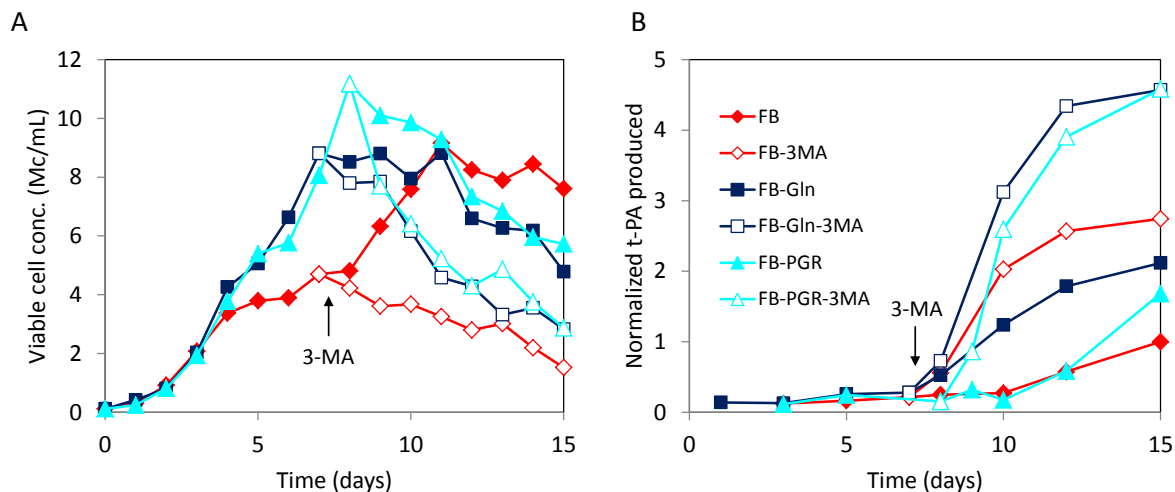
Figure 4.5.   Viable cell concentration and total t-PA produced with partial glutamine replacement.
Legend: FB (red): control fed-batch with 4 mM initial glutamine and no further glutamine supplementation; FB-Gln (dark blue): fed-batch with glutamine supplementation, matching the cellular consumption; FB-PGR (light blue): fed-batch with partial glutamine replacement. Open symbols refer to cultures treated with 3-MA and closed symbols to the equivalent non-treated controls. The arrow indicates time of 3-MA treatment.

4.3.4   Investigation of other chemicals to inhibit autophagy and enhance protein production

Given the remarkably increased CHO cell t-PA production obtained with 3-MA addition, a major question becomes whether the approach can be generalized to other systems. An investigation using 3-MA as an additive for monoclonal antibody producing CHO cell fed-batch cultures is being investigated by another student with promising and interesting results. Alternatively, selection and testing of inhibitors acting on related pathways could provide additional insights into the mechanism by which autophagy decreases protein production as well as perhaps further increased recombinant protein yields.

It is likely that the mechanism by which autophagy decreases cell-specific productivity (Jardon et al., 2012) involves sequestration of vesicles in the secretory pathway carrying the recombinant protein or elimination of components of the translation machinery, such as ribosomes (ribophagy) or parts of the endoplasmic reticulum (reticulophagy). TEM imaging appears to support at least the second hypothesis, since upon glutamine deprivation, the granular, electron-dense mass of ribosomes decreases visibly within one day. Effective

63

autophagy inhibitors for enhanced protein production should interfere with early stages of the pathway, i.e. preventing vesicle nucleation, or in even upstream pathways, preventing autophagy induction. Autophagy inhibitors such as chloroquine or bafilomycin A1 are not suitable for this purpose, since they prevent fusion between autophagosomes and lysosomes and so do not block autophagosome generation. Preliminary verification in fed-batch experiments using chloroquine was consistent with this hypothesis. Furthermore, since most lysosomal chemical inhibitors act by increasing the pH of acidic compartments, they could also disrupt the glycosylation machinery, since the Golgi system is also acidic and slight increases in the Golgi pH have caused mislocalization of glycosyltransferases and disrupted proper protein glycosylation (Rivinoja et al., 2009).

The most widely used chemical inhibitors of early stage autophagy are the PI3K inhibitors, such as 3-MA. Wortmannin is another PI3K inhibitor that could be investigated in this context since it has a longer-term effect than 3-MA (Wu et al., 2010). However, it is less specific than 3-MA for the class III PI3K (Miller et al., 2010) and so does not only inhibit the kinase activity that signals the autophagy process.

Thus, it was chosen instead to inhibit upstream positive regulators of autophagy. The best characterized upstream pathways that lead to activation of autophagy are the mTOR pathway, the AMPK pathway and the ER stress response, also known as UPR, for unfolded protein response (Kroemer et al., 2011). The UPR and AMPK pathways are positive regulators, whereas mTOR is a negative regulator of autophagy. The AMPK pathway is a master sensor of energy stress (Mihaylova et al., 2011) and thus likely to be involved in the stress leading to autophagy under glutamine limited culture conditions.

When the adenosine monophosphate–activated protein kinase (AMPK) is activated, it interacts with ULK1/2 to initiate autophagy (Egan et al., 2011). When calcium is mobilized into the cytoplasm, CAMKK2β is activated, which functions as a potent inducer of autophagy and that can be inhibited by the naphthoyl-fused benzimidazole kinase inhibitor, STO-609 (Høyer-Hansen et al., 2007). In order to establish a proof of concept for the use of STO-609, the short-term scaled-down fed-batch methodology described previously was used for a factorial design experiment (Table 4.1).

Table 4.1.   Experimental design for evaluation of STO-609 as an additive

Condition	Glutamine Concentration (mM)	STO-609 Concentration (μM)	Description
1	0	0	Negative control, baseline conditions with induction of autophagy upon glutamine depletion
2	0	25	Test of STO-609 to overcome the loss of productivity expected by glutamine deprivation (main purpose of experiment)
3	4	0	Positive control for high protein production, result that the treatment could match if effective (though high ammonia)
4	4	25	Double positive control, not relevant to fed-batch conditions

The results of this simple experiment (Figure 4.6) are useful in determining the potential for STO-609 to increase protein production in CHO cell fed-batch cultures. The negative control produced, as expected, the lowest t-PA concentration (26 μg/mL), whereas the glutamine positive control produced 35% more t-PA. The culture treated production with STO-609 exceeded the glutamine control, with a t-PA concentration 52% higher than the negative control. Interestingly, the double-positive culture obtained a considerable increase, yielding 120% more t-PA than the negative control. This result is consistent with those observed in shake flask cultures, where supplementation with glutamine or PGR, along with autophagy inhibition using 3-MA also resulted in increased t-PA production (Figure 4.5). The double-positive highest production result could mean that glutamine supplementation alone is not sufficient to prevent autophagy at later time points, as other autophagic stimuli may begin to appear. Another explanation could be that the basal autophagy activity of these cells already decreases their productivity and therefore its inhibition results in increased production, even in nutrient-rich conditions. Overall, the effectiveness of using STO-609 also reveals that there may be calcium and AMPK-mediated mechanisms by which autophagy is being triggered in this system.

A 14-day fed-batch cultivation (Figure 4.7) was operated according to the established baseline control FB protocol (not using the PGR approach for maximal cell proliferation). Similar to the 3-MA treatment, STO-609 was supplemented as a single addition on day 7. Addition of this chemical resulted in a 1.6-fold increase in t-PA over the control fed-batch. This fed-batch experiment has not yet been replicated.
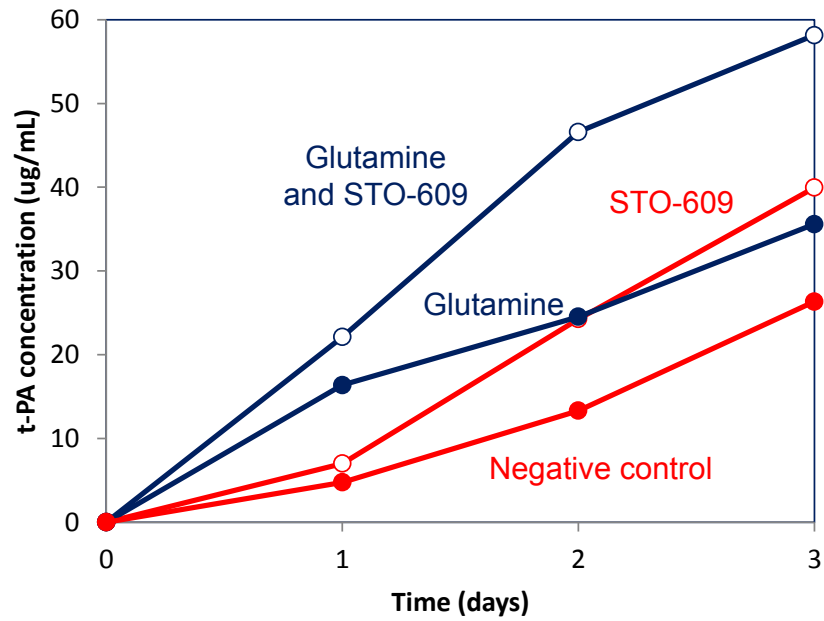
Figure 4.6. STO-609: another small molecule candidate to increase production
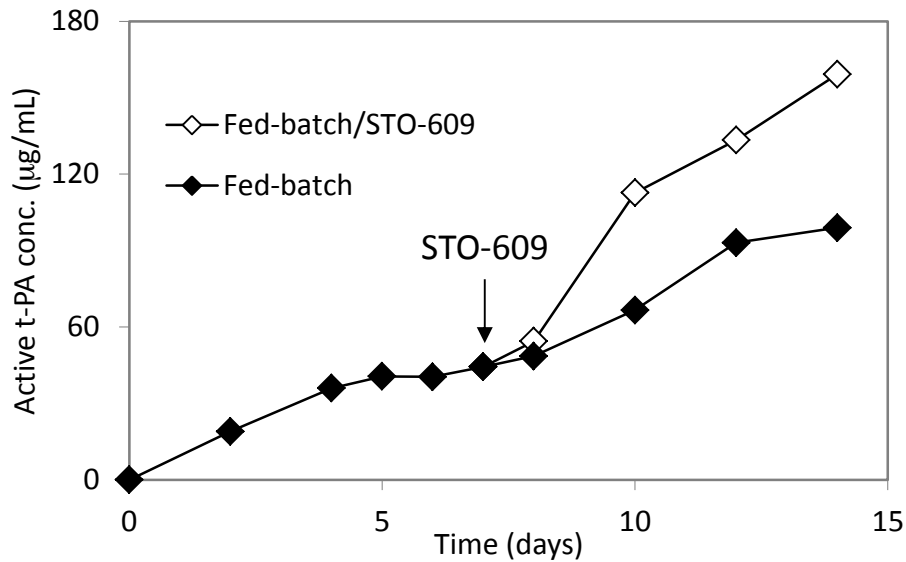
Figure 4.7. Production of t-PA in fed-batch culture with STO-609 treatment.
On day 7 (indicated by the arrow), the fed-batch culture was split and half of it treated with 25 μM STO-609.

4.4 Conclusions

This chapter described further developments and insights to increase bioprocess performance, resulting in the partial glutamine replacement (PGR) strategy that enabled maximization of cell proliferation, even though it did not entirely preclude autophagic stimuli. Combination of the PGR strategy with autophagy inhibition resulted in the further increase from a 2.8-fold, as reported in Chapter 2, to a maximum of 4.6-fold in t-PA production. A biphasic approach was needed, since the inhibition of autophagy resulted in cytotoxic side-effects and severely limited proliferation.

Various studies have reported loss of productivity over fed-batch culture time (Yu et al., 2011; Stansfield et al., 2007). ER processing may be part of the bottleneck, since overexpression of the UPR mediator XBP-1, which expands the ER capacity, has shown some benefit in increasing protein production (Ku et al., 2008). However, the considerable rescue of productivity wrought by inhibition of autophagy in this study, brings a new perspective to these studies and to the bioprocessing field in general, i.e. that increasing recombinant protein yield should take in account not only protein biosynthesis, but also its clearance by autophagy. Overall, the mass balance of recombinant protein production in mammalian cells risks being incomplete if it neglects the removal by autophagy.

This work suggests that glutamine has a unique role in process performance that is related to autophagy. Follow-up work should include bioreactor studies to more consistently control pH and oxygen. A concern about oxygen in the shake flask cultures is that the higher growth cultures could have been exposed to significantly different oxygen levels. Further study could also identify the optimal dosage and timing of STO-609 additions as well as determine if there are effects on protein glycosylation. An important follow-up of this chapter should include the comparison of additions of 1 mM glutamine alone with the combination of 1 mM and α-ketoglutarate, in order to distinguish the effects of each.

 Overall this Chapter shows again the crucial role of autophagy in modulating cell-specific productivity and the influence of glutamine on cell proliferation. Also, these findings establish a basis for follow-up investigations on the use of chemical inhibitors as well as cell line engineering and RNAi approaches to increasing bioprocess performance. For the latter, preliminary efforts are described in Appendix C.

5 Exploring autophagy and glutamine metabolism in cancer cell lines

The work presented in this dissertation has mainly related to the link between autophagy and glutamine metabolism in CHO cells with the aim of increasing recombinant protein production in fed-batch processes. The present chapter describes related studies in a different model system and biological context. As in bioprocess engineering, cell proliferation, viability and survival are fundamental topics in cancer biology, albeit from an opposite perspective where they are a problem to be eliminated. Thus, the interplay between autophagy and glutamine metabolism in cancer cells was briefly investigated.

This work was also stimulated by the availability of Raman spectroscopy, a technology that enables the label-free, non-destructive analysis of living biological cells and tissues. The response of mouse and human cancer cells to glutamine deprivation was probed by Raman spectroscopy and compared to fluorescence microscopy results. The recovery dynamics of starved cells using this technology were also evaluated. Overall, this study establishes a precedent on the use of Raman spectroscopy to detect changes in live cells under conditions that trigger autophagy. A brief preliminary exploration of glutamine-mediated responses of cancer cells to chemical treatments can be found in Appendix D.

5.1 Introduction

The numerous physiological roles of autophagy in health and disease make this cellular process relevant to a wide variety of fields in biological research, both fundamental and applied. Studies on autophagy come from very diverse biological contexts, such as cancer, neurodegenerative disorders, infectious diseases, inflammatory disorders and aging (Mizushima et al., 2010), using a variety of model systems (Kourtis and Tavernarakis, 2009).

The established analytical techniques to study autophagy include electron microscopy, fluorescence microscopy and immunoblotting of autophagy-related proteins (Klionsky et al., 2008; Mizushima et al., 2010). However, the limitations of these techniques make new methods of detection a persistent need, particularly for in-vivo and non-invasive analysis. Raman spectroscopy does not require labeling or staining and can be non-invasive. This

technology has been successfully used to monitor cellular processes such as apoptosis (Zoladeck et al., 2011) and embryonic cell differentiation (Schulze et al., 2010).

Autophagy is mainly a survival response to cellular stress (Kroemer et al., 2010), in contrast to apoptosis (type I cell death) where beyond a threshold level apoptosis leads irreversibly to a termination of cellular function. The characteristic phenotype of autophagy is the appearance of double membrane vesicles, named autophagosomes that sequester the intracellular components targeted for degradation. Once they mature, autophagosomes fuse with lysosomes and their contents are degraded (Mizushima et al., 2010). If the stimuli that triggered autophagy disappear, cells can revert to their original physiological state (Lum et al., 2005) by downregulating autophagosome generation and allowing clearance of the autophagosomes already present in the cell.

This study establishes a precedent on the use of Raman spectroscopy to detect changes in live cells under conditions that trigger autophagy. The link between autophagy and amino acid deprivation is widely recognized (Mizushima et al., 2010). Among the amino acids, glutamine exerts a singular role as a potent modulator of autophagy, though its particular mechanism has been established only recently (Nicklin et al., 2009). We produced Raman signatures in cancer cells undergoing glutamine deprivation as a first approach to analyze autophagy using this technolgy.

5.2 Materials and methods

5.2.1 Cell culture

Two cancer cell lines were used for the present study. Human breast carcinoma MCF7 cells stably expressing the autophagy reporter GFP-LC3 were cultured in DMEM supplemented with 10% FBS, 1X essential amino acids and 4 mM glutamine (GIBCO-Invitrogen, Grand Island, NY). Metastatic prostate carcinoma mouse cells LMD (Setiadi et al., 2007) were generously provided by Dr. Wilfred Jefferies. LMD cells were cultured in DMEM supplemented with 10% FBS, 1X penicillin/streptomycin and 4 mM glutamine (GIBCO-Invitrogen). Both cell types were cultured in static conditions at 37°C, 90% relative humidity and 5% CO_2.

In order to generate an autophagy reporter cell line from LMD cells, the hrGFP-LC3 construct previously described (Jardon et al., 2012) was used. LMD cells were transfected with the construct containing the GFP-LC3 sequence, using Lipofectamine 2000 in OptiMEM transfection medium (Invitrogen, Carlsbad, CA), according to the manufacturer's protocol. The transfected cells were sorted after expansion and then a second round of sorting was used to isolate clones. A clone displaying intermediate levels of fluorescence was selected for further work in this study.

Gold mirrors for Raman spectroscopy (Thorlabs, Newton, NJ) were precoated with matrigel (StemCell Technologies, Vancouver, Canada) for 45 min at room temperature. After removing excess matrigel, the mirrors were placed into 6-well plates and seeded with 120 μL of freshly trypsinized cells resuspended in fresh medium at a concentration of ca. 1×10^5 cells/mL. The cells were allowed to settle and adhere overnight in an incubator. Then 5 mL of complete medium was added and cells were cultured for a day. On the day of treatment, the mirrors were transferred to 6 well plates containing 5 mL of medium in each well in one of the following conditions: nutrient-rich conditions (same media as described above), glutamine deprivation (same media as described above, but not supplemented with glutamine), or amino acid starvation. Amino acid starvation medium consisted of HBSS (GIBCO-Invitrogen) supplemented with 10% FBS.

5.2.2 Fluorescence microscopy

GFP-LC3-expressing cells were seeded in FluoroDish culture dishes with cover glass bottom (World Precision Instruments, Sarasota, FL) that had been pre-coated with matrigel. Nutrient-rich, glutamine deprivation and amino acid deprivation conditions were the same as described above. For treatment, culture medium was removed and replaced with the respective fresh medium. After treatment, cells were imaged in confocal mode using an IX81 motorized inverted microscope (Olympus Life Science, Hamburg, Germany) with a water-immersion 60X objective and a filter set for GFP, at Z-increments of 0.5 μm. Image acquisition, deconvolution and projection was performed using Slidebook (Leeds Precision Instruments, Minneapolis, MN).

Table 5.1. **Description of Raman peaks of interest in the spectra**

Raman band   Assignment

Raman band	Assignment
718 cm^{-1}	Lipids (phospholipids → C-N stretch); DNA/RNA (adenine → ring breathing)
724 cm^{-1}	DNA/RNA (adenine → ring breathing)
757 cm^{-1}	Proteins (symmetric ring breathing in tryptophan)
784 cm^{-1}	782 cm^{-1}: DNA/RNA (pyrimidines → ring breathing); 788 cm^{-1}: DNA (backbone → O-P-O stretching)
811 cm^{-1}	RNA (backbone → O-P-O stretching); proteins (collagen → C-C stretching of proline and hydroxyproline)
827 cm^{-1}	Proteins (proline, hydroxyproline, out-of-plane ring breathing in tyrosine); DNA/RNA (asymmetric O-P-O stretching)
853 cm^{-1}	Proteins (collagen → C-C stretch in proline; also other proteins → ring breathing in tyrosine); carbohydrates (glycogen, polysaccharides → C-O-C stretching)
874 cm^{-1}	Proteins (collagen → C-C stretching in hydroxyproline, proteins → ring deformation in tryptophan); lipids (phospholipids → asymmetric stretch of choline); carbohydrates (C-O-C stretching)
937 cm^{-1}	Proteins (collagen type I → C-C stretching, α-helix → C-C stretching); carbohydrates (glycogen)
972 cm^{-1}	C-C BK stretching b-sheet (proteins), -CH bend (lipids)
1003 cm^{-1}	Proteins (symmetric ring breathing in phenylalanine)
1031 cm^{-1}	Proteins (collagen, keratin, C-N stretching in proteins, C-H in-plane bending of phenylalanine); lipids (phospholipids); carbohydrates (polysaccharides)

5.2.3   Raman Spectroscopy

Before spectral acquisition, the mirrors with cells were removed from the culture medium, rinsed gently, and transferred to a culture dish containing medium without serum. Spectra were generated at room temperature by scanning randomly chosen areas using an In Via Raman microscope system (Renishaw, Gloucestershire, UK). A water-immersion 40X objective was used to focus the laser beam to an area of approximately 3 x 30 μm. Raman

scattering, generated with 80 mW of 785 nm radiation, was collected for 100 s per spectrum. Each spectrum typically included contributions from at least three cells. The 400 cm^{-1} to 1800 cm^{-1} spectral interval was used to obtain general Raman spectra of each sample. To reduce collection times and cellular stress during acquisition outside the incubator environment in basal medium, most spectra were obtained only in the fingerprint region from ca. 660 cm^{-1} to 1050 cm^{-1}. For each sample four background spectra were obtained, two before and two after recording cell spectra.

5.2.4 Data analysis

Raman spectra were inspected individually for gross inconsistencies, and artifacts such as the cosmic radiation spikes were removed. The background spectra in all samples were averaged and subtracted from each of the culture spectra. Baseline flattening was then performed with a 50-point moving average, peak stripping, semi-automated procedure in two passes (with 50 iterations on the first and 25 iterations on the second pass) and thereafter smoothed by an automated smoothing filter using 30 iterations per spectrum. A list of relevant band assignments, assembled from literature, is given in Table 5.1. Statistical significance was determined using a two-tailed t-test.

5.3 Results and discussion

5.3.1 Glutamine deprivation increases autophagosome content in mouse and human cancer cells

The response of MCF7 (human breast carcinoma) and LMD (mouse metastatic prostate carcinoma) cells under glutamine deprivation was evaluated by fluorescence microscopy. Increased numbers of GFP-LC3-positive puncta were clearly visible after one day of glutamine deprivation (Figure 5.1). These punctate structures are indicative of autophagosomes, since upon induction of autophagy, soluble LC3 (known as LC3-I), is lipidated (becoming LC3-II) and associates with the luminal and external membranes of autophagosomes. This change in LC3 configuration involves a change of fluorescence pattern from diffuse (LC3-I) to punctate (LC3-II). In lower numbers, a few punctate

structures could also be detected in the glutamine-supplemented cultures. These baseline vesicle levels correspond to basal physiological autophagic activity in the cells.
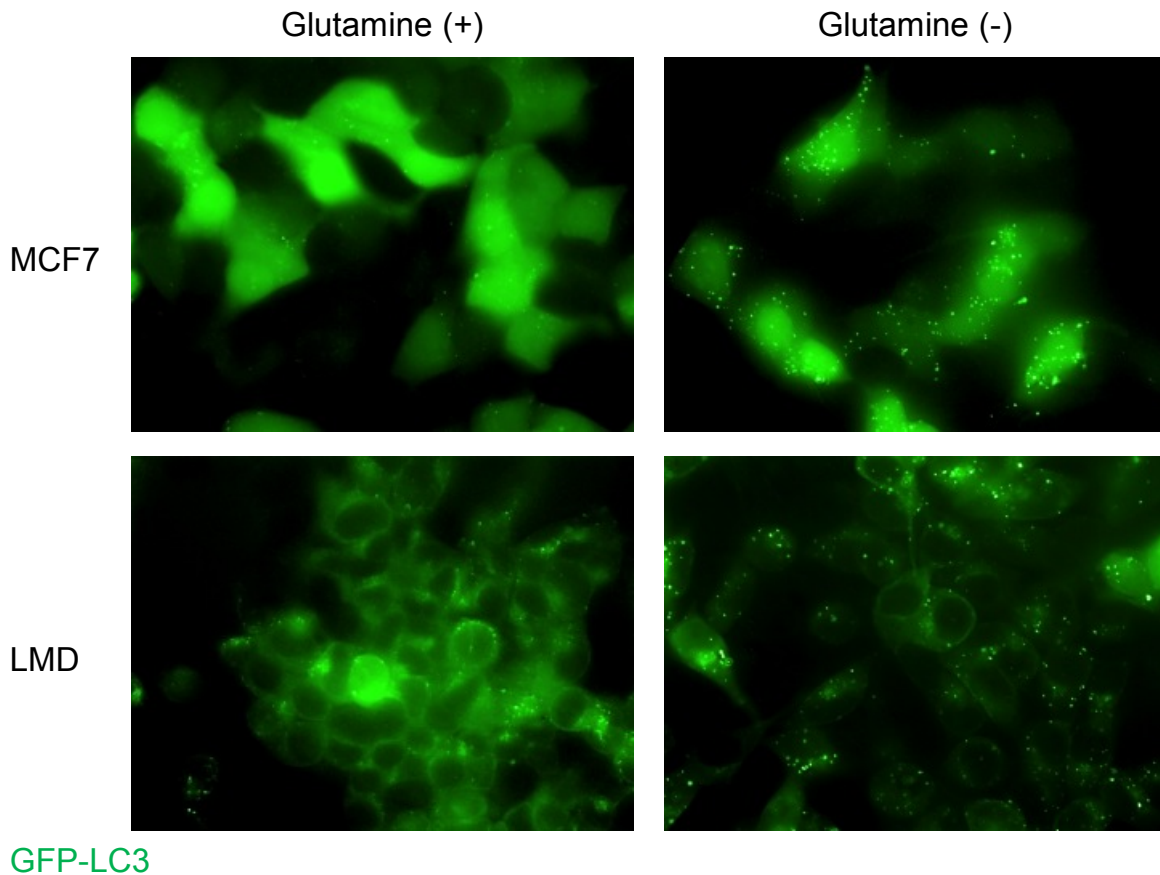
Figure 5.1. Effect of glutamine deprivation on MCF7 and LMD cells expressing GFP-LC3
Representative fluorescence micrographs of cells cultured one day in the presence (+, 4 mM) or absence (-) of glutamine.

The numbers of autophagic puncta per cell were quantified manually from fluorescence micrographs of at least 50 cells (Figure 5.2). In MCF7 cells, the average autophagosome content per cell increased 2.9 times (from 9.1 to 26.4) in the absence of glutamine. LMD cells had lower initial levels of autophagosomes but glutamine deprivation resulted in these cells in a 2.1 fold increase (from 5.5 to 11.6) of the autophagosomal compartment. The size of cells, ability to upregulate the autophagic machinery and susceptibility to glutamine deprivation may account for the quantitative differences observed between the cell lines.
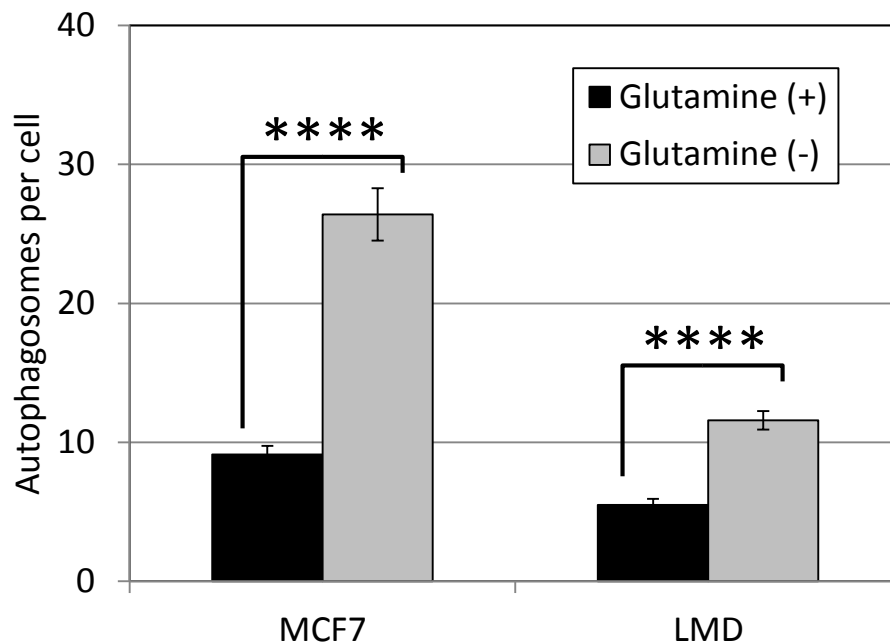
Figure 5.2.   Autophagosome levels in MCF7 and LMD cells expressing GFP-LC3.
Cells were cultured one day in the presence (+, 4 mM) or absence (-) of glutamine. Error bars represent the SEM with n $\geq$ 50. **** p value < 0.001

5.3.2   Raman spectroscopy can detect changes in live cells exposed to conditions that trigger autophagy

First, a baseline Raman signature of cells was generated over a wide range (300 to 1800 cm^{-1}) from LMD cells from unstressed growth conditions (complete medium, supplemented with glutamine) on the second day after passaging (Figure 5.3). To reduce collection times and cellular stress during acquisition, most spectra were obtained only in the fingerprint region from ca. 660 cm^{-1} to 1050 cm^{-1} for each sample. The averaged Raman spectra (n>36) of LMD cells in various conditions are presented in Figure 5.4. Spectra from cells in complete culture medium with glutamine for 2 days (Q+, blue) and in the absence of glutamine for 2 days (Q-, green) or 5 days (Q-, red) are normalized to the nucleic acid Raman band around 784 cm^{-1}. Several bands in the Raman spectra reveal differences between cells in the presence or absence of glutamine. The clearest differences appear around 718, 937, and 972 cm^{-1}.
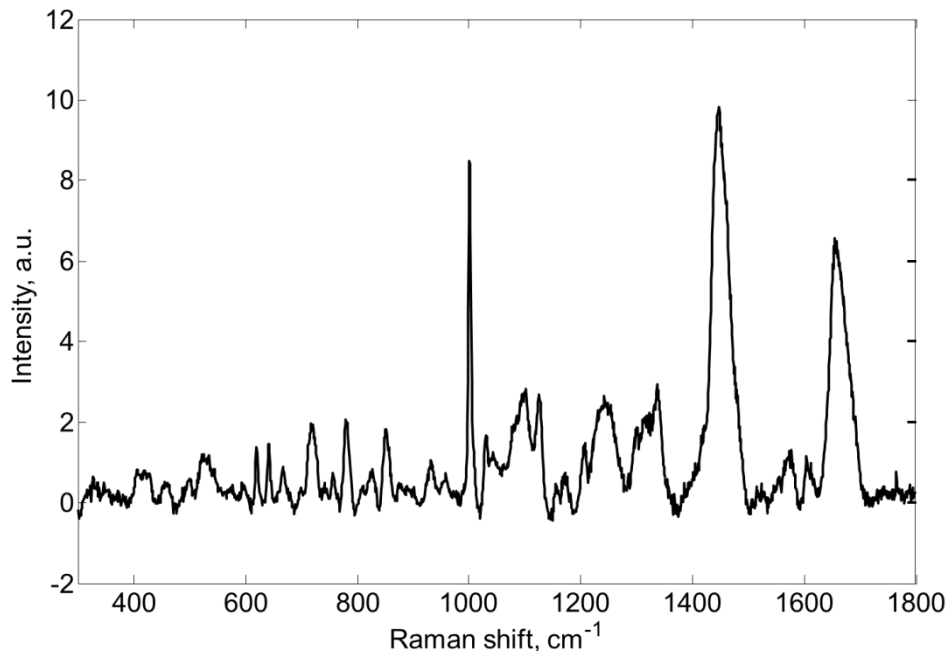
Figure 5.3. **Baseline Raman spectrum from LMD cells.**
Averaged Raman spectra from LMD cells in regular culture medium with glutamine.

The most salient difference appears in the 718 cm^{-1} Raman line that corresponds mainly to phospholipids. Since the process of autophagy involves the generation of double-membrane vesicles, it is possible that the detected increase in phospholipids reveals the increasing abundance of autophagic organelles. Further investigation is required to determine the identity and localization of the phospholipids detected, since this observation could also be non-specific for autophagy. Accumulation of membrane phospholipids has been reported in other stress conditions, particularly in apoptotic cells (Zoladek et al., 2011). It is however unlikely that the cells were undergoing apoptosis, since cell viability was retained and, as shown below, these spectral changes were reversible. The variations in the Raman line around 972 cm^{-1} are consistent with these observations, since they can also can be attributed to lipids. This Raman band has a higher intensity in glutamine-deprived cells.
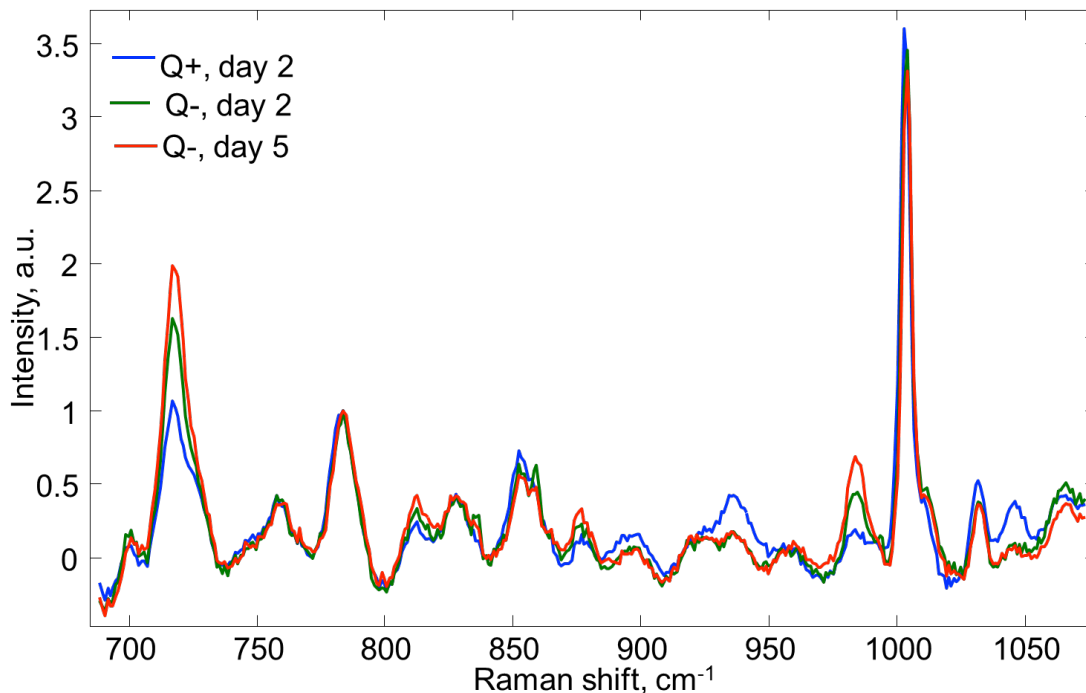
Figure 5.4.   Raman spectra of LMD cells cultured with or without glutamine.
Averaged Raman spectra (n > 36) from LMD cells in culture medium with glutamine for 2 days (Q+, blue) and in the absence of glutamine for 2 (Q-, green) and 5 days (Q-, red). Q stands for glutamine.

Another detectable difference between the two treatments (presence or absence of glutamine) appears around 937 cm^{-1}. This Raman line is formed by the contribution from proteins and glycogen. However, glycogen also produces a pronounced Raman line around 482 cm^{-1}, which is not observed in these spectra. Therefore, the difference around 937 cm^{-1} could be attributed to the expression of different proteins due to the different conditions, rather than changes in glycogen content. The reduction observed in the 1003 cm^{-1} Raman line in cells without glutamine can also be attributed to proteins (symmetric ring breathing in phenylalanine, Table 5.1). However, this change is not statistically significant. The ratio of the Raman line around 718 cm^{-1} (phospholipids) to the Raman line around 784 cm^{-1} (nucleic acid) could be proposed as a glutamine starvation indicator feature for LMD cells (Figure 5.5).
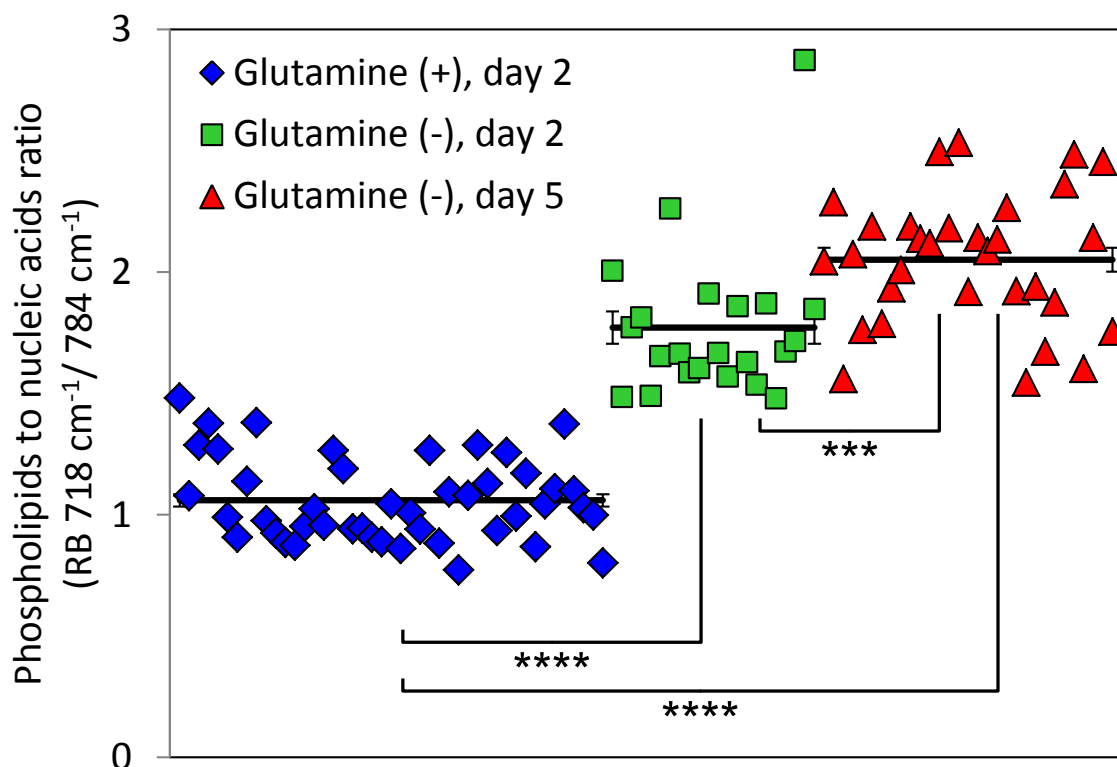
Figure 5.5. **Ratio of phospholipids / nucleic acids Raman bands in LMD cells.**
Ratio of the Raman band around 718 cm^{-1} (phospholipids) to the Raman band around 784 cm^{-1} (nucleic acid) for all collected data from LMD cells in culture medium with glutamine for 2 days (blue) and in the absence of glutamine for 2 (green) and 5 days (red). *** p value < 0.005; **** p value < 0.001

5.3.3 Raman spectroscopy can detect the recovery of cells upon removal of the conditions that activate autophagy

A major advantage of Raman microspectroscopy includes that this technology does not require labeling and that it can be non-invasive. Therefore, live cells can be returned to physiological conditions after spectroscopy and analyzed again at later time points. Taking advantage of this feature, the recovery dynamics of LMD cells from glutamine deprivation was studied. LMD cells that had been exposed to glutamine deprivation for two days were placed in complete medium containing glutamine and then reanalyzed at multiple time points (Figure 5.6). The cells were placed in a humidified incubator at 37 ºC and 5% CO$_2$ between readings.
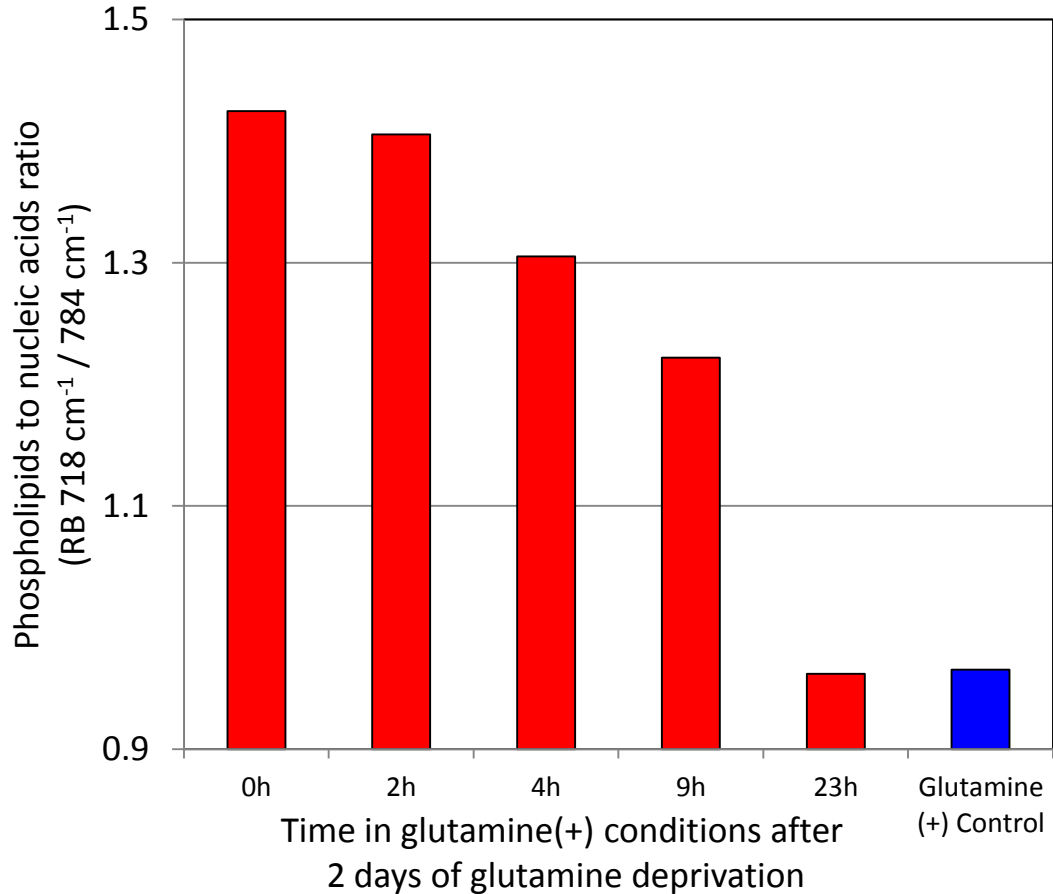
Figure 5.6.   Recovery dynamics after glutamine starvation.
Ratio of the 718 cm^{-1} Raman line (phospholipids) to the 784 cm^{-1} Raman line (nucleic acid) collected from LMD cells that had been exposed to the absence of glutamine for two days and placed back in medium with glutamine, for 2, 4, 9 and 23 hours (black circles). The baseline condition (with glutamine, red circle) is presented as a reference point.

As shown in Figure 5.6, Raman spectroscopy allowed detection of the recovery of the LMD cells 718 cm^{-1} (phospholipids) to 784 cm^{-1} (nucleic acids) ratio, once the starvation condition had been removed. By 4 hours, a detectable difference was already clear, but the recovery process continued. By 23 hours, the cells had reverted to the baseline nutrient-rich (Glutamine+) ratio.

The same glutamine deprivation experiments as described above were performed on MCF7 cells. Raman spectra were generated after 3 days of culture in the presence or absence of glutamine (Figure 5.7). Consistent with results obtained with LMD cells, the largest

differences between the two conditions were observed in the 718 and 972 cm^{-1} Raman lines, suggesting that the change in the phospholipid Raman signature as a potential indicator of this nutrient deprivation. However, the increase of the phospholipid-associated Raman lines was much less intense than the one observed in LMD cells. In MCF7 cells, the ratio of Raman lines 718 cm^{-1} (phospholipid-associated) to 784 cm^{-1} (DNA-associated) is 1.24 for cells in the presence of glutamine and 1.52 for cells in the absence of this amino acid. This appears to indicate that the phospholipids concentration relatively to nucleic acid is less affected by glutamine deprivation in MCF7 cells and potentially corresponds to a lower susceptibility to glutamine-dependent autophagy than was the case for the LMD cells.
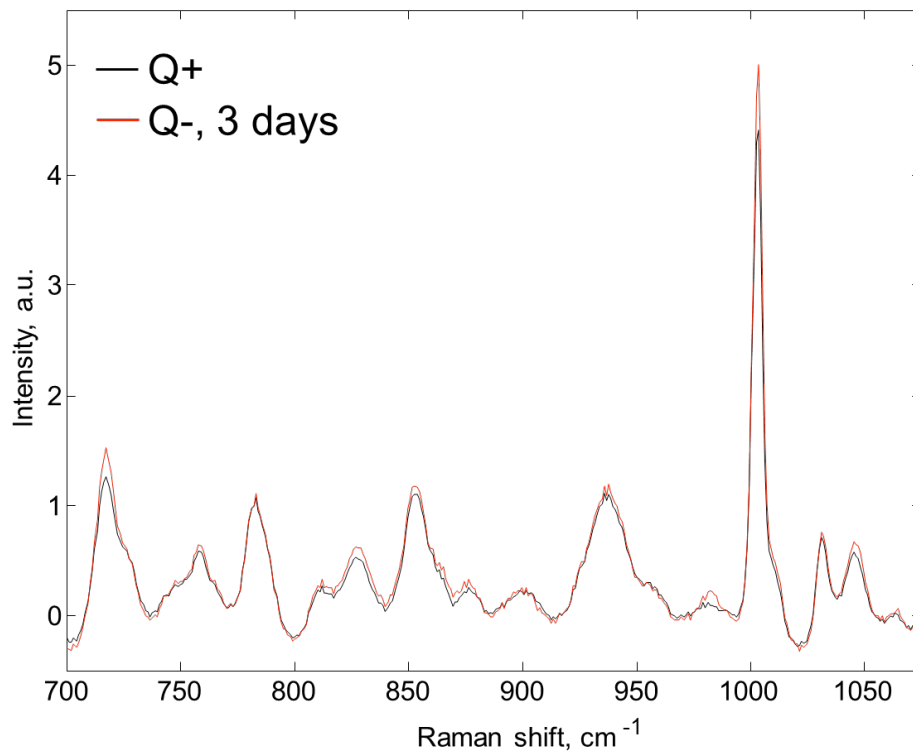
Figure 5.7.   Raman spectra from MCF7 cells cultured with or without glutamine.
Averaged Raman spectra (n > 36) from MCF7 cells obtained from cells cultured with (black) and without (red) glutamine for 3 days.

The lower susceptibility of MCF7 cells to glutamine limitation suggested by these observations is consistent with recent studies reporting that these cells express glutamine synthetase (Kung et al., 2011). Glutamine synthetase (GS) enables cells to produce glutamine

from ammonia and glutamate (Matsuno and Hirai, 1989). Expression of GS distinguishes breast tumour subtypes according to the differentiated tissue niche from which they arise. Breast cancer subtypes of basal origin do not express GS and are thus sensitive to glutamine deprivation, while breast cancer cells of luminal origin (such as MCF7 cells) do express GS and are thus less sensitive to glutamine deprivation (Kung et al., 2011). Based on these results, it would be interesting to probe with Raman spectroscopy the glutamine starvation response of human breast cancer cells that do not express glutamine synthetase, such as MDAMB231 cells. The efficacy of cancer treatments has been linked to the expression of glutamine synthetase (Todorova et al., 2011), and therefore, these Raman observations could provide new perspectives to develop a better understanding of the responsiveness of cancer cells to glutamine deprivation (DeBerardinis and Cheng, 2010).

5.3.4 Raman spectroscopy can reveal population inhomogeneity in cells exposed to conditions triggering autophagy

The apparent low responsiveness of MCF7 cells to glutamine deprivation was partly due to a greater heterogeneity across the sample. In order to examine if a stronger starvation stimulus could enable a clearer Raman signature, MCF7 cells were exposed to deprivation of all amino acids for 27 hours. Figure 5.8 presents the results of this experiment. The spectrum from the complete medium control (black spectrum, identified as Q+) is shown as a baseline, to provide a reference to the spectra taken from two different areas in the amino acid deprived culture (blue and red spectra, identified as areas 1 and 2, respectively). Stark differences were observed in the 718, 853, 937 and 1031 cm^{-1} spectral regions. On the one hand, these results confirm some of the findings from the glutamine deprivation experiment (particularly the increase in the 718 cm^{-1} phospholipid band). On the other hand, the profile differences (especially in the 853 and 937 cm^{-1} spectral regions), could be indicative that a different type of starvation involving glycogen was taking place in the cells.

Spectral heterogeneity was observed within the same sample only in MCF7 and not in LMD cells (data not shown). This observation may be explained by the fact that LMD cells are a clonal population (all originated from a single cell), whereas MCF7 cells are not. Thus, this result may be revealing a likewise heterogeneous response to starvation by different

MCF7 cells and even niche-related differences in a colony or aggregate of cells (Konorov et al., 2011), for which Raman spectroscopy could provide a particularly valuable analytic tool.
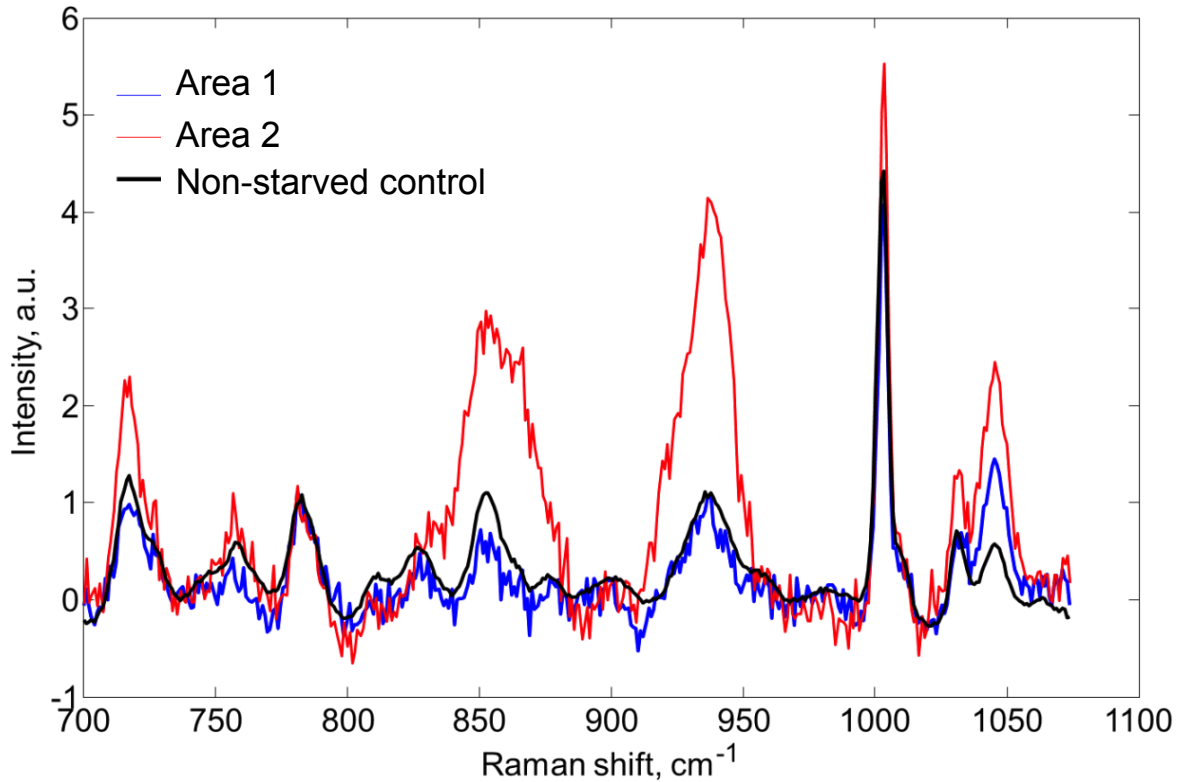
Figure 5.8.   Population inhomogeneity of Raman spectra in MCF7 cells under amino acid starvation.
Averaged Raman spectra from MCF7 cells (n > 36) cultured in the presence of glutamine (black) and after 27 hours in amino-acid free medium collected at 2 different areas (red and blue).

5.4   Conclusions

Using adherent cancer cells of mouse and human origin, Raman spectroscopy analyzed the cellular chemical composition during the physiological response of live cells to conditions that trigger autophagy. This study suggested that the 718 cm^{-1} Raman line associated with phospholipids could be used as a signature associated with starvation stimuli. The dynamics of recovery from glutamine starvation as well as cell population heterogeneity in the response to starvation were analyzed effectively.

More investigation of these promising results is required in order to establish the full potential of Raman spectroscopy in the study of autophagy. It is possible that the Raman signatures observed are not exclusively related to the cellular process of autophagy, since other cellular adaptation processes could influence the cellular composition. Nonetheless, this work opens new perspectives and establishes a precedent in the use of Raman microspectroscopy to analyze autophagy in live cells with non-invasive, label-free methods.

6 Conclusions and future directions

CHO cells are widely used to produce valuable biopharmaceuticals for human use. Finding means of expanding the production capacity can facilitate more general access and greater benefits from modern biotechnology therapeutics. An improved understanding of the physiological factors that affect cell proliferation, survival, productivity and product quality have contributed to advances in that direction. This dissertation discusses the investigation of autophagy and glutamine metabolism as critical physiological factors affecting process performance. Specifically, this work has shown that:

1. Cellular autophagy can play a significant role in process performance by decreasing the production capacity of cells. In this work, inhibiting autophagy using 3-methyl adenine (3-MA) resulted in a 2.8-fold increase in recombinant tissue plasminogen activator produced in fed-batch processes. This remarkable enhancement of protein production did not compromise the glycosylation capacity of cells.

2. Glutamine is a strong mediator of cell proliferation and metabolic activity in all cell lines used in this study. However, the susceptibility to glutamine-dependent autophagy was cell-line dependent. The most susceptible cells displayed the most decreased productivity and greatest changes in the lysosomal and mitochondrial compartments.

3. Combining the effects of enhanced proliferation (achieved through modulation of glutamine metabolism) and inhibition of autophagy (by treatment with 3-MA) resulted in a maximum 4.6-fold increase of recombinant tissue plasminogen activator production in fed-batch cultures of glutamine-sensitive cells.

4. Raman spectroscopy has considerable potential to probe the dynamic response of live cells to starvation stimuli in a non-invasive and label-free manner.

These results represent significant advances particularly in the bioprocess engineering field, but could also make positive contributions in other areas of biological research, applied and fundamental. The close link between autophagy and glutamine metabolism that this

investigation uncovered could be explored in other fields of research, particularly in cancer biology.

A most interesting direction for future work is to engineer cell lines so as to modulate autophagy at a genetic level. Preliminary investigations of genetic approaches (Appendix C) have suggested that the dosage of the gene product is a key factor. For cell line engineering, the most straightforward approach would be to overexpress a gene expected to have anti-autophagy function, i.e. negative regulators of autophagy. A candidate would be the PI3P phosphatase Jumpy (Vergne et al., 2009), which inhibits autophagy by a mechanism equivalent to 3-MA (PIK3C3 inactivation). Other negative regulators of PIK3C3, such as CDK1 (Furuya et al., 2010) would be alternative candidates. The use of an inducible system should provide the means to optimize the timing and dosage of regulatory gene products. Once the engineered cell line expresses the gene of interest, it would then be important to quantify the effect of those levels of expression on autophagy. Another possibility for intervention with genetic approaches would be to use gene knock-down by RNA interference. This approach can be more laborious, and a previous assessment of feasibility should be performed. For this approach to succeed, the sequences of the CHO gene target would allow the design and evaluation of candidate siRNA or shRNAs sequences. Candidate genes to down-regulate could be positive regulators of autophagy or essential genes required for early autophagy. Example candidates would be: AMPK or some of the autophagy core genes (Vps34/PIK3C3, Atg14L, Beclin-1, Atg5, Atg7, Atg16). It would even be possible to design a library of constructs with genes and shRNAs to include in such an inducible system. This library could then be used to probe systematically the autophagy responses. Such a system also could benefit other autophagy-related fields.

Identifying metabolites or gene products that make some cell lines less susceptible to glutamine deprivation could be another direction for future work with potential to produce valuable results. Culturing cells in two matching conditions, presence and absence of glutamine (such as was done in Chapter 3) could be used to establish the differential profile of the metabolome, proteome or transcriptome. This simple approach may be an efficient means to uncover potential points of intervention to engineer cell lines and processes that are both high-performance and robust.

The effect of 3-MA on glycosylation could also be followed-up. Based on the results of this work, it could be hypothesized that the glycosylation profile of a protein may be tailored by extrinsic manipulation of the cellular conditions through the use of regulators of autophagy. An unlimited supply of glutamine resulted in lower glycan processing, most likely due to excess ammonia accumulation, whereas 3-MA treatment resulted in higher levels of complex glycans. The optimal levels of these two factors may provide control on the glycosylation pattern of a protein. Since chloroquine affects the pH of acidic organelles, it can be expected to produce a similar effect as ammonia, decreasing glycosylation capacity. This "glycosylation optimization" study could thus consist in finding the right doses of 3-MA and chloroquine to match a particular glycosylation profile, a particularly valuable capability in the emerging era of biosimilars seeking to match already marketed biotherapeutics.

Another outcome of this project that could be explored in future work is the development of adaptive control strategies based on the monitoring of lysosomal content. Such a study could start by testing in a given cell line if the lysosomal content is a robust indicator of cell-specific productivity. If that is the case, then a control strategy could be developed in order to feed the cultures the minimum required to prevent excessive lysosomal accumulation and thus maintain the cells in a productive state.

The mathematical modeling of autophagy is another direction to explore in future work. A conceptual framework to model autophagy is presented in Appendix B. The use of reporter cell lines that have been generated in the context of this project can facilitate the task. For example, the use of the tandem mRFP-GFP-LC3 reporter can be used to model autophagic flux, since it permits the distinction of LC3 in autophagosomes and in autolysosomes. Another interesting modeling case could be the mutual inhibition of autophagy and apoptosis. For this second project, the Omi-mCherry reporter could be used in combination with the GFP-LC3 reporter. A list of reporter cell lines generated in the context of the present project or other related activities is shown in Appendix E.

Finally, the Raman spectroscopy (RS) investigation produced in the course of this project should also have a positive impact on various fields of research. Since current methods of detection of autophagy are either destructive or require genetic manipulation, a label-free, non-invasive technology such as RS would represent a considerable advance if a robust autophagy-specific Raman signature can be demonstrated. A more detailed

investigation of the Raman spectrum profile of cells under autophagy-inducing conditions is thus required. Such investigation should perform the RS profiling of live cells under autophagy-inducing stimuli, in the presence (preferentially 3-MA, to prevent autophagy initiation) and in the absence of autophagy inhibitors. This approach would ideally generate, two different signatures, one of functional and another of defective autophagy. An alternative would be to perform the comparison between cells in which the functional or defective state of autophagy would be obtained by genetic means (knock-out cells for particular autophagy genes, or by knock-down using RNA interference).

Indeed the questions that this Ph.D. project has raised are more numerous than the answers it provided. Yet, the results delivered are also substantial and beneficial. The research presented in this dissertation provides the foundations for sustained contributions of engineering disciplines to applied and fundamental knowledge.

Bibliography

Aggarwal S. 2010. What's fueling the biotech engine-2009-2010. Nature Biotechnology, 28(11): 1165-1171.

Bell A, Wang ZJ, Arbabi-Ghahroudi M, Chang TA, Durocher Y, Trojahn U, Baardsnes J, Jaramillo ML, Li S, Baral TN, O'Connor-McCourt M, MacKenzie R, Zhang J. 2010. Differential tumor-targeting abilities of three single-domain antibody formats. Cancer Letters 289: 81-90.

Bensaad K, Tsuruta A, Selak MA, Calvo Vidal MN, Nakano K, Bartrons R, Gottlieb E, Vousden KH. 2006. TIGAR, a p53-inducible regulator of glycolysis and apoptosis. Cell, 126: 107-120.

Betenbaugh MJ, Arden N. 2004. Life and death in mammalian cell culture: Strategies for apoptosis inhibition. Trends in Biotechnology, 22(4):174–180.

Bibila TA, Ranucci CS, Glazomitsky K, Buckland BC, Aunins JG. 1994. Monoclonal Antibody Process Development Using Medium Concentrates. Biotechnology Progress, 10: 87-96.

Bibila TA, Robinson DK. 1995. In pursuit of the optimal fed-batch process for monoclonal antibody production. Biotechnology Progress, 11(1): 1-13.

Bouchier-Hayes L, Muñoz-Pinedo C, Connell S, Green DR. 2008. Measuring apoptosis at the single cell level. Methods, 44: 222-228.

Boya P, Gonzalez-Polo RA, Casares N, Perfettini JL, Dessen P, Larochette N, Metivier D, Meley D, Souquere S, Yoshimori T, Pierrot G, Codogno P, Kroemer G. 2005. Inhibition of macroautophagy triggers apoptosis. Molecular and Cellular Biology, 25(3): 1025-1040.

Brasse-Lagnel C, Lavoinne A, Husson A. 2009. Control of mammalian gene expression by amino acids, especially glutamine. FEBS Journal, 276: 1826-1844.

Burky JE, Wesson MC, Young A, Farnsworth S, Dionne B, Zhu Y, Hartman TE, Qu L, Zhou W, Sauer PW. 2007. Protein-Free Fed-Batch Culture of Non-GS NS0 Cell Lines for Production of Recombinant Antibodies. Biotechnology and Bioengineering, 96(2): 281-293.

Butler M. 2005. Animal cell cultures: recent achievements and perspectives in the production of biopharmaceuticals. Applied Microbiology and Biotechnology, 68: 283-291.

Butler M. 2006. Optimisation of the cellular metabolism of glycosylation for recombinant proteins produced by mammalian cell systems. Cytotechnology, 50: 57-76.

Buzzai M, Bauer DE, Jones RG, DeBerardinis RJ, Hatzivassiliou G, Elstrom RL, Thompson CB. 2005. The glucose dependence of Akt-transformed cells can be reversed by pharmacologic activation of fatty acid β-oxidation. Oncogene, 24: 4165-4173.

Buzzai M, Jones RG, Amaravadi RK, Lum JJ, DeBerardinis RJ, Zhao F, Viollet B, Thompson CB. 2007. Systemic Treatment with the Antidiabetic Drug Metformin Selectively Impairs p53-Deficient Tumor Cell Growth. Cancer Res, 67(14): 6745-6752.

Cao Y, Klionsky DJ. 2007. Physiological functions of Atg6/Beclin 1: a unique autophagy-related protein. Cell Research, 17: 839-849.

Cardenas C, Miller RA, Smith I, Bui T, Molgo J, Muller M, Vais H, Cheung KH, Yang J, Parker I, Thompson CB, Birnbaum MJ, Hallows KR, Foskett JK. 2010. Essential regulation of cell bioenergetics by constitutive InsP$_3$ receptor Ca^{2+} transfer to mitochondria. Cell, 142: 270–283.

Chipuk JE, Green DR. 2006. Dissecting p53-dependent apoptosis. Cell Death and Differentiation, 13: 994-1002.

Christie A, Butler M. 1999. The Adaptation of BHK Cells to a Non-Ammoniagenic Glutamate-Based Culture Medium. Biotechnology and Bioengineering, 64(3): 298-309.

Chu L, Robinson DK. 2001. Industrial choices for protein production by large-scale cell culture. Current Opinion in Biotechnology, 12: 180-187.

Combs RG, Yu E, Roe S, Piatchek MB, Jones HL, Mott J, Kennard ML, Goosney DL, Monteith D. 2011. Fed-batch bioreactor performance and cell line stability evaluation of the artificial chromosome expression technology expressing an IgG1 in Chinese hamster ovary cells. Biotechnology Progress, 27(1): 201-208.

Cuervo AM. 2004. Autophagy: in sickness and in health. Trends in Cell Biology, 14(2): 70-77.

Dang CV, Hamaker M, Sun P, Le A, Gao P. 2011. Therapeutic targeting of cancer cell metabolism. J Mol Med, 89: 205-212.

DeBerardinis RJ, Mancuso A, Daikhin E, Nissim I, Yudkoff M, Wehrli S, Thompson CB. 2007. Beyond aerobic glycolysis: Transformed cells can engage in glutamine metabolism that exceeds the requirement for protein and nucleotide synthesis. PNAS 104(49): 19345-19350.

DeBerardinis RJ, Sayed N, Ditsworth D, Thompson CB. 2008. Brick by brick: metabolism and tumor cell growth. Current Opinion in Genetics & Development, 18: 54-61.

DeBerardinis RJ, Cheng T. 2010. Q's next: the diverse functions of glutamine in metabolism, cell biology and cancer. Oncogene, 29: 313-324.

Dempsey J, Ruddock S, Osborne M, Ridley A, Sturt S, Field R. 2003. Improved Fermentation Processes for NS0 Cell Lines Expressing Human Antibodies and Glutamine Synthetase. Biotechnology Progress, 19: 175-178.

Dorai H, Kyung YS, Ellis D, Kinney CA, Lin C, Jan D, Moore G, Betenbaugh MJ. 2009. Expression of anti-apoptosis genes alters lactate metabolism of Chinese Hamster Ovary cells in culture. Biotechnology and Bioengineering, 103(3): 592-608.

Drouin H, Ritter JB, Gorenflo GM, Bowen BD, Piret JM. 2007. Cell Separator Operation within Temperature Ranges to Minimize Effects on Chinese Hamster Ovary Cell Perfusion Culture. Biotechnology Progress, 23(6): 1473-1484.

Durocher Y, Butler M. 2009. Expression systems for therapeutic glycoprotein production. Current Opinion in Biotechnology, 20: 700-707.

Egan DF, Shackelford DB, Mihaylova MM, Gelino S, Kohnz RA, Mair W, Vasquez DS, Joshi A, Gwinn DM, Taylor R, Asara JM, Fitzpatrick J, Dillin A, Viollet B, Kundu M, Hansen M, Shaw RJ. 2011. Phosphorylation of ULK1 (hATG1) by AMP-Activated Protein Kinase Connects Energy Sensing to Mitophagy. Science, 331: 456-461.

Eng CH, Yu K, Lucas J, White E, Abraham RT. 2010. Ammonia Derived from Glutaminolysis Is a Diffusible Regulator of Autophagy. Science Signaling, 3(119): 1-9.

Erlichman JS, Hewitt A, Damon TL, Hart M, Kurascz J, Li A, Leiter JC. 2008. Inhibition of Monocarboxylate Transporter 2 in the Retrotrapezoid Nucleus in Rats: A Test of the Astrocyte–Neuron Lactate-Shuttle Hypothesis. The Journal of Neuroscience, 28(19):4888 – 4896.

Fann CH, Guirgis F, Chen G, Lao MS, Piret JM. 2000. Limitations to the amplification and stability of human tissue-type plasminogen activator expression by Chinese Hamster Ovary cells. Biotechnol Bioeng 69(2):204-212.

U.S. Department of Health and Human Services, Food and Drug Administration (USDHHS-FDA). September 2004. Guidance for industry. PAT - A framework for innovative pharmaceutical development, manufacturing, and quality assurance.

Ferraro E, Cecconi F. 2007. Autophagic and apoptotic response to stress signals in mammalian cells. Archives of Biochemistry and Biophysics, 462: 210-219.

Fischer U, Janicke RU, Schulze-Osthoff K. 2003. Many cuts to ruin: a comprehensive update of caspase substrates. Cell Death and Differentiation, 10: 76-100.

Frahm B, Lane P, Markl H, Portner R. 2003. Improvement of a mammalian cell culture process by adaptive, model-based dialysis fed-batch cultivation and suppression of apoptosis. Bioprocess and Biosystems Engineering, 26(1): 1-10.

Franco R, Cidlowski JA. 2009. Apoptosis and glutathione: beyond an antioxidant. Cell Death and Differentiation, 16: 1303-1314.

Furuya T, Kim M, Lipinski M, Li J, Kim D, Lu T, Shen Y, Rameh L, Yankner B, Tsai LH, Yuan J. 2010. Negative Regulation of Vps34 by Cdk Mediated Phosphorylation. Molecular Cell, 38: 500–511.

Gawlitzek M, Ryll T, Lofgren J, Sliwkowski MB. 2000. Ammonium Alters N-Glycan Structures of Recombinant TNFR-IgG: Degradative Versus Biosynthetic Mechanisms. Biotechnology and Bioengineering, 68(6): 637-646.

Genzel Y, Ritter JB, Ko1nig S, Alt R, Reichl U. 2005. Substitution of Glutamine by Pyruvate To Reduce Ammonia Formation and Growth Inhibition of Mammalian Cells. Biotechnology Progress, 21: 58?69.

Green DR, Reed JC. 1998. Mitochondria and apoptosis. Science, 281: 1309-1312.

Guile GR, Rudd PM, Wing DR, Prime SB, Dwek RA. 1996. A rapid high-resolution high-performance liquid chromatographic method for separating glycan mixtures and analyzing oligosaccharide profiles. Anal. Biochem, 240: 210-226.

Hamiel CR, Pinto S, Hau A, Wischmeyer PE. 2009. Glutamine enhances heat shock protein 70 expression via increased hexosamine biosynthetic pathway activity. Am J Physiol Cell Physiol 2987: C1509-C1519.

Han YK, Ha TK, Lee SJ, Lee JS, Lee GM. 2011. Autophagy and apoptosis of recombinant Chinese Hamster Ovary Cells during fed-batch culture: effect of nutrient supplementation. Biotechnology and Bioengineering, 108(9): 2182-2192.

Hossler P, Khattak SF, Li ZJ. 2009. Optimal and consistent protein glycosylation in mammalian cell culture. Glycobiology, 19(9): 936-949.

Høyer-Hansen M, Bastholm L, Szyniarowski P, Campanella M, Szabadkai G, Farkas T, Bianchi K, Fehrenbacher N, Elling F, Rizzuto R, Stenfeldt Mathiasen I, Jäättelä M. 2007. Control of Macroautophagy by Calcium, Calmodulin-Dependent Kinase Kinase-β, and Bcl-2. Molecular Cell, 25: 193-205.

Hu WS, Aunins JG. 1997. Large-scale mammalian cell culture. Current Opinion in Biotechnology, 8(2): 148-153.

Hwang SO, Lee GM. 2008. Nutrient deprivation induces autophagy as well as apoptosis in Chinese Hamster Ovary cell culture. Biotechnology and Bioengineering, 99(3): 678-685.

Jaiswal McEligot A, Yang S, Meyskens Jr FL. 2005. Redox regulation by intrinsic species and extrinsic nutrients in normal and cancer cells. Annu. Rev. Nutr., 25: 261-295.

Jang JD, Barford JP. 2000. Effect of feed rate on growth rate and antibody production in the fed-batch culture of murine hybridoma cells. Cytotechnology, 32(3): 229-242.

Jardon MA, Sattha B, Braasch K, Leung AO, Côté HCF, Butler M, Gorski SM, Piret JM. 2012. Inhibition of glutamine-dependent autophagy increases t-PA production in CHO cell fed-batch processes. Biotechnology and Bioengineering, 109(5): 1228-1238.

Jeong YH, Wang SS. 1995. Role of glutamine in hybridoma cell culture: Effects on cell growth, antibody production and cell metabolism. Enzyme and Microbial Technology 17: 47-55.

Jo EC, Park HJ, Kim DI, Moon HM. 1993. Repeated fed-batch culture of hybridoma cells in nutrient-fortified high-density medium. Biotechnology and Bioengineering, 42: 1229-1237.

Jones AJS, Papac DI, Chin EH, Keck R, Baughman SA, Lin YS, Kneer J, Battersby JE. 2007. Selective clearance of glycoforms of a complex glycoprotein pharmaceutical caused by terminal N-acetylglucosamine is similar in humans and cynomolgus monkeys. Glycobiology, 17(5): 529-540.

Kennard ML, Goosney DL, Monteith D, Zhang L, Moffat M, Fischer D, Mott J. 2009. The generation of stable, high MAb expressing CHO cell lines based on the artificial chromosome expression (ACE) technology. Biotechnology and Bioengineering 104(3): 540-553.

Kim I, Rodriguez-Enriquez S, Lemasters JJ. 2007. Selective degradation of mitochondria by mitophagy. Archives of Biochemistry and Biophysics, 462: 245-253.

Kim YG, Kim JY, Mohan C, Lee GM. 2009. Effect of Bcl-xL overexpression on apoptosis and autophagy in recombinant Chinese Hamster Ovary cells under nutrient-deprived condition. Biotechnology and Bioengineering, 103(4): 757-766.

Klionsky DJ, Cregg JM, Dunn WA Jr, Emr SD, Sakai Y, Sandoval IV, Sibirny A, Subramani S, Thumm M, Veenhuis M, Ohsumi Y. 2003. A unified nomenclature for yeast autophagy-related genes. Dev Cell., 5(4):539-45.

Klionsky DJ. 2007. Autophagy: from phenomenology to molecular understanding in less than a decade. Nature Reviews in Molecular Cell Biology, 8: 931-937.

Klionsky DJ, Cuervo AM, Seglen PO. 2007. Methods for Monitoring Autophagy from Yeast to Human. Autophagy, 3(3): 181-206.

Klionsky DJ, et al. 2008. Guidelines for the use and interpretation of assays for monitoring autophagy in higher eukaryotes. Autophagy, 4(2): 151-175.

Konorov SO, Schulze HG, Piret JM, Aparicio SA, Turner RF, Blades MW. 2011. Raman microscopy-based cytochemical investigations of potential niche-forming inhomogeneities present in human embryonic stem cell colonies. Appl Spectrosc, 65(9):1009-16.

Kourtis N, Tavernarakis N. 2009. Autophagy and cell death in model organisms. Cell Death and Differentiation, 16: 21-30.

Kroemer G, Levine B. 2008. Autophagic cell death: the story of a misnomer. Nature Reviews Molecular Cell Biology, 9(12): 1004-1010.

Kroemer G, Mariño G, Levine B. 2010. Autophagy and the Integrated Stress Response. Molecular Cell 40: 280-293.

Ku SCY, Ng DTW, Yap MGS, Chao SH. 2008. Effects of Overexpression of X-Box Binding Protein 1 on Recombinant Protein Production in Chinese Hamster Ovary and NS0 Myeloma Cells. Biotechnology and Bioengineering, 99(1): 155-164

Kundu M, Lindsten T, Yan CY, Wu J, Zhao F, Zhang J, Selak MA, Ney PA, Thompson CB. 2008. Ulk1 plays a critical role in the autophagic clearance of mitochondria and ribosomes during reticulocyte maturation. Blood, 112: 1493-1502.

Kundu M, Thompson CB. 2008. Autophagy: Basic principles and relevance to disease. Annual Review of Pathology: Mechanisms of Disease, 3: 427-455.

Kundu M, Thompson CB. 2005. Macroautophagy versus mitochondrial autophagy: a question of fate? Cell Death and Differentiation, 12: 1484-148.

Kung HN, Marks JR, Chi JT. 2011. Glutamine Synthetase Is a Genetic Determinant of Cell Type–Specific Glutamine Independence in Breast Epithelia. PLoS Genetics 7(8): e1002229.

Kurokawa H, Park YS, Iijima S, Kobayashi T. 1994. Growth characteristics in fed-batch culture of hybridoma cells with control of glucose and glutamine concentrations. Biotechnology and Bioengineering, 44: 95-103.

Levine B, Sinha S, Kroemer G. 2008. Bcl-2 family members, dual regulators of apoptosis and autophagy. Autophagy, 4(5): 600-606.

Li F, Zhao L, Sun Y, Kou T, Zhou Y, Tan WS. 2009. A high-yielding, generic fed-batch process for recombinant antibody production of GS-engineered cell lines. Journal of Microbiology and Biotechnology, 19(12): 1695–1702.

Li J, Wong CL, Vijayasankaran N, Hudson T, Amanullah A. 2012(a). Feeding lactate for CHO cell culture processes: Impact on culture metabolism and performance. Biotechnology and Bioengineering, Early View.

Li J, Gu W, Edmondson DG, Lu C, Vijayasankaran N, Figueroa B, Stevenson D, Ryll T, Li F. 2012(b). Generation of a cholesterol-independent, non-GS NS0 cell line through chemical treatment and application for high titer antibody production. Biotechnology and Bioengineering, Early View.

Lum JJ, Bauer DE, Kong M, Harris MH, Li C, Lindsten T, Thompson CB. 2005. Growth Factor Regulation of Autophagy and Cell Survival in the Absence of Apoptosis. Cell, 120: 237–248.

Luo J, Vijayasankaran N, Autsen J, Santuray R, Hudson T, Amanullah A, Li F. 2012. Comparative Metabolite Analysis to Understand Lactate Metabolism Shift in Chinese

Hamster Ovary Cell Culture Process. Biotechnology and Bioengineering 109(1): 146–156.

Luzio JP, Pryor PR, Bright NA. 2007. Lysosomes: fusion and function. Nature Reviews in Molecular Cell Biology, 8: 622-632.

Maiuri MC, Zalckvar E, Kimchi A, Kroemer G. 2007. Self-eating and self-killing: crosstalk between autophagy and apoptosis. Nature Reviews in Molecular Cell Biology, 8: 741-752.

Majors BS, Pederson NE, Chiang GG, Betenbaugh MJ. 2009. Mcl-1 overexpression leads to higher viabilities and increased production of humanized monoclonal antibody in Chinese hamster ovary cells. Biotechnol. Prog., 25: 1161–1168.

Malicdan MC, Noguchi S, Nonaka I, Saftig P, Nishino I. 2008. Lysosomal myopathies: An excessive build-up in autophagosomes is too much to handle. Neuromuscular Disorders 18: 521-529.

Mancuso A, Sharfstein ST, Fernandez EJ, Clark DS, Blanch HW. 1998. Effect of extracellular glutamine concentration on primary and secondary metabolism of a murine hybridoma: An *in vivo* 13C nuclear magnetic resonance study. Biotechnology and Bioengineering 57(2): 172-186.

Matsuno T, Hirai H. 1989. Glutamine synthetase and glutaminase activities in various hepatoma cells. Biochem Int, 19:219-225.

Mathew R, Kongara S, Beaudoin B, Karp CM, Bray K, Degenhardt K, Chen G, Jin S, White E. 2007. Autophagy suppresses tumor progression by limiting chromosomal instability. Genes & Development, 21: 1367-1381.

Meijer AJ, Codogno P. 2004. Regulation and role of autophagy in mammalian cells. The International Journal of Biochemistry & Cell Biology, 36: 2445-2462.

Meneses-Acosta A, Mendonça RZ, Merchant H, Covarrubias L, Ramírez OT. 2001. Comparative Characterization of Cell Death Between Sf9 Insect Cells and Hybridoma Cultures. Biotechnology and Bioengineering, 72(4): 441-457.

Mihaylova MM, Shaw RJ. 2011. The AMPK signalling pathway coordinates cell growth, autophagy and metabolism. Nature Cell Biology, 13(9): 1016-1023.

Miller S, Tavshanjian B, Oleksy A, Perisic O, Houseman BT, Shokat KM, Williams RL. 2010. Shaping Development of Autophagy Inhibitors with the Structure of the Lipid Kinase Vps34. Science, 327: 1638-1642.

Mizushima N. 2007. Autophagy: process and function. Genes & Development, 21: 2861-2873.

Mizushima N, Klionsky DJ. 2007. Protein turnover via autophagy: Implications for metabolism. Annual Review of Nutrition, 27: 19-40.

Mizushima N, Yoshimori T. 2007. How to Interpret LC3 Immunoblotting. Autophagy, 3(6): 542-545.

Mizushima N, Levine B, Cuervo AM, Klionsky DJ. 2008. Autophagy fights disease through cellular self-digestion. Nature Reviews, 451: 1069-1075.

Mizushima N, Yoshimori T, Levine B. 2010. Methods in Mammalian Autophagy Research. Cell, 140: 313-326.

Moran EB, McGowan ST, McGuire JM, Frankland JE, Oyebade IA, Waller W, Archer LC, Morris LO, Pandya J, Nathan SR, Smith L, Cadette ML, Michalowski JT. 2000. A systematic approach to the validation of process control parameters for monoclonal antibody production in fed-batch culture of a murine myeloma. Biotechnology and Bioengineering, 69(3): 242-255.

Neermann J, Wagner R. 1996. Comparative analysis of glucose and glutamine metabolism in transformed mammalian cell lines, insect and primary liver cells. Journal of Cellular Physiology 166: 152-169.

Nicklin P, Bergman P, Zhang B, Triantafellow E, Wang H, Nyfeler B, Yang H, Hild M, Kung C, Wilson C, Myer VE, MacKeigan JP, Porter JA, Wang K, Cantley LC, Finan PM, Murphy LO. 2009. Bidirectional Transport of Amino Acids Regulates mTOR and Autophagy. Cell, 136: 521-534.

Pavlou AK, Reichert JM. 2004. Recombinant protein therapeutics - success rates, market trends and values to 2010. Nature Biotechnology, 22(12): 1513-1519.

Petiot A, Ogier-Denis E, Blommaart EFC, Meijer AJ, Codogno P. 2000. Distinct Classes of Phosphatidylinositol 3-Kinases Are Involved in Signaling Pathways That Control Macroautophagy in HT-29 Cells. The Journal of Biological Chemistry, 275(2): 992-998.

Rivinoja A, Hassinen A, Kokkonen N, Kauppila A, Kellokumpu S. 2009. Elevated Golgi pH Impairs Terminal N-Glycosylation by Inducing Mislocalization of Golgi Glycosyltransferases. Journal of Cellular Physiology, 220: 144-154.

Rodriguez-Enriquez S, He L, Lemasters JJ. 2004. Role of mitochondrial permeability transition pores in mitochondrial autophagy. The International Journal of Biochemistry & Cell Biology, 36: 2463-2472.

Royle L, Radcliffe CM, Dwek RA, Rudd PM. 2006. Detailed Structural Analysis of N-Glycans Released From Glycoproteins in SDS-PAGE Gel Bands Using HPLC Combined With Exoglycosidase Array Digestions. Methods in Molecular Biology - Glycobiology Protocols, 347: 125-143.

Rubinsztein DC. 2006. The roles of intracellular protein-degradation pathways in neurodegeneration. Nature, 443: 780-786.

Rubinsztein DC, Cuervo AM, Ravikumar B, Sarkar S, Korolchuk V, Kaushik S, Klionsky DJ. 2009. In search of an autophagomometer. Autophagy 5(5): 585-589.

Ryu JS, Lee GM. 1999. Application of hypoosmolar medium to fed-batch culture of hybridoma cells for improvement of culture longevity. Biotechnology and Bioengineering, 62(1): 120-123.

Sanfeliu A, Cairo JJ, Casas C, Sola C, Godia F. 1996. Analysis of nutritional factors and physical conditions affecting growth and monoclonal antibody production of the hybridoma KB-26.5 cell line. Biotechnology Progress, 12: 209-216.

Sauer PW, Burky JE, Wesson MC, Sternard HD, Qu L. 2000. A high-yielding, generic fed-batch cell culture process for production of recombinant antibodies. Biotechnology and Bioengineering, 67(5): 585-597.

Schafer FQ, Buettner GR. 2001. Redox environment of the cell as viewed through the redox state of the glutathione disulfide/glutathione couple. Free Radical Biology & Medicine 30(11): 1191-1212.

Scherz-Shouval R, Elazar Z. 2007. ROS, mitochondria and the regulation of autophagy. Trends in Cell Biology, 17(9): 422-427.

Schneider M, Marison IW, vonStockar U. 1996. The importance of ammonia in mammalian cell culture. Journal of Biotechnology,46(3): 161-185.

Schulze HG, Konorov SO, Caron NJ, Piret JM, Blades MW, Turner RFB. 2010. Assessing Differentiation Status of Human Embryonic Stem Cells Noninvasively Using Raman Microspectroscopy. Anal. Chem., 82(12): 5020–5027.

Sellick CA, Croxford AS, Maqsood AR, Stephens G, Westerhoff HV, Goodacre R,3,5 Dickson AJ. 2011. Metabolite profiling of recombinant CHO cells: Designing tailored feeding regimes that enhance recombinant antibody production. Biotechnology and Bioengineering, 108(12): 3025–3031.

Setiadi AF, David MD, Seipp RP, Hartikainen JA, Gopaul R, Jefferies WA. 2007. Epigenetic control of the immune escape mechanisms in malignant carcinomas. Mol Cell Biol, 27: 7886–94.

Shanware NP, Mullen AR, DeBerardinis RJ, Abraham RT. 2011. Glutamine: pleiotropic roles in tumor growth and stress resistance. J Mol Med 89: 229-236.

Smedsrod B, Eiarsson M. 1990. Clearance of tissue plasminogen activator by mannose and galactose receptors in the liver. Thrombosis and Haemostasis, 63(1): 60-66.

Stansfield SH, Allen EE, Dinnis DM, Racher AJ, Birch JR, James DC. 2007. Dynamic analysis of GS-NS0 cells producing a recombinant monoclonal antibody during fed-batch culture. Biotechnology and Bioengineering, 97(2): 410-424.

Stelling J, Sauer U, Szallasi Z, Doyle III, FJ, Doyle J. 2004. Robustness of cellular functions. Cell, 118: 675-685.

Tabuchi H, Sugiyama T, Tanaka S, Tainaka S. 2010. Overexpression of taurine transporter in Chinese hamster ovary cells can enhance cell viability and product yield, while promoting glutamine consumption. Biotechnology and Bioengineering, 107(6): 998–1003.

Takagi M, Hia HC, Jang JH, Yoshida T. 2001. Effects of high concentrations of energy sources and metabolites on suspension culture of Chinese Hamster Ovary cells producing tissue plasminogen activator. Journal of Bioscience and Bioengineering, 91(5): 515-521.

Tasdemir E, Maiuri MC, Galluzzi L, Vitale I, Djavaheri-Mergny M, D'Amelio M, Criollo A, Morselli E, Zhu C, Harper F, Nannmark U, Samara C, Pinton P, Vicencio JM, Carnuccio R, Moll UM, Madeo F, Paterlini-Brechot P, Rizzuto R, Szabadkai G, Pierron

G, Blomgren K, Tavernarakis N, Codogno P, Cecconi F, Kroemer G. 2008. Regulation of autophagy by cytoplasmic p53. Nat Cell Biol., 10(6):676-87.

Todorova VK, Kaufmann Y, Luo S, Klimberg VS. 2011. Tamoxifen and raloxifene suppress the proliferation of estrogen receptor-negative cells through inhibition of glutamine uptake. Cancer Chemother Pharmacol (67):285–291.

Trachootham D, Lu W, Ogasawara MA, Rivera-del Valle N, Huang P. 2008. Redox regulation of cell survival. Antioxidants & Redox Signaling, 10(8): 1343-1374.

Valko M, Leibfritz D, Moncol J, Cronin MTD, Mazur M, Telser J. 2007. Free radicals and antioxidants in normal physiological functions and human disease. The International Journal of Biochemistry & Cell Biology, 39: 44-84.

Vander Heiden MG, Cantley LC, Thompson CB. 2009. Understanding the Warburg Effect: The Metabolic Requirements of Cell Proliferation. Science 324: 1029-1033.

Vaughn AE, Deshmukh M. 2008. Glucose metabolism inhibits apoptosis in neurons and cancer dells by redox inactivation of cytochrome c. Nature Cell Biology, 10(12): 1477-1483.

Vergne I, Roberts E, Elmaoued RA, Tosch V, Delgado MA, Proikas-Cezanne T, Laporte J, Deretic V. 2009. Control of autophagy initiation by phosphoinositide 3-phosphatase jumpy. The EMBO Journal, 28: 2244–2258

Wang J, Honda H, Lenas P, Watanabe H, Kobayashi T. 1995. Effective tPA production by BHK cells in nutrients-controlled culture using an on-line HPLC measuring system. Journal of Fermentation and Bioengineering, 80(1): 107-110.

Weiss P, Ashwell G. 1989. The asialoglycoprotein receptor: properties and modulation by ligand. Progress in Clinical and Biological Research, 300:169-84.

Werner RG. 2004. Economic aspects of commercial manufacture of biopharmaceuticals. Journal of Biotechnology, 113: 171-182.

Wong DCF, Wong NSC, Goh JSY, May LM, Yap MGS. 2010. Profiling of N-glycosylation gene expression in CHO cell fed-batch cultures. Biotechnology and Bioengineering, 107(3): 516-528.

Wu YT, Tan HL, Shui G, Bauvy C, Huang Q, Wenk MR, Ong CN, Codogno P, Shen HM. 2010. Dual role of 3-methyladenine in modulation of autophagy via different temporal

patterns of inhibition on class I and II phosphoinositide 3-kinase. Journal of Biological Chemistry, 285: 10850-10861.

Wurm FM. 2004. Production of recombinant protein therapeutics in cultivated mammalian cells. Nature Biotechnology, 22(11): 1393-1398.

Xie L, Wang DIC. 1994. Fed-batch cultivation of animal cells using different medium design concepts and feeding strategies. Biotechnology and Bioengineering, 43: 1175-1189.

Xie L, Wang DIC. 1996. High Cell Density and High Monoclonal Antibody Production Trough Medium Design and Rational Control in a Bioreactor. Biotechnology and Bioengineering, 51: 725-729.

Yang Z, Klionsky DJ. 2010. Mammalian autophagy: core molecular machinery and signaling regulation. Current Opinion in Cell Biology 22:124-131.

Yu M, Hu Z, Pacis E, Vijayasankaran N, Shen A, Li F. 2011. Understanding the intracellular effect of enhanced nutrient feeding toward high titer antibody production process. Biotechnology and Bioengineering, 108(5): 1078-1088.

Yuneva M, Zamboni N, Oefner P, Sachidanandam R, Lazebnik Y. 2007. Deficiency in glutamine but not glucose induces MYC-dependent apoptosis in human cells. The Journal of Cell Biology, 178(1): 93-105.

Zhang J, Robinson D, Salmon P. 2006. A novel function for Selenium in biological system: Selenite as a highly effective iron carrier for Chinese hamster ovary cell growth and monoclonal antibody production. Biotechnology and Bioengineering, 95(6): 1188-1197.

Zhang L, Shen H, Zhang YX. 2004. Fed-batch culture of hybridoma cells in serum-free medium using an optimized feeding strategy. Journal of Chemical Technology and Biotechnology, 79(2): 171-181.

Zhou WC, Rehm J, Hu WS. 1995. High viable cell concentration fed-batch cultures of hybridoma cells through online nutrient feeding. Biotechnology and Bioengineering, 46(6): 579-587.

Zhou WC, Chen CC, Buckland B, Aunins J. 1997a. Fed-batch culture of recombinant NS0 myeloma cells with high monoclonal antibody production. Biotechnology and Bioengineering, 55(5): 783-792.

Zhou WC, Rehm J, Europa A, Hu WS. 1997b. Alteration of mammalian cell metabolism by dynamic nutrient feeding. Cytotechnology, 24(2): 99-108.

Zielke HR, Sumbilla CM, Sevdalian DA, Hawkins RL, Ozand PT. 1980. Lactate: a major product of glutamine metabolism by human diploid fibroblasts. Journal of Cellular Physiology 104: 433-441.

Zoladek A, Pascut FC, Patel P, Notingher I. 2011. Journal of Raman Spectroscopy, 42(3):251–258.

**Appendix A. Supplementary data**
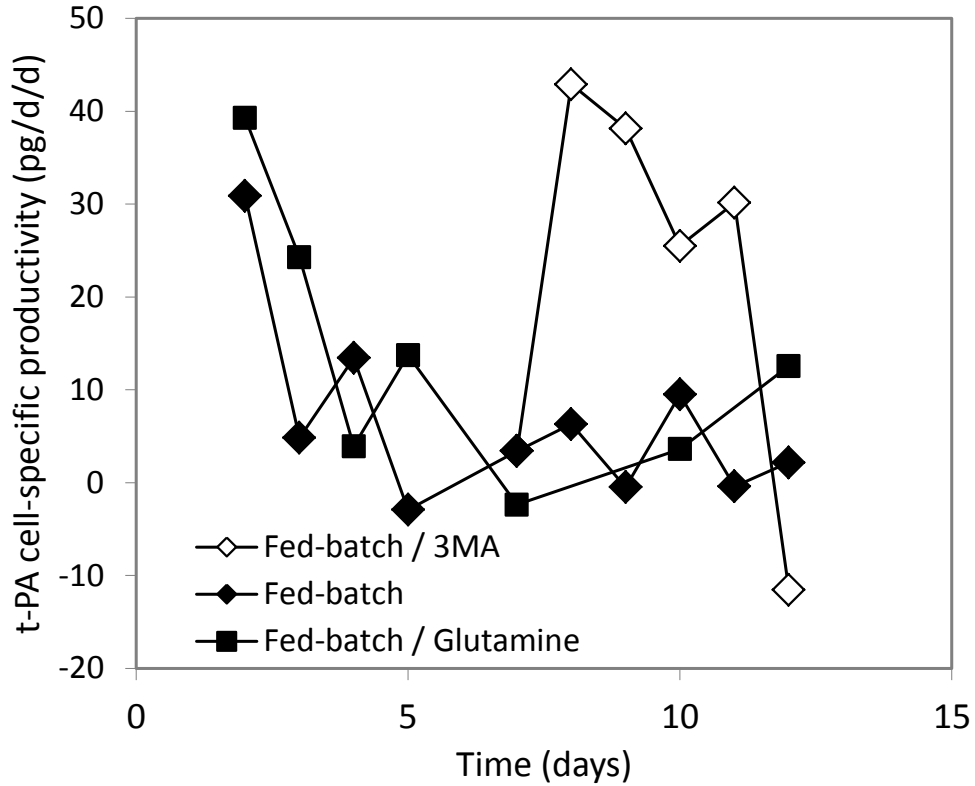
Figure A.1.   Effect of 3-MA treatment on cell-specific t-PA productivity.
Treatment of fed-batch culture with 3-MA restored t-PA cell-specific productivity to initial levels. Data calculated from one of the replicate experiments used to generate Figure 2.3. After 4 days of treatment the cell-specific productivity declines again. This decline could be due to a dilution effect of the feeding additions on 3-MA concentration, to metabolic clearance of 3-MA or to decreased cell viability.
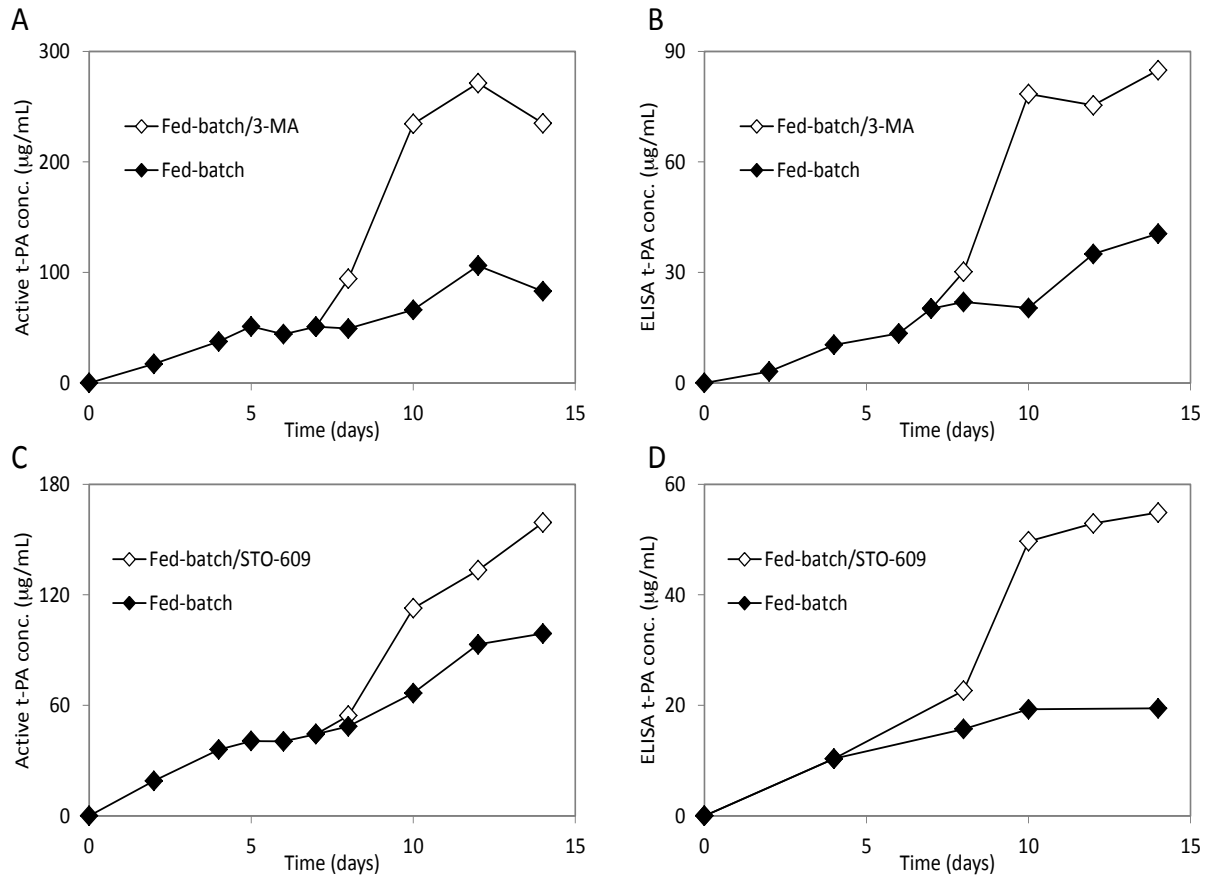
Figure A.2.   Comparison of t-PA activity assay and ELISA.
Two assays (t-PA activity and ELISA) were compared to show that the effect observed on t-PA production after treatment with 3-MA or STO-609 was not due to a change in specific activity of the t-PA produced. 3-MA concentration was 10 mM; STO-609 concentration was 25 μM. ELISA detects the target protein regardless of its activity, whereas the t-PA activity assay detects only active t-PA. Two parallel fed-batch cultures (closed symbols, panels A to D) were split on day 7. Half of the original culture was kept without treatment to serve as a control and half treated with 3-MA (open symbols, panels A and B) or with STO-609 (open symbols, panels C and D). Since the two assays provide similar trends, it can be concluded that the increased levels of t-PA observed upon treatment correspond to more t-PA being produced and not to a change in its specific activity.
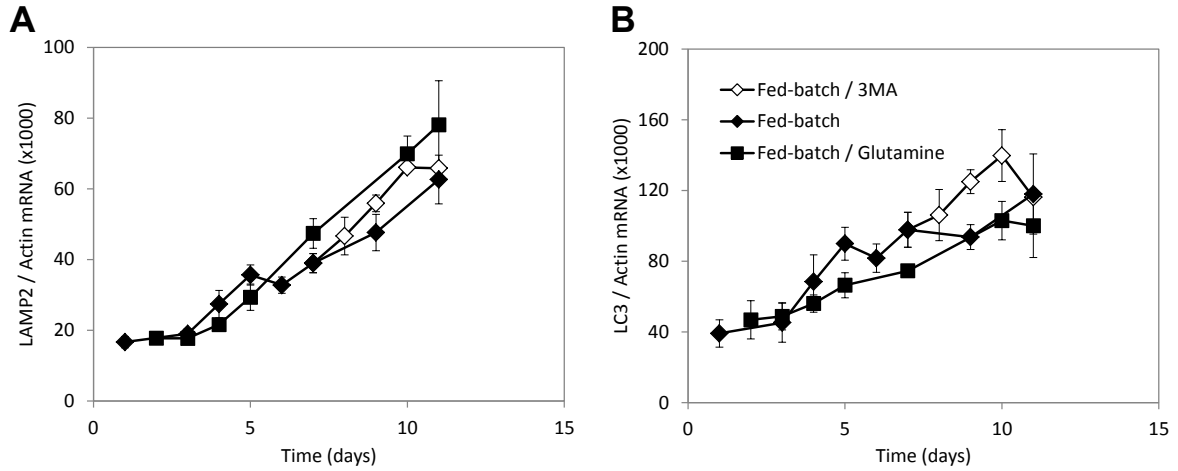
Figure A.3.   Quantification of mRNA levels for LAMP2 and MAP1-LC3B.
Legend: Control fed-batch (◆), fed-batch treated with 10 mM 3-MA on day 7 (◇) and fed-batch supplemented with excess glutamine (■). Results are normalized to cellular β–actin. Error bars represent the SEM of biological triplicates.
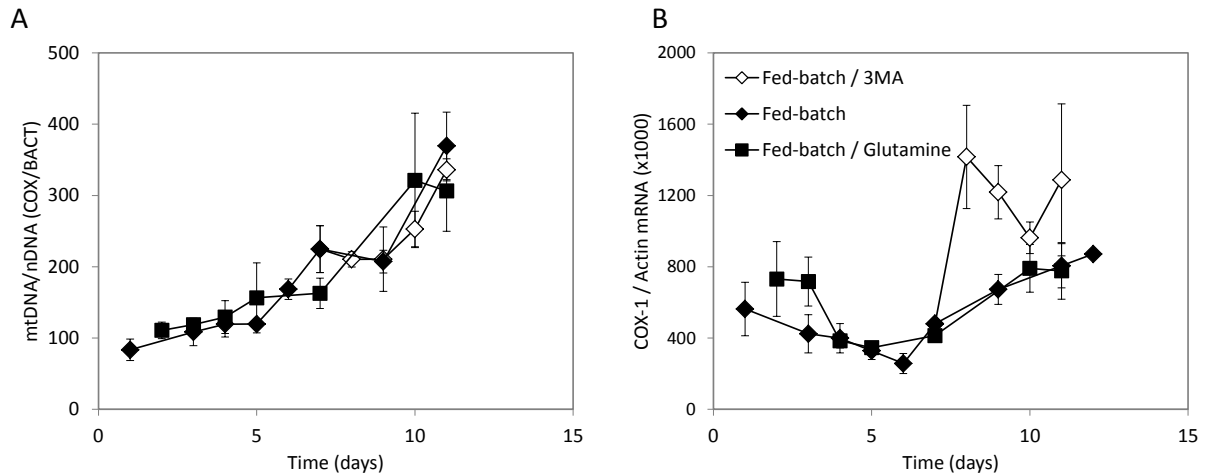

Figure A.4.   Quantification of mitochondrial DNA and mRNA content.
Legend: Control fed-batch (◆), fed-batch treated with 10 mM 3-MA on day 7 (◇) and fed-batch supplemented with excess glutamine (■).Results are normalized to cellular β–actin. Error bars represent the SEM of biological triplicates.

Early-stage culture   Late-stage culture

LTG, Hoechst 33342
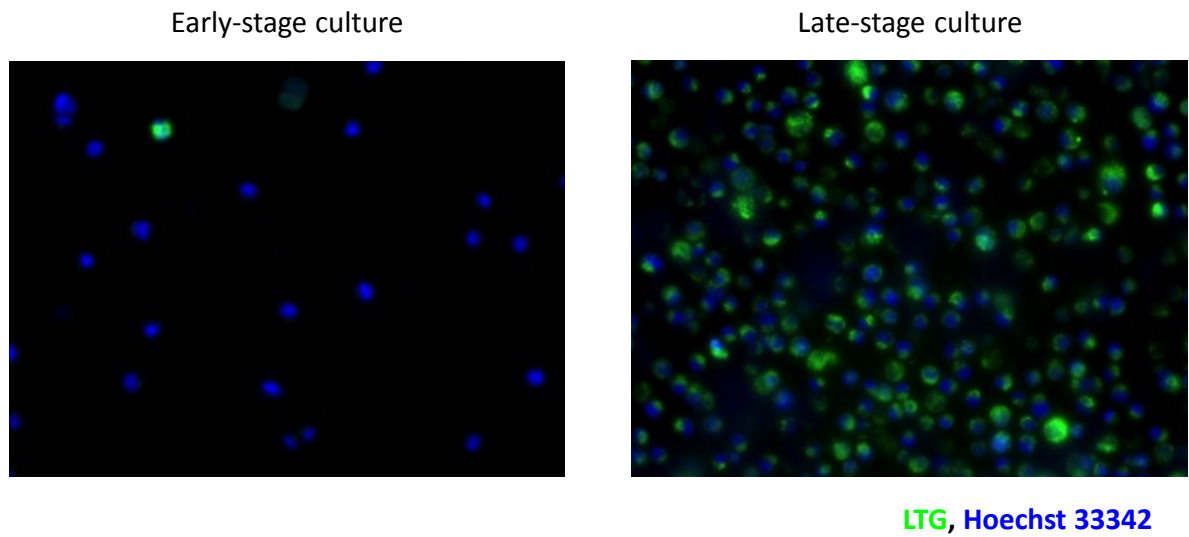
Figure A.5.   **Comparison of lysosomal content between early and late-stage cultures.**
These fluorescence micrographs were generated using t-PA producing CHO cells. Two cultures in early (left pannel) or late (right pannel) stage were compared in terms of lysosomal content. Cells were stained with 75 nM LysoTracker Green (LTG) and 1 µM Hoechst 33342 for 15 min at 37 ºC.

Untreated   3MA-treated, 24 h

**Propidium iodide, YO-PRO1, Hoechst 33342**
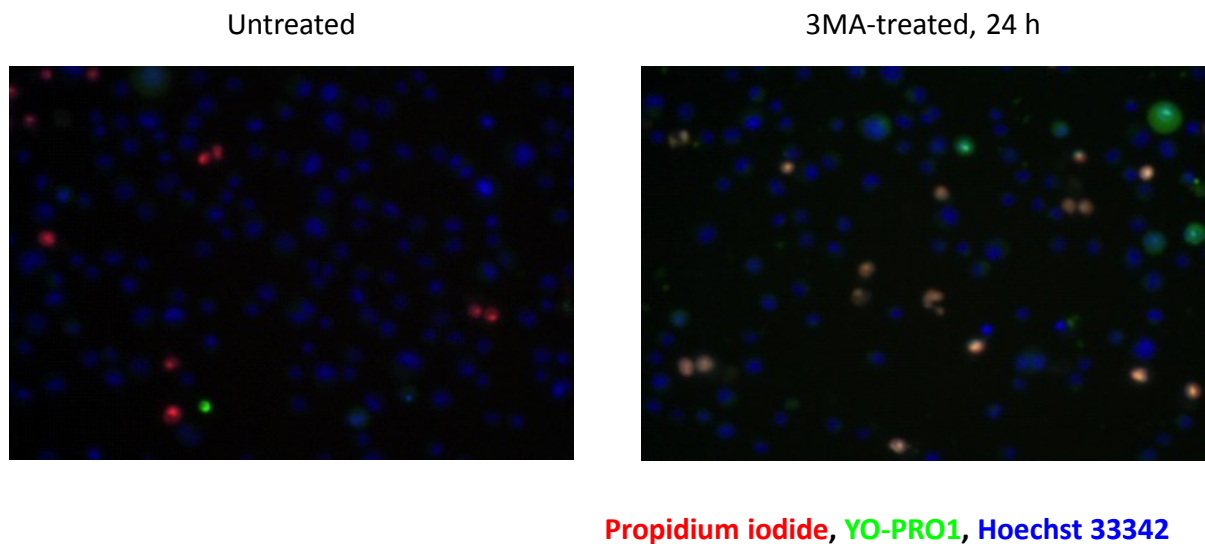
Figure A.6.   **Preliminary characterization of 3-MA toxicity.**
Dead cells are propidium iodide-positive; apoptotic cells are YO-PRO1-positive and cells that are only Hoechst 33342-positive are alive.
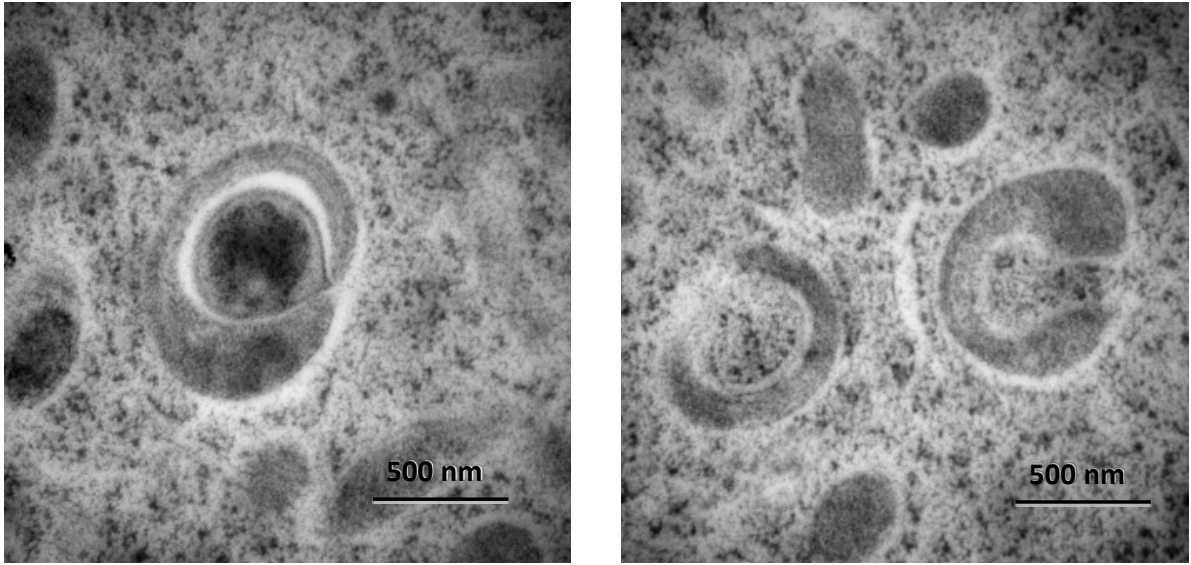
Figure A.7.   Transmission electron micrographs of phagophores.
Images were captured 1 day after glutamine withdrawal in t-PA producing CHO cells.
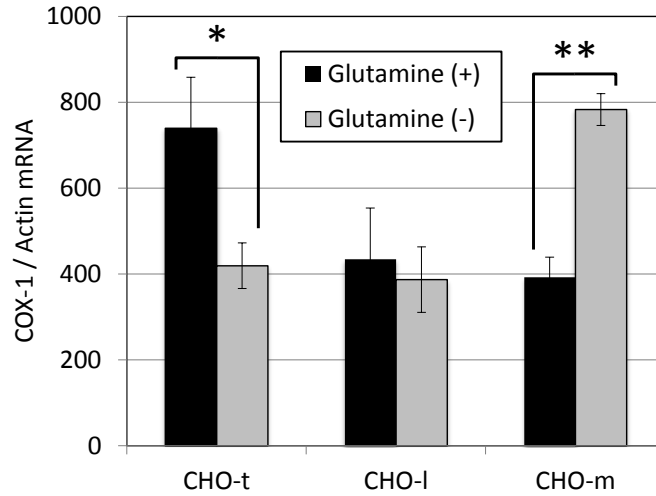
Figure A.8.   Effect of glutamine deprivation on mitochondrial RNA content.
Error bars represent the SEM of biological triplicates. * p value < 0.1; ** p value < 0.05
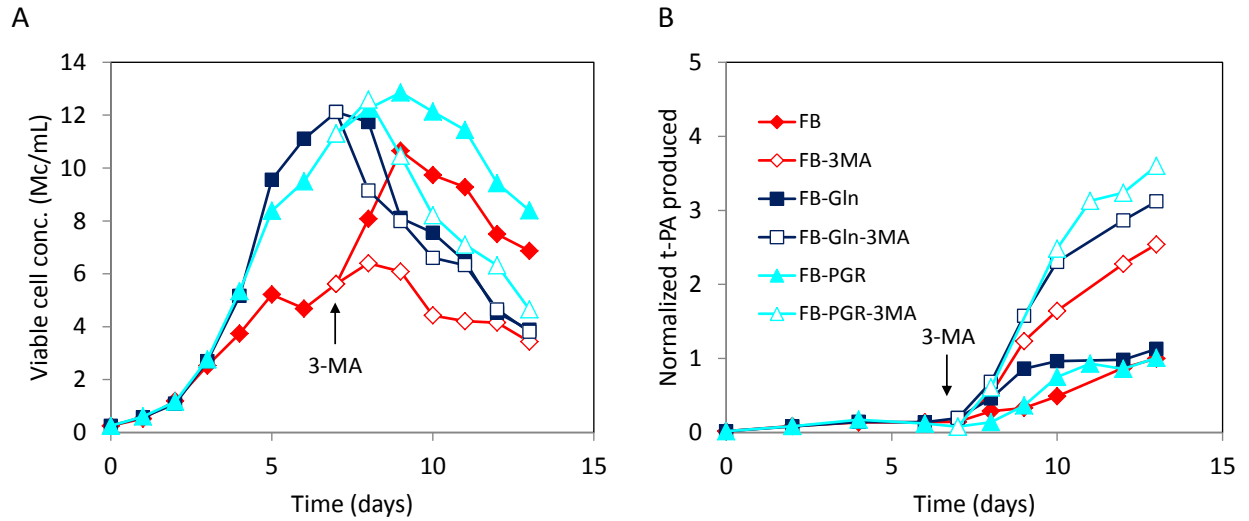
Figure A.9. Viable cell concentration and total t-PA produced under PGR.
Duplicate experiment to data shown in Chapter 4. Legend: FB (red): control fed-batch with 4 mM initial glutamine and no further glutamine supplementation; FB-Gln (dark blue): fed-batch with glutamine supplementation, matching the cellular consumption; FB-PGR (light blue): fed-batch with partial glutamine replacement. Open symbols refer to cultures treated with 3-MA and closed symbols to the equivalent non-treated controls. The arrow indicates time of 3-MA treatment.

Appendix B.   Conceptual framework for the mathematical modeling of autophagy

The mass balance on autophagosomes can be established as:

$$\frac{dA}{dt} = r_A - A(k_f + \mu)$$

(Equation 1)

Table B.1.   Mass balance parameters for modeling of autophagy

Parameter	Description	Units
A	Autophagosome content	organelles
t	Time	d
r_A	Rate of autophagosome biogenesis (induction)	organelles/d
k_f	Rate constant for autophagosome degradation (flux)	1/d
μ	Cell-specific growth rate	1/d

In the presence of chloroquine, there is no degradation and therefore, $k_f = 0$

$$\frac{dA}{dt} = r_A - A\mu$$

(Equation 2)

Considerations:

- LC3-II is proportional to the mass of autophagosomes and Western Blot data is generally normalized to the cellular levels of actin, so A is proportional to LC3-II/Actin.
- μ can be determined experimentally.

Therefore:

r_A can be estimated from the Chloroquine (+) values using Equation 2.

k_A can be estimated from the Chloroquine (-) values, using Equation 1, once r_A is known.

Using the data generated in Chapter 2 (Figure 2.2.C), with $\mu = 0$ since this cell line does not proliferate under the conditions of glutamine deprivation used for the experiment.

Using the following constants on Equation 1:

$r_A = 0.847$ organelles/day

$k_A = 0.262$ 1/day,

the curves in Figure B.1 are obtained, where *Total autophagosomes produced* (biogenesis) correspond to the chloroquine (+) data; *Physiological autophagosome levels* to the chloroquine (-) data; and *Autophagosomes cleared* is the difference between the two curves.
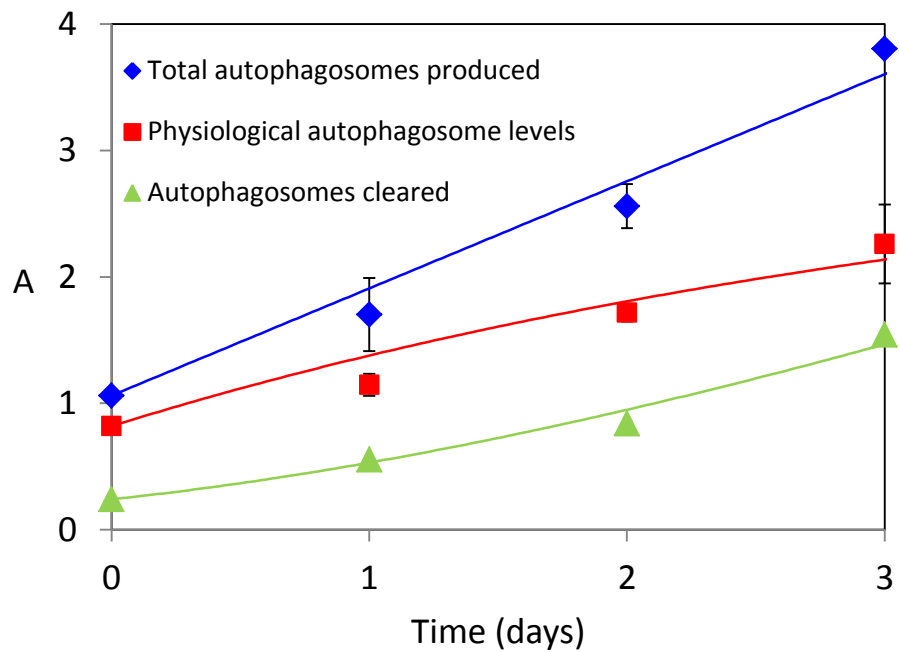

Figure B.1.   Estimation of autophagosome biogenesis and clearance rates

Appendix C. Investigation of genetic strategies to modulate autophagy

Use of RNAi to inhibit autophagy in CHO cells

The first attempt at genetic strategies to inhibit autophagy consisted in the use of siRNA. Beclin-1 was chosen as the target for various reasons. On one hand, beclin-1 interacts with PIK3C3 (3-MA target) during early stages of autophagy. Also, since beclin-1 haploinsufficiency caused by monoallellic deletion leads to defective autophagy, it was hypothesized that its downregulation would be more readily achievable and noticeable. Finally, beclin-1 was chosen as a target, since the primers developed in this study (sequences listed previously in Table 2.1) could be used to demonstrate effective mRNA silencing by qRT-PCR.

Various siRNA sequences (Table C.1) targeting human beclin-1 effectively decreased the mRNA levels of this protein in CHO cells as well (Figure C.1). Human 293F cells were used as a control to compare silencing efficiency. Sequence D was selected to pursue this study.
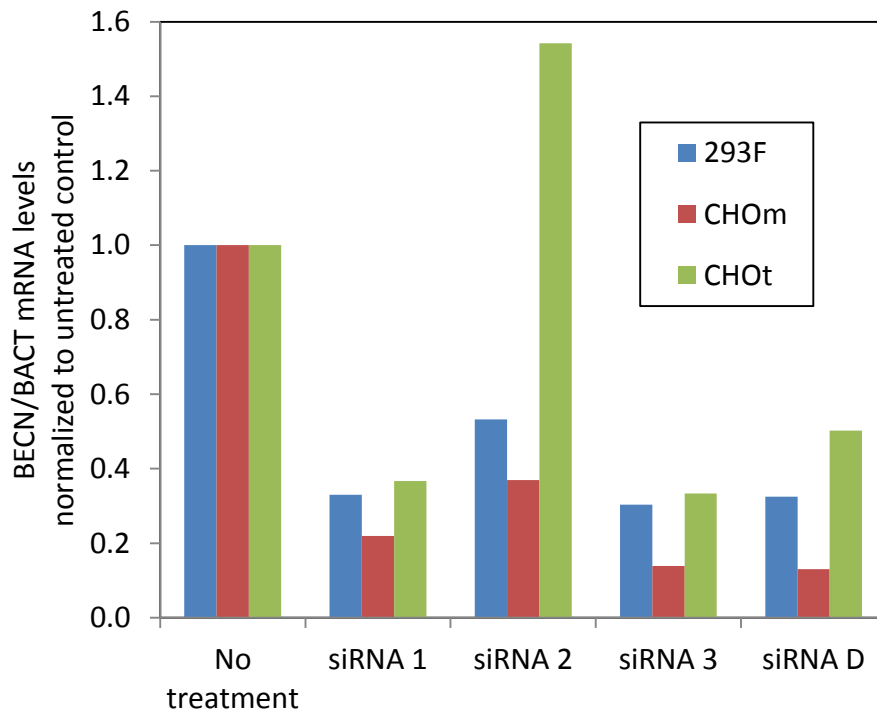

Figure C.1.   Effect of siRNA for human beclin-1 on CHO beclin-1 mRNA levels.

A transfection protocol was developed to deliver siRNA to cells in suspension without need for trypsinisation. Transfections with Beclin-1 siRNA resulted generally in low viability and proliferation, as well as lower overall production.

Later efforts consisted in using siRNAs targeting Atg5 and Atg7 (3 different sequences for both, listed in Table C.1). Transfections with Atg5 or Atg7 siRNA were generally less toxic than transfections with Beclin-1, but little overall difference was observed for protein production, in terms of protein concentration and of cell-specific productivity (Figure C.2). Furthermore, since the sequence of Atg5 and Atg7 was not available for CHO cells, it was not possible to design primers to test for levels of knock-down.
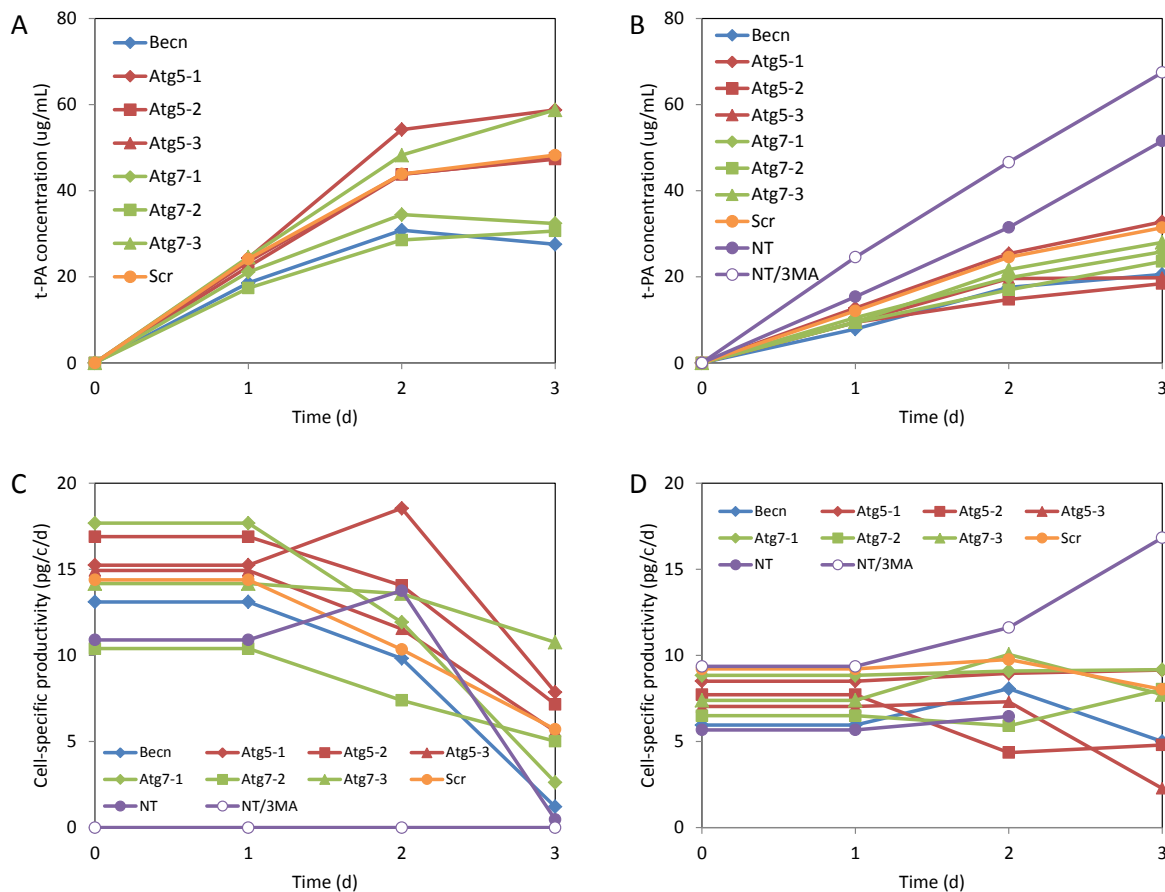
Figure C.2. Effect of the transfection of siRNA against Beclin-1, Atg5 and Atg7 in CHO-t cells on t-PA concentration and cell-specific productivity.
Left-side panels correspond to cultures in the presence of glutamine; right-side panels to cultures in the absence of glutamine. The sequence of beclin-1 (Becn) was Beclin-1/D. Scr stands for Scramble control. NT stands for non-treated with siRNA or Lipofectamine. NT/3MA stands for non-treated with siRNA or Lipofectamine, but treated with 10 mM 3MA.

Finally, two different doses of siRNA were tried on CHO-m cells (Figure C.3). Trying these transfections on a different cell line was based on the observation that the CHO-m cells were more susceptible to transfections than the CHO-t cells. Similarly to the results observed with the previous cell line, transfections with Beclin-1 siRNA resulted in lower viability, proliferation and overall protein production. Neither Atg5 nor Atg7 enhanced protein production.
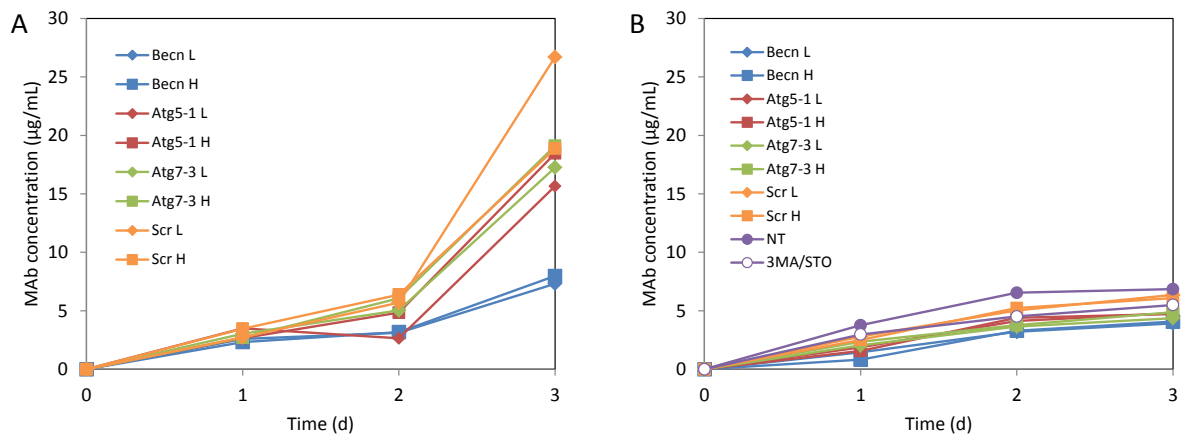
**Figure C.3.   Effect of the transfection of siRNA against Beclin-1, Atg5 and Atg7 in CHO-m cells on MAb concentration.**
Left-side panel corresponds to cultures in the presence of glutamine; right-side panel to cultures in the absence of glutamine. The sequence of beclin-1 (Becn) was Beclin-1/D. Scr stands for Scramble control. L or H refer to low or high siRNA concentration. NT stands for non-treated with siRNA or Lipofectamine. 3MA/STO stands for non-treated with siRNA or Lipofectamine, but treated with 10 mM 3MA or 25 μM STO-609, respectively.

In conclusion, this preliminary investigation on the use of siRNA to downregulate essential autophagy genes produced experience that can be useful for future efforts in this direction. Dosage of the interfering RNA, the effect on target mRNA levels and effect on autophagic activity should be carefully evaluated. Also, since the effect of the siRNA could decrease within a few days, the time courses may not be long enough to demonstrate effects on protein production. In this perspective, an inducible system expressing shRNA sequences that target the gene of interest would potentially be a more suitable option to test this approach.

Table C.1.   siRNA sequences for Beclin-1, Atg5 and Atg7

Target	ID	Sequence
Beclin-1	1	GCUGUUUGGAGAUCUUAGAGCAAAU
		AUUUGCUCUAAGAUCUCCAAACAGC
	2	UAUCUGUGCAUUCCUCACAGAGUGG
		CCACUCUGUGAGGAAUGCACAGAUA
	3	GGAUGAUGAGCUGAAGAGUGUUGAA
		UUCAACACUCUUCAGCUCAUCAUCC
	D	UUCAACACUCUUCAGCUCAUCAUCC
		GGAUGAUGAGCUGAAGAGUGUUGAA
Atg5	1	GAUCACAAGCAACUCUGGAUGGGAU
		AUUCCAUGAGUUUCCGAUUGAUGGC
	2	GCCAUCAAUCGGAAACUCAUGGAAU
		AAACAAGUUGGAAUUCGUCCAAACC
	3	GGUUUGGACGAAUUCCAACUUGUUU
		AUCCCAUCCAGAGUUGCUUGUGAUC
Atg7	1	GCUGGAUGAAGCUCCCAAGGACAUU
		AAUGUCCUUGGGAGCUUCAUCCAGC
	2	CCAAGGAUGGUGAACCUCAGUGAAU
		AUUCACUGAGGUUCACCAUCCUUGG
	3	AAACCUUUGAUCCAAACCCACUGGC

Genetic engineering approaches to inhibit autophagy in CHO cells

The second genetic strategy explored in this project to inhibit autophagy in CHO cells consisted in the heterologous expression of Jumpy (MTMR14), a PI3P phosphatase that interferes with the early stages of autophagy (Vergne et al. 2009). Jumpy dephosphorylates the position 3 of phosphatidyl inositol, which is required for induction of autophagy. Since the action of Jumpy counteracts the activity of PIK3C3 (Vps34), Jumpy thus functions in an analogous manner to 3-MA.

Two constructs of Jumpy, wild-type and catalytically inactive mutant C330S, were obtained from Dr. Jocelyn Laporte. Both constructs express Jumpy fused with YFP as a reporter. CHO-t and CHO-m cells were used to generate stable cell lines with wild-type

(functional) and mutant (inactive) Jumpy-YFP. Positive transfectants were enriched by flow cytometry and expanded until further use. Figure C.4 shows the effects of Jumpy on cell proliferation and overall t-PA production. Wild-type Jumpy seems to produce more t-PA than the parental (non-transfected) cell line, with no negative effect on cell proliferation. The inactive mutant Jumpy seemed to decrease slightly the proliferation, but the effect on protein production is not clear.
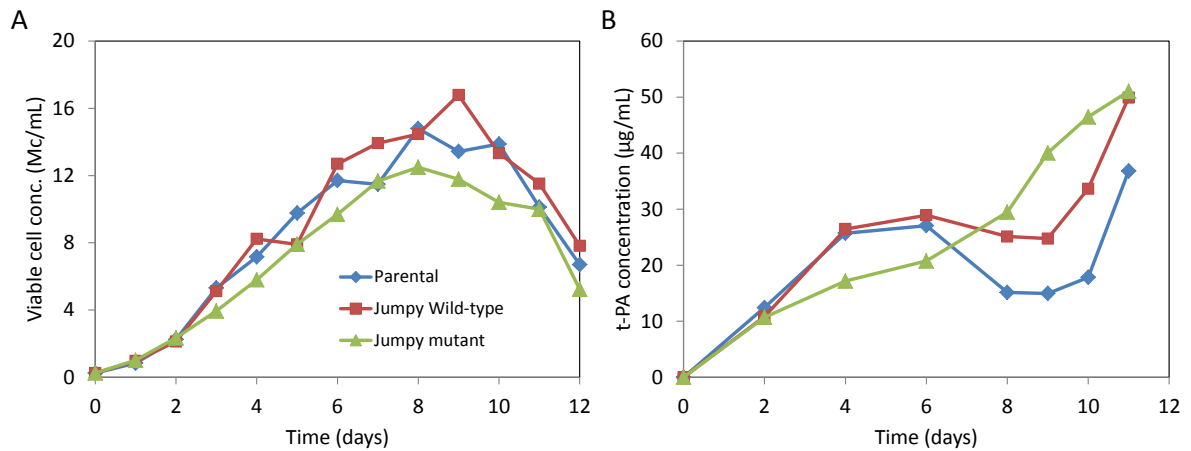

Figure C.4.   Effect of jumpy overexpression on viable cell and t-PA concentrations. Graphs show the average of two biological duplicates.
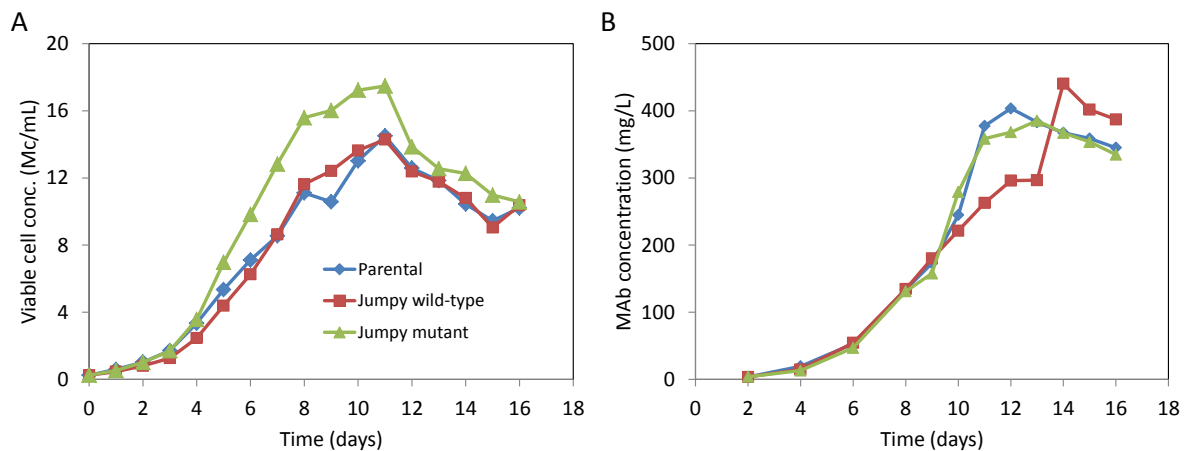

Figure C.5.   Effect of jumpy overexpression on viable cell and MAb concentrations. Graphs show the average of two biological duplicates.

113

Heterologous expression of wild-type Jumpy on CHO-m cells did not affect their proliferation, but the benefit for enhanced protein production is not clear (Figure C.5). As with the CHO-t cells, further investigation would be required. The stable cell line expressing mutant Jumpy had an increased proliferation capacity, but did not increase the protein production ability of the cells.

In conclusion, this preliminary investigation on the use of heterologous expression of proteins with anti-autophagic activity did not provide definitive results, but produced useful experience for future efforts. In a similar way to the study with RNA interference, the dosage of the transgene, the expression timing and the effect on autophagic activity need to be evaluated to optimize this system. An inducible system expressing the gene of interest would be a most valuable tool to determine the optimal timing and dosage of autophagy inhibition.

Appendix D. Glutamine-mediated responses of cancer cells to chemical treatments

The purpose of the experiments described in this Appendix was to explore briefly the relevance of glutamine metabolism and autophagy in cancer cells, mainly from the perspective of survival to chemical treatments.

In a preliminary assessment, the overall responsiveness of human and mouse cancer cells to glutamine deprivation was tested by its effect on cell proliferation and viability. Human cancer carcinoma MCF7 cells and mouse metastatic prostate carcinoma LMD cells have been described in Chapter 5. Other mouse cancer cells were generously provided by Dr. Wilfred Jefferies. Briefly, the cell lines used (Setiadi et al., 2007) were PA (prostate primary carcinoma), TC1 (lung primary carcinoma), A9 and D11 (both of which were clones derived from lung metastatic carcinoma).

Consistent with the results observed on CHO cells, human MCF7 cells (Figure D.1) and mouse cancer cells (Figure D.2) proliferated more slowly in the absence of glutamine. The proliferation of mouse cancer cells was more drastically affected by glutamine deprivation. MCF7 cells seem to be less sensitive, likely due to their endogenous glutamine synthetase (GS) activity (Kung et al., 2011) and yet, their proliferation was significantly affected by the presence or absence of exogenous glutamine. These results are reminiscent to those obtained with the GS-expressing cells studied in chapter 3.
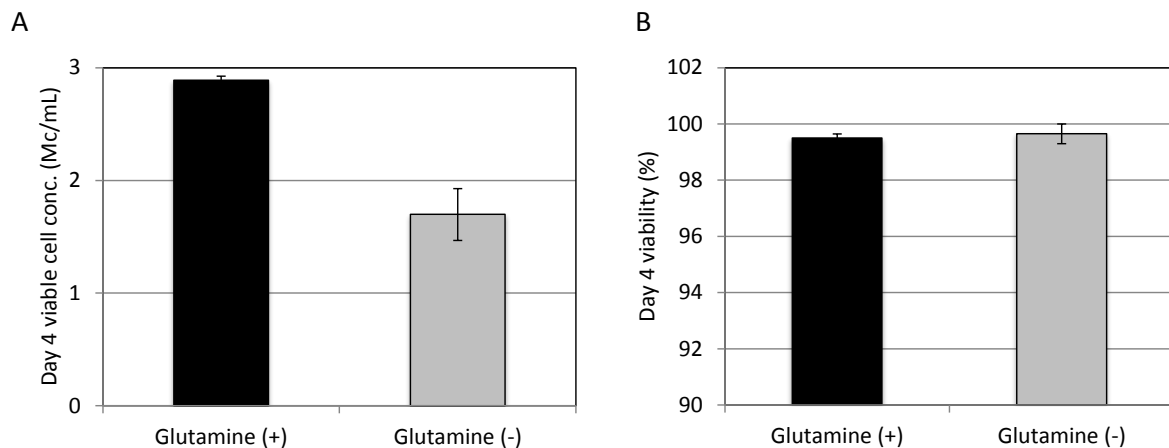

Figure D.1. Effect of glutamine on viable cell concentration and viability of MCF7 cells.
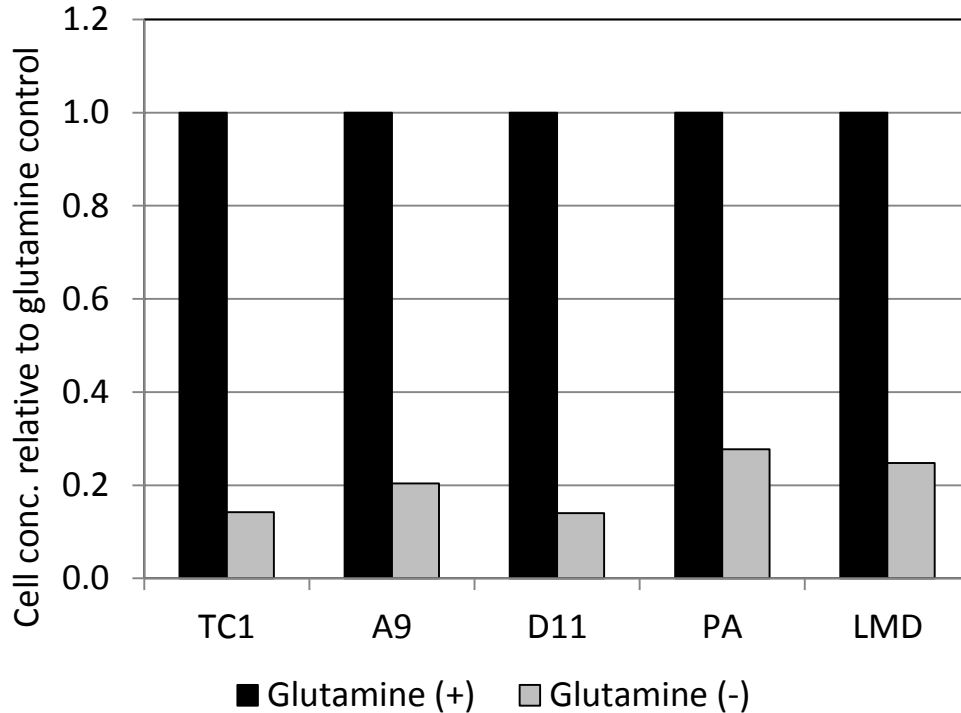
Figure D.2.   Effect of glutamine on viable cell concentration of mouse cancer cells.
Values of viable cell concentration are normalized to the respective culture in the presence of glutamine. All cell lines tested, metastatic or pre-metastatic, lung or prostate tissue-derived, responded in a similar way.

The next idea tested was whether the presence of glutamine would provide cells an advantage to survive chemically-induced stress. The ultimate purpose of this study was to suggest combinations of chemicals to eradicate cancer cells more effectively. Three chemicals were used to generate different kinds of stress. Chloroquine (20 μM) was used as an inhibitor of autophagic degradation. Metformin (was chosen as an AMPK activator (Buzzai et al., 2007) and therefore as an inducer of autophagy via energy stress. In previous observations, treatment with 4 mM metformin heavily increased lactate production in MCF7 cells. Thus, as an additional stress, cells were treated with 500 μM α-cyano-4-hydroxy-cinnamate (4-CIN), which inhibits the monocarboxylate transporter (MCT) mediated lactate efflux (Erlichman et al., 2008). Treatment with these chemicals alone or in combination was done in matched cultures to compare responses in the presence or absence of glutamine.

After 4 days of treatment, cells were harvested to determine the viable cell concentration (Figure D.3.A) and viability (Figure D.3.B). Concentrations of glucose (Figure D.4.A), lactate (Figure D.4.B), glutamine (Figure D.5.A) and glutamate (Figure D.5.B) were determined from medium collected at the same time points.
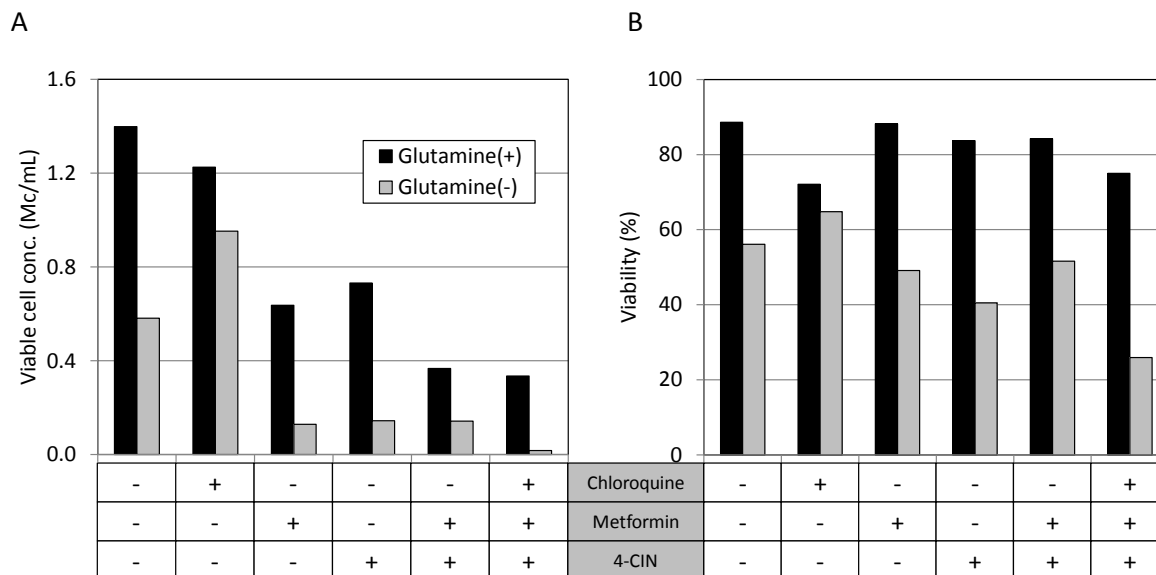

Figure D.3.   Viable cell concentration and viability of MCF7 cells in response to treatment with various chemicals.
After a 4 day culture in the conditions described here above, cells were trypsinized and counted for viable cell concentration and viability using the trypan blue exclusion method. The (+) conditions are chloroquine: 20 μM; metformin: 4 mM; 4-CIN: 500 μM.

Consistent with previous results, cell proliferation and viability after 4 days of culture were maximal in the glutamine-positive control, not treated with any chemicals, i.e. 1.4×10^6 c/mL and 89%, respectively. Viable cell concentrations in all other conditions will be discussed as percentages of this control. Absence of glutamine alone resulted in decreased cell proliferation (42% of the control) and viability (56%). Treatment with chloroquine alone in the presence of glutamine resulted in a slight decrease of cell proliferation (88% of the control) and viability (72%). In the absence of glutamine, chloroquine alone seemed to have a beneficial effect on proliferation and viability compared to glutamine deprivation alone, since viable cell concentration was 68% of the glutamine-positive control and viability was 65%.

117

Metformin and 4-CIN had similar effects as single treatments, decreasing cell proliferation to 45% and 52% of the control, respectively, in the presence of glutamine. The effect of these single treatments on viability was not noticeable 88% and 84%. However, in the absence of glutamine, both metformin and 4-CIN alone decreased further cell proliferation to 9% and 10% of the control, respectively. These single treatments were also more toxic in the absence of glutamine, reducing viability to 49% and 40%, respectively. Combination of both treatments resulted in a cell proliferation of 26% and 10% of the control in the presence or absence of glutamine, respectively. This combination did not result in additional toxicity neither in the presence nor in the absence of glutamine, since viability was 84% and 52%, respectively.

The combination of all three chemical treatments resulted in lowest proliferation in the presence of glutamine (24% of the control), even though the viability was not so severely impaired (75%). However, the combined treatment was considerably stronger in the absence of glutamine, practically eliminating proliferation (1% of the control) and reducing cell viability to 26%, the lowest recorded in this experiment.
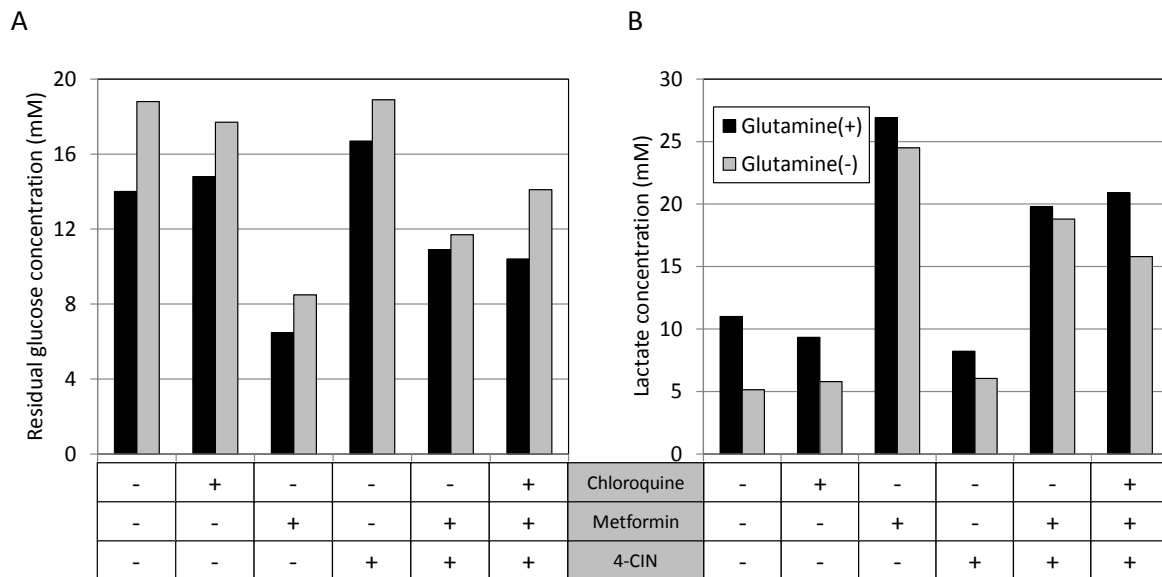

Figure D.4.   Effect of chloroquine, metformin and 4-CIN treatment on glucose uptake and lactate production.
Medium samples were taken after a 4 day culture in the conditions described here above. The (+) conditions are chloroquine: 20 μM; metformin: 4 mM; 4-CIN: 500 μM.

Figure D.4 shows that neither chloroquine nor 4-CIN alone affected considerably glucose consumption or lactate production. However, under metformin treatment cells consumed more glucose and produced more lactate, suggesting a perturbation of oxidative metabolism. Treatment with 4-CIN seemed to attenuate metformin treatment in terms of total glucose uptake and total lactate formation. Finally, combination of metformin, 4-CIN and chloroquine resulted in similar residual glucose and final lactate levels to the double-treated culture in the presence of glutamine. In the absence of glutamine, cells with triple treatment consumed less glucose and produced less lactate, which reflects the lower proliferation in these conditions.
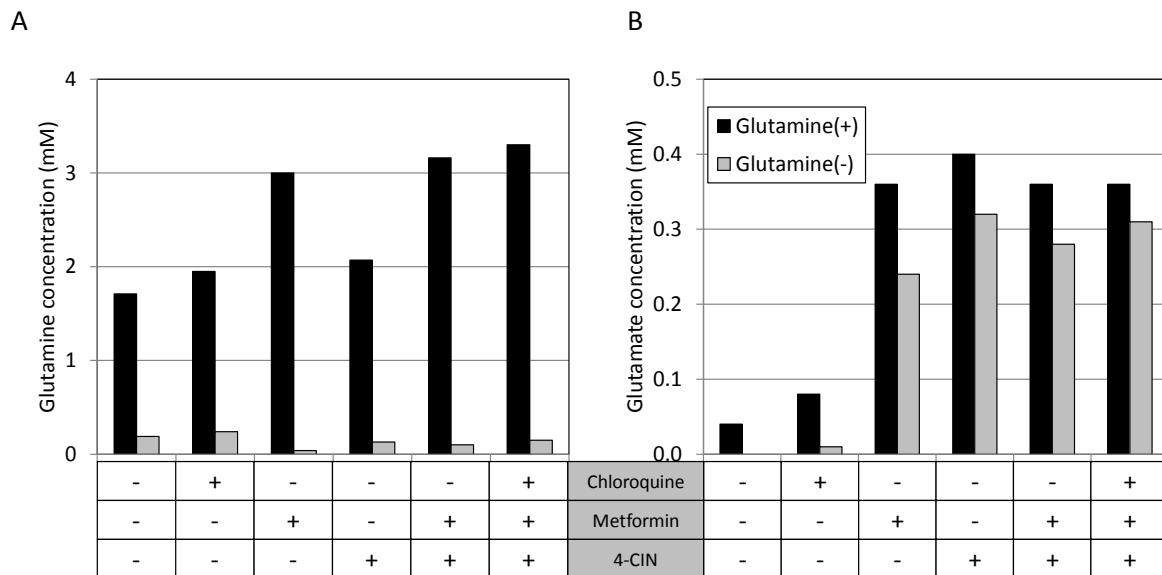

Figure D.5.   Effect of chloroquine, metformin and 4-CIN treatment on glutamine and glutamate consumption.
Medium samples were taken after a 4 day culture in the conditions described here above. The (+) conditions are chloroquine: 20 μM; metformin: 4 mM; 4-CIN: 500 μM.

Glutamine and glutamate concentrations in culture medium under these cultivation conditions were also evaluated. Cultures treated with chloroquine alone had similar profiles to the non-treated cultures and thus appears to be the less toxic of the chemicals. Metformin-treated cultures had the lowest glutamine consumption and 4-CIN treatment resulted in similar glutamine consumption as the non-treated cells, even though cell proliferation had been reduced by almost half.

119

| Chl	Met	4-CIN	Glutamine (+)	Glutamine (-)
-	-	-		
+	-	-		
-	+	-		
-	-	+		
-	+	+		
+	+	+		
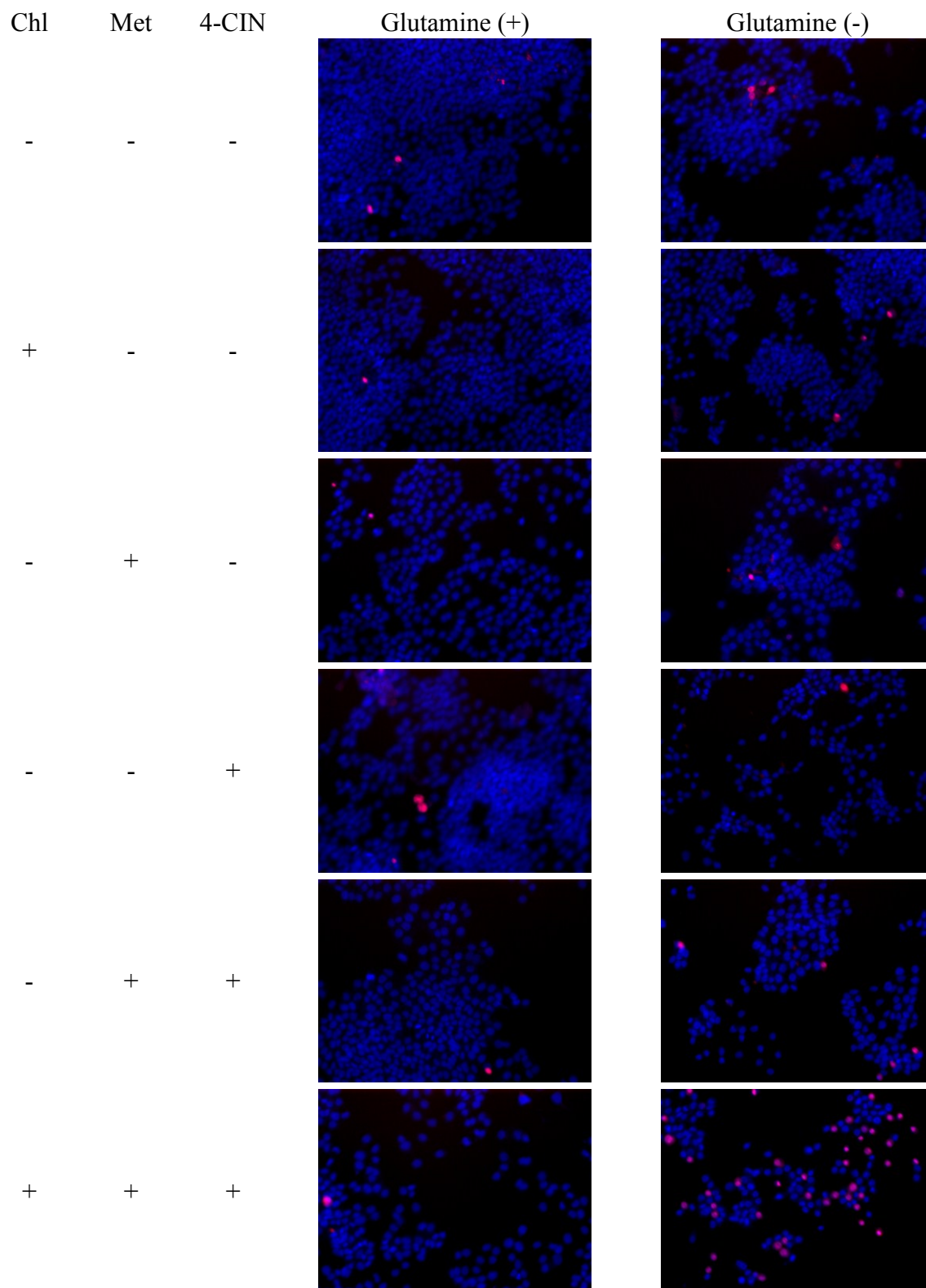
Figure D.6.   Effect of chloroquine, metformin and 4-CIN treatment on survival of MCF7 cells.
Fluorescence images were collected after a 4 day culture. Dead cells are stained red (Propidium Iodide); live cells are only blue (Hoechst 33342).

| Chl	Met	4-CIN	Glutamine (+)	Glutamine (-)
-	-	-		
+	-	-		
-	+	-		
-	-	+		
-	+	+		
+	+	+		
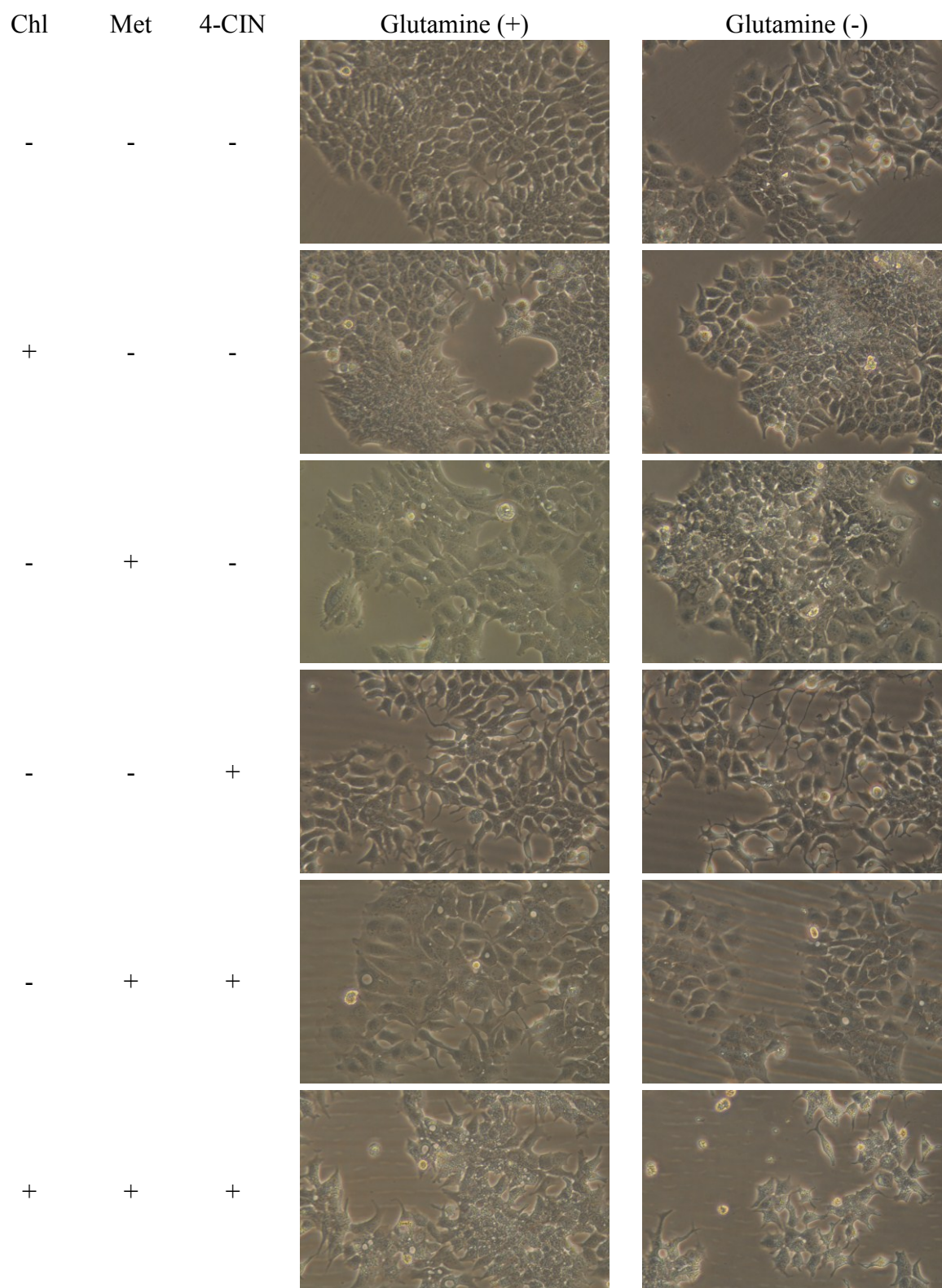
Figure D.7. **Effect of chloroquine, metformin and 4-CIN treatment on morphology of MCF7 cells.**
Bright field micrographs collected after a 3 day culture in the conditions described here above.

121

In order to determine the statistical significance of these observations, replicate experiments should be performed. These results reveal nonetheless glutamine as a strong mediator of cellular repair in the presence of chemical and metabolic stress. From the metabolic profiles, the main findings are that chloroquine is the least toxic of the three, not disturbing metabolism if provided alone. However, when combined with metformin and 4-CIN, the toxic effects were significantly higher. Such toxicity was more remarkable if that combination took place in the absence of glutamine. Metformin treatment, on the other hand was noticeable for its effect on increasing lactate production, which could be an indicator of mitochondrial dysfunction.

These experiments suggest that combining impairment of respiratory metabolism, inhibition of lactate efflux and impairment of autophagy could be a strategy for treatment of cancer cells. This strategy is likely to be more effective in the absence of the repair functions provided by glutamine.

Appendix E.   Reporter cell lines

Various reporter cell lines were generated in the context of the present Ph.D. work and/or supervising related projects.

Table E.1.   Description of reporter cell lines

Cell line name	Reporter protein	Parental cell line	Comments	Prepared by
CHOma	hrGFP-LC3	ChK2 437.89.56	Autophagy reporter	Mario Jardon
CHOmjw	eYFP-Jumpy	ChK2 437.89.56	Active Jumpy reporter	Mario Jardon
CHOmjm	eYFP-Jumpy mutant C330S	ChK2 437.89.56	Catalytically inactive Jumpy reporter	Mario Jardon
CHOlj	eYFP-Jumpy	CHO EG2 1A7	Active Jumpy reporter	Nicole Stichling
CHOld	Tandem eGFP/mRFP-LC3	CHO EG2 1A7	Autophagy flux reporter	Amy Yu
CHOtjw	eYFP-Jumpy	CHO540/24	Active Jumpy reporter	Mario Jardon
CHOtjh	eYFP-Jumpy	CHO540/24	Active Jumpy reporter, sorted for high fluorescence	Mario Jardon
CHOtjl	eYFP-Jumpy	CHO540/24	Active Jumpy reporter, sorted for low fluorescence	Mario Jardon
CHOtjm	eYFP-Jumpy mutant C330S	CHO540/24	Catalytically inactive Jumpy reporter	Mario Jardon
CHOa	hrGFP-LC3	CHO540/24	Autophagy reporter	Mario Jardon
LMDa	hrGFP-LC3	LMD	Autophagy reporter	Mario Jardon
293a	hrGFP-LC3	HEK 293	Autophagy reporter	Leslie Chan
293o	Omi-mCherry	HEK 293F	Apoptosis reporter	Mario Jardon
293d	hrGFP-LC3	293a	Dual autophagy and apoptosis reporter	Leslie Chan

Appendix F. Colorimetric t-PA activity assay

The enzymatic t-PA activity was determined with a colorimetric assay that measures plasmin activity using the chromogenic peptide substrate D-Val-Leu-Lys-p-Nitroanilide dihydrochloride (Sigma, St. Louis MO). In the presence of a stimulator (fibrinogen fragments), t-PA converts plasminogen into plasmin. To produce the stimulator, fibrinogen (Calbiochem, La Jolla, CA) was digested with a 70% solution of formic acid and 122.75 mM CNBr (Sigma) and dialysed with distilled water. Human plasminogen (Roche, Manheim, Germany) was prepared in distilled water, aliquoted and stored at -20 ºC. The standards were prepared from human tissue plasminogen activator (Calbiochem) by serial dilution to a range of 0.25 to 10 U/mL in 0.1 M Tris-HCl; 0.1% Tween 80; pH 8.0 (Tris DB).

Assay Procedure

1. The reaction mixture should be prepared just prior to use. For one 96-well plate prepare 10.7 mL of reaction mixture in a 15 mL polypropylene tube by adding the reagents in the following order and amount, vortexing gently after addition of each reagent:

    Tris DB: 6 mL

    Plasminogen 1 mg/mL: 113 μL

    Substrate 14.477 mg/mL : 204 μL

    Stimulator 5.465 mg/mL: 236 μL

    Tris DB: 4.711 mL

2. Mix reaction by gentle inversion or gentle vortexing.

3. Add 50 μL of each standard and samples prediluted with Tris DB, in duplicate wells.

4. Using a multichannel pipette, add 100 μL of reaction mixture to all wells. Cover the plate with plate sealer and incubate at 37 ºC until color develops (between 2 and 3 hours).

5. Read the plate on the microplate reader at 405 nm, using endpoint analysis. The standard curve is generated using a 4-parameter logistic fitting.